Hydrological Approaches of Wadi System Considering Flash Floods in Arid Regions

Mohamed Saber Mohamed Sayed Ahmed

Department of Urban Management
Graduate School of Engineering
Kyoto University, Japan
September, 2010

ABSTRACT

The arid regions of the world are facing the problems of water scarcity and flash floods threat. However, more than one third of the world areas are suffering from aridity conditions, the increasing population and the expanding urbanization and industrialization lead to great need of water which has become one of the key factors of sustainable development in the arid countries. The hydrological conditions of arid regions are represented in the following three main problems: (1) the water resources deficiency, where both of surface and subsurface water are not enough for people demand in arid regions due to the paucity and high variability of rainfall events as well as missing of the appropriate strategies of water use management. (2) They are suffering from the threat of flash floods which become the big catastrophic cause for the human being, Environment, etc, due to the climate change. (3) The lack of powerful hydrological models and good support tools for flash floods and water resources management. The reasons are due to, i) the paucity of observational data and high quality data, ii) several modeling techniques and tools have been widely developed for humid area applications but arid and semi-arid regions have received little attention although their severe situation of water resources scarcity and flash floods threat. Thus, developing the comprehensive, innovative and powerful physical-based approaches (i.e., models explicitly based on the best available understanding of the physics of hydrological processes of wadi system) which could be applied as effective and sustainable management tools for water resources and flash floods are desperately needed in arid and semi-arid regions.

With regard to the aforementioned problems of arid and semi-arid regions, the main objectives of this study are: (1) To develop a physically-based distributed

hydrological model to overcome the prescribed struggles for wadi runoff and flash floods simulation, (2) to propose a homogenization method of upscaling hydrological parameters related to a distributed runoff model from microscopic aspects up to macroscopic ones. The essential idea of homogenization is to average inhomogeneous media in some way in order to capture global properties of the medium, (3) To present a consistency of empirical and physical methodology to estimate the initial and transmission loss in wadi basins, throughout the empirical approaches with the physical approaches have been connected to develop a new methodology for this purpose, (4) To evaluate the initial and transmission losses and their effect on both surface and subsurface water due to their importance in the hydrological processes in the arid regions, (5) To understand distributed wadi runoff behaviors in space and time throughout a comparative study between some Arabian wadi basins. The comparison between such wadi basins is focusing on the effect of topographical conditions of the catchments, the difference of degree of urbanization, the difference of basin's scales or shapes, the difference of total amounts of rainfall or rainfall duration in the upstream and mountainous areas, the difference of soil permeability on the river channels, and the difference of runoff features in wadi basins, (6) To simulate flash floods using Satellite Remote Sensing Data to overcome the paucity of data in such regions and to protect the human life and their properties from flash floods devastating effect, (7) To assess and evaluate the contribution of wadi basins to the Nile River which is representing the main water resource for Egypt and the other sharing countries. In some extend, flash flood water could be managed as useful new water resources.

In this study, proposing and developing of hydrological approaches for simulation of distributed runoff in wadi systems have been achieved in regard to water resources management and flash floods. Understanding of wadi system characteristics and hence its hydrological processes are accomplished and depicted,

for instance, depicting the potentially discontinuous occurrence of flow in both time and space in the ephemeral streams have been done as pioneering work. Furthermore, study of runoff behaviors and factors affecting it, initial and transmission losses and their effect on both surface flow and subsurface storage are successfully evaluated.

This thesis also presents homogenization method of upscaling hydrological parameters related to a distributed runoff model from microscopic aspects up to macroscopic ones. The homogenized parameters are equivalently derived from the mathematically formulated descriptions based on the conservation of surface and subsurface water quantities, these parameters are relied on Darcy's law and Manning's law.

A trial is made to adopt Hydrological Basin Environmental Assessment Model (Hydro-BEAM) which has been originally developed for humid regions application. The adopted Hydro-BEAM is a physically-based numerical model and it mainly consists of: (1) the watershed modeling using GIS technique is processed. (2) Surface runoff and stream routing modeling based on using the kinematic wave approximation is applied. (3) The initial and transmission losses modeling are estimated by using SCS method and Walter's equation respectively. (4) Groundwater modeling based on the linear storage model is used. Additionally, the consistency and compatibility between empirical (empirically proposed transmission losses) and theoretical (kinematic wave) models are also originally established. With finding the observed data of transmission losses in wadi basins for calibration, this approach could be deliberated as adequate contribution to the hydrological modeling in arid regions.

Hydro-BEAM is used to simulate the surface runoff and transmission loss in the ephemeral streams throughout comparative studies between some Arabian wadis basins (wadi Alkhoud in Oman, wadi Ghat in Saudi Arabia, and wadi Assiut

in Egypt). The model has been calibrated and the parameters have been identified at wadi Al-Khoud of Oman. The simulated runoff behaviors are showing reasonable agreement with the monitored one that prove an appropriate performance of the proposed model to predict the flash floods events in the arid regions. In addition to, the runoff features are affected by the catchments area, slope, and rainfall events frequency and duration. Runoff features in the ephemeral streams are characterized by different behaviors from the runoff in the humid area based on the results as follow: i) the time to peak is short. ii) Flash floods event period including starting and cessation of flow is short. iii) Initial and transmission losses are considered the main source of subsurface water recharge. v) The occurrence of discontinuous surface flow in space and time.

Due to the scarcity of high quality observational data in arid regions, an attempt is made to use Global Satellite Mapping of Precipitation (GSMaP) for flash floods simulation in wadi basins at the Nile River and wadi El-Arish, Sinai Peninsula, Egypt in Egypt. GSMaP product has been compared with the monitored data of Global Precipitation Climatology Centre (GPCC) which are gauge-based gridded monthly precipitation data sets. Statistics analysis has been done to calculate the bias of these data for different arid areas. The results of comparative show an acceptable agreement between GSMaP and GPCC but with the occurrence of overestimated or underestimated systematic seasonal bias which is variable relying on the selected arid regions. Relying on these results, GSMaP product has been corrected in the target basin. HydroBEAM as a physical-based hydrological model is used to simulate various flash floods events at wadi outlets of the Nile River and and wadi El-Arish using GSMaP data. The simulation has been done to the flood event which hit Egypt on Jan. 18-20, 2010, Feb. 2003, Dec. 2004, and Apr. 2005 for more understanding of the flash flood behaviors and characteristics.

The simulated results present remarkable characteristics of flash flood

hydrograph as reaching to maximum peak flow throughout a few hours. The distribution maps of flash flood events of in the whole catchment of the Nile River and wadi El-Arish in Egypt show that there are highly variations of flash flood distribution in space and time in the selected wadi basins. It reveals the high variability of discharge distribution due to the spatiotemporal variability of rainfall during the selected four events. Also, the flash floods of wadis can contribute into the Nile River as additional water resources however its difficulty to control and management it to avoid or avert the devastating effect on the downstream areas along the Nile River. The contributed water flow volume in the downstream point of wadis is varying from one wadi to the others. It can be inferred that GSMaP precipitation product is very effective in use with the physical-based hydrological model (HydroBEAM) to predict the flash flood not only in the Nile River and wadi El-Arish but also in different arid regions. It can also be used as linkages with the flood forecasting technique in order to provide the flash flood forecast well in advance for taking the emergency actions for evacuating the people so that their lives may be saved and the losses of the properties may be minimized.

The findings and advantages of this study are summarized in the following points: (1) Adopting of Hydro-BEAM to simulate the runoff and transmission loss in arid regions, (2) Developing upsaling technique using the homogenization theory for the hydrological parameters which could be more applicable than the conventional average method of parameters, (3) Depicting of the discontinuous flow in wadi system successfully using the proposed model of Hydro-BEAM, (4) Proposing of the theoretical approach to estimate the transmission losses throughout the original establishing of the compatibility between empirical (empirically proposed transmission losses) and theoretical (kinematic wave) models, (5) Understanding of the hydrological conditions of wadi runoff which are deduced from the comparative study between some wadi basins in arid regions, (6)

Simulating of flash flood has been successfully achieved in wadi basins in very large catchment of the Nile River basin and wadi El-Arish, Sinai Peninsula, Egypt, (7) Using Remote Sensing Data, GSMaP product, to overcome the problem of data paucity in arid regions. They are analyzed and calibrated in order to simulate the flash floods, and (8) Evaluating of water contribution of sub-catchments of the Nile River and wadi El-Arish, Egypt, during the flash floods events.

Comprehensively, it is concluded that the proposed approaches could be considered as remarkable contribution to the hydrological modeling tools in the arid areas in order to estimate distributed surface runoff and transmission losses as well as simulation of flash floods.

Keywords: wadi system, hydrological approach, flash floods, arid regions, transmission losses, homogenization theory, Egypt, the Nile River

Table of Contents

List of Figures

List of Photos

List of Tables

Chapter One

INTRODUCTION

1.1. MOTIVATION AND BACKGROUND

A wadi is a stream that runs fully for only a short time, mostly during and after a rainstorm. Not every rainstorm, however, necessarily produces surface runoff. It is seldom that wadi flow at a certain section can be described as perennial, if so, the flow is then extremely variable from one event to another. In other words; a wadi is an Arabic term traditionally referring to a valley. It can be used to describe the ephemeral streams in the arid regions, and they are a vital source of water in most arid and semi-arid countries. In some cases, it may refer to a dry riverbed that contains water only during infrequently heavy rain. It is characterized by scarcity of fresh water resources, an ever-increasing demand on water supplies, the paucity of data and flash flood threat.

Catastrophic flash floods occurring in wadis are, on one hand, a threat to many communities and, on the other hand, a representative of major groundwater recharges sources after storms. Moreover, infrequent surface water flow in wadi system may cause natural flood hazards but it can be managed to be valuable water resources throughout an appropriate decision support system based on effective methodologies.

Despite the critical importance of water in arid and semi-arid areas,

hydrological data have historically been severely limited. The scarcity of data and the lack of high quality observations as well as the potentially discontinuous occurrence of flow in both space and time are important characteristics of the ephemeral streams in the arid regions and consequently the difficulty of developing the powerful hydrological models.

In general, wadi basins are suffering from the dryness or drought condition for all the year except during the infrequent flash flood events as shown in **Photos 1.1a and 1.1b.** They are affected by infrequent rainfall events which are coming in a short time with the form of flash flood if the rainfall is severe. If the rainfall is not strong, the surface flow will be consequently low. The ephemeral streams are characterized by discontinuous flow especially at the starting of flow as in **Photo 1.2a** and also at the cessation of the flow as depicted in **Photo 1.2b**. The flash flood in wadi basin is very vital natural phenomena which is occurring within short duration and rapidly rising water flow level due to the causative event of intense rainfall or dam failure resulting in a greater danger to human life and severe structural damages as shown in **Photo 1.3**. It is almost accompanying with landslides, mudflows and debris flows.

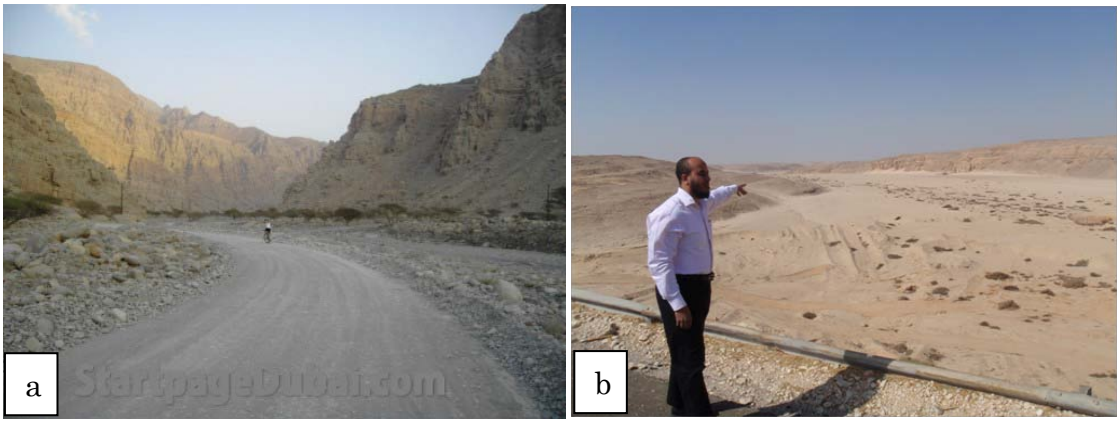

Photo 1.1 Wadi in dry condition; (a) Wadi Baih (Emirates); (b) Eastern Desert (Egypt, March 2010).

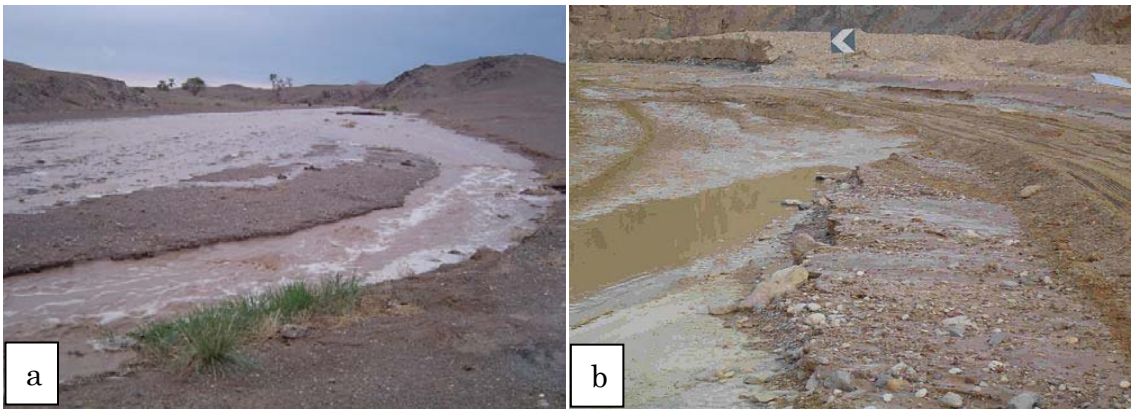

Photo 1.2 Wadi channel showing the discontinuous flow at the starting of flood; (a) flash flood in the Gobi of Mongolia, 2004); and at the ending of it (b) wadi Watier (Sinai, Egypt).

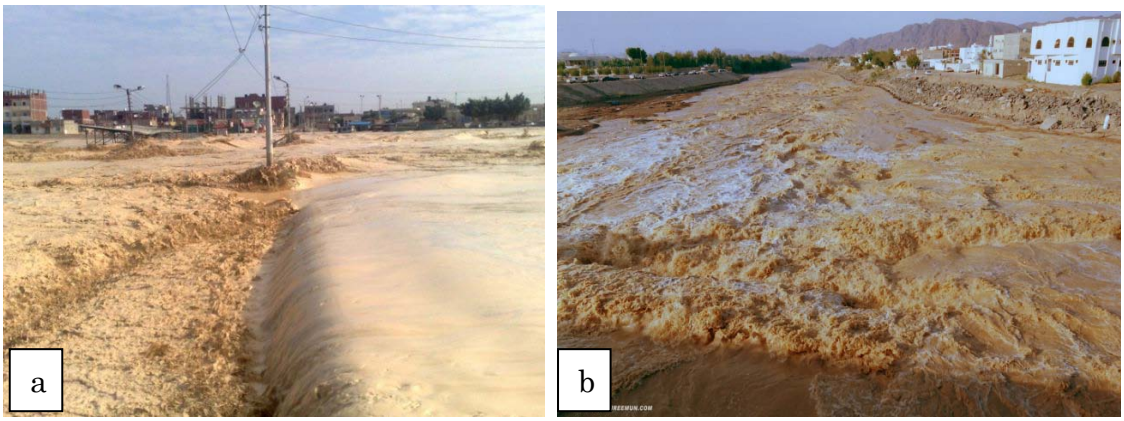

Photo 1.3 (a) Flash floods of Jan., 18th, 2010 (Egypt); (b) Wadi Aqeeq after heavy rainfall, (Madina, Saudi Arabia).

Ephemeral streams are characterized by much higher flow variability, extended periods of zero surface flow and the general absence of low flow except during the recession periods immediately after moderate to large high flow events (Knighton and Nanson, 1997).

Furthermore, those countries of arid areas are facing the problem of overpopulation, and consequently the demand of water resources for the agricultural, manufacturing and domestic purposes, which means that these regions are undergone to severe and increasing water stress due to expanding populations,

increasing per capita water use, and limited water resources. In arid and semi-arid regions, an appropriate utilization and strong management of renewable sources of water in wadis is the only optimal choice to overcome water deficiency problems. One third of the world's land surface is classified as arid or semi-arid (Zekai, 2008). As stated by Pilgrim et al. (1988) and according to UNESCO (1977) classification, nearly half of the countries in the world are suffering from aridity problems. Also, forty percent of Africa's population lives in arid, semi-arid, and dry sub-humid areas (WMO, 2001). Thus, understanding of hydrological processes of wadi system in the arid regions is so important due to the importance of water resources in such areas.

A set of different models is available to represent rainfall-runoff relationships, but they have limitations in the hydrologic parameters that are used to describe the rainfall–runoff process in wadi systems (Wheater et al., 1993). It has been widely stated that the major limitation of the development of arid-zone hydrology is the lack of high quality observations (McMahon, 1979; Pilgrim et al., 1988). Transmission loss in the arid regions has been discussed in different literatures (Jordan (1977), Lane (1984), Vivarelli and Perera (2002), Walters (1990), Andersen et al. (1998), and Abdulrazzak and Sorman (1994) due to its significant role on wadi basins. The behavior of flow discharge takes about 25 min, on average, to reach the target of $100m^3$/sec (Nouh, 2006). A few direct studies of channel transmission losses have been done in arid regions (Crerar et al., 1988; Hughes and Sami, 1992), despite the fact that this process has been recognized as one of the most important components of the water balance of many of arid and semi-arid basins.

Arid and semi-arid regions are defined as areas where water is at its most scarce. The hydrological conditions in these areas are extreme and highly variable, where flash floods from a single large storm can exceed the total runoff from yearly hydrographs. Globally, these areas are facing the greatest pressures to manage the available water resources for their needs due to increasing of population, water

demand, agriculture area, pollution, and threat of climate change. Although, there is not enough powerful hydrological modeling and good support tools for management water resources in such areas. Additionally, they are suffering from the threat of flash flood which become the big catastrophic cause due to the climate change and its frequency in the arid regions as well as its damage for the human being, Environment, etc.

Different modeling techniques and tools have been widely used for a variety of purposes, but almost all have been primarily developed for humid area applications. However, arid and semi-arid regions have particular challenges that have received little attention however their very severe situation of scarcity of water resources and flash flood threat.

Developing the powerful physical-based models (i.e., models explicitly based on the best available understanding of the physics of hydrological processes) is desperately needed in arid and semi-arid regions.

Stream flow in arid and semi-arid regions tends to be dominated by rapid responses to intense rainfall events. Such events frequently have a high degree of spatial variability, coupled with poorly gauged rainfall data. This sets a fundamental limit on the capacity of rainfall-runoff model to reproduce the observed flow (Wheater et al. 2008). Rainfall-runoff models fall into several categories: metric, conceptual, and physics-based models (Wheater et al., 1993). Metric models are typically the most simple, using observed data (rainfall and stream flow) to characterize the response of a catchment. Conceptual models impose a more complex representation of the internal processes involved in determining catchment response, and can have a range of complexity depending on the structure of the model. Physics-based models involve numerical solution of the relevant equations of motion.

Using the ratio of mean annual precipitation to represent mean annual potential evapotranspiration, the world is divided into six aridity zones: hyper-arid, arid, semi-arid, dry sub- humid, moist sub-humid, and humid. As shown on this map

(**Figure 1.1**), the humid zone is the most extensive, covering about 46.5 million km^2 (or 34 percent of total land area). This zone covers most of Europe and Central America, and large portions of Southeast Asia, Eastern North America, Central South America, and Central Africa. The hyper-arid zone is the least extensive, covering approximately 11 million km^2 (or 8 percent of total land area), and is represented most predominantly by the Saharan Desert. Hyper-arid lands generally are unsuitable for growing crops (WRI, 2002). Dry lands, as defined by the United Nations Convention to Combat Desertification (UNCCD), include the arid, semi-arid, and dry sub-humid zones and cover almost 54 million km^2 of the globe. Semi-arid areas are most extensive, followed by arid areas and then dry sub-humid lands. These dry land zones are spread across all continents, but are found most predominantly in Asia and Africa (WRI, 2002)

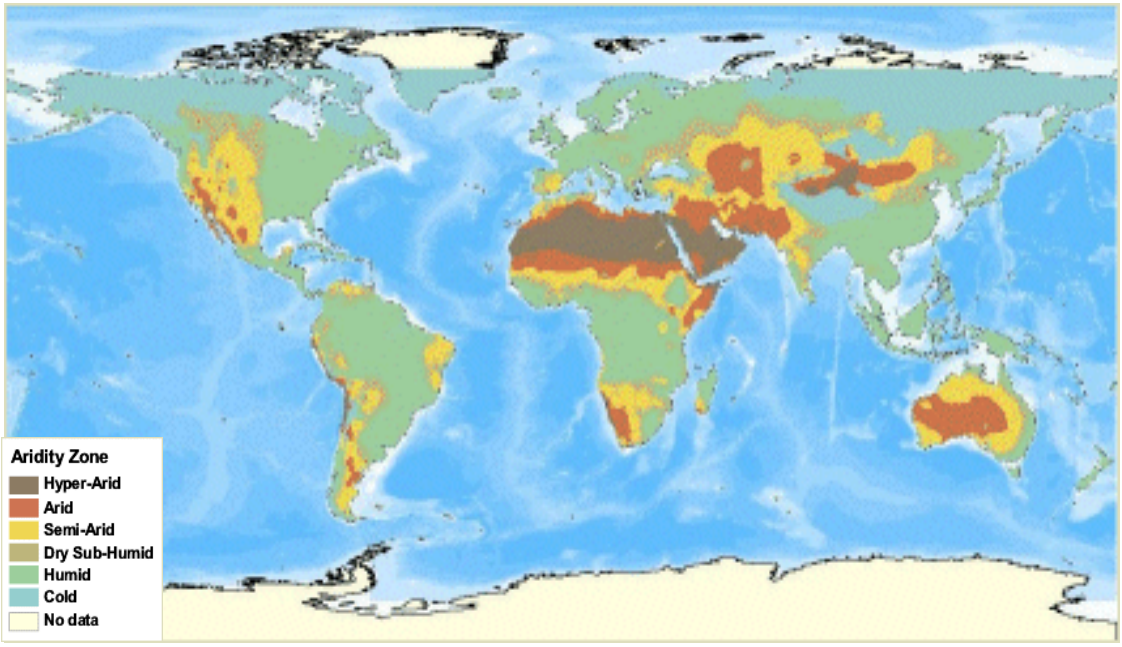

Figure 1.1 Map showing the arid zones (WRI, 2002)

In arid climates, limited water resources for crop production and industrial and domestic use present a critical factor that affects development. Such issues are vital in most arid regions including the Southwestern part of United States, the

western coast of South America, Northern Africa, the Arabian Gulf, Australia, and Northern China (**Figure 1.1**).

Aridity in climate terms relates principally to paucity of precipitation, which in turn dictates the opportunity for groundwater recharge and the sustainability of naturally occurring groundwater resources. The sporadic distributions, frequencies, intensities, and amounts of precipitation that characterize the very low precipitation areas of the world inherently constrain recharge opportunity and, coupled with ground conditions, result in very complex and little-understood recharge processes. The simplistic boundary between arid and semi-arid reflects the onset of opportunity for direct recharge to occur as precipitation increases above 200 mm per annum (Goosen and Shayya, 1999)

In particular, the Arabian countries lack permanent and renewable surface water resources such as streams and lakes because they lie within the arid belt of the earth. The people of these countries are depending on groundwater (from both shallow and deep aquifers), and a small number of springs. The two latter resources are being seriously depleted at present as a result misuse, excessive pumping and poor maintenance. Because of the large volume needed for domestic, agriculture and other purposes. Groundwater is being depleted which means that these countries are facing a real water shortage problem. Currently, they are also using desalinated water however the high cost of its production.

Generally the majority of countries in arid and semi-arid regions depend either on groundwater (from both shallow and deep aquifers) or on desalinization for their water supply, both of which enable them to use water in amounts far exceeding the estimated renewable fresh water in the country (IPCC, 1997). However, there are some important water-related problems in these countries are the depletion of aquifers in several areas, saline-water intrusion problems, and water quality problems such as those associated with industrial, agricultural, domestic activities as well as human effect. Flash floods are infrequent, but extremely damaging and represent a threat for human lives stability and their

infrastructure, especially with the effect of regional climatic change all over the world. The Arabian Peninsula as an arid to semi-arid region is suffering from low rainfall and high temperatures in addition to a high humidity in the coastal areas. Water resources are so limited, yet the availability of a sufficient supply of high quality water is the major requirement for social, industrial, agricultural and economic development of the region.

Thorough the prescribed information and explanation about the severe situation of water resources paucity and flash flood threat in arid regions, it is recommended that effective water management, utilization of wadi surface flow and appropriate decision support systems, including modeling tools based on the availability of the data, as well as of their analysis are urgently needed.

1.2. PROBLEMS STATEMENT AND RESEARCH OBJECTIVES

More than one third of the world areas are suffering from aridity conditions. The current situation of arid regions are represented in three main problems; hydrological modeling problems due to the data deficiency and data accuracy where the data in arid regions are rare and it is not complete as well as not accurate because of the lack of new technologies in most of these areas. The second problem is the water resources shortage in arid areas. Both of subsurface and surface water are the main water resources for human kind use but in arid regions, the available surface water is infrequently occurred due to the paucity and high variability of rainfall events. Additionally, the subsurface water is so important but it has some quality problem or aquifers depletion due to the misuse strategies.

The third problem is, most of arid regions are suffering from the aridity conditions all the year except during the infrequent rainfall events which almost they will be in the form of flash flood which is highly devastating for human life and their properties as shown in the chart diagram of **Figure 1.2**

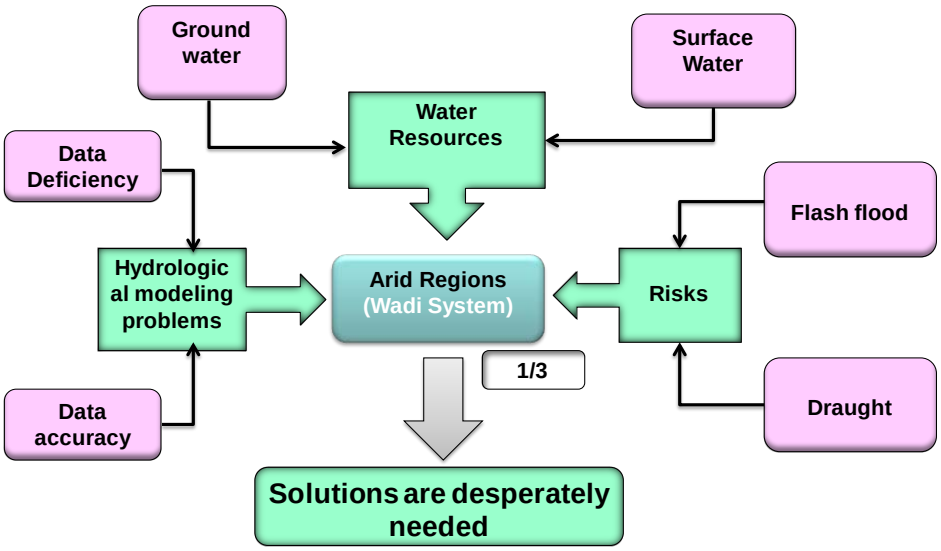

Figure 1.2 Chart diagram showing main problems of arid regions.

Furthermore, the scarcity of data and the lack of high quality observations as well as the potentially discontinuous occurrence of flow in both space and time are important characteristics of the ephemeral streams in the arid regions and consequently the difficulty of developing the powerful hydrological models. All these problems present practical difficulties in arid areas for water resources planning, development, management studies, and developing the powerful rainfall-runoff physical-based hydrological models.

Wheater et al. (1997) and Telvari et al. (1998) stated that surface water and groundwater interactions depend strongly on the local characteristics of the underlying alluvium and the extent of their connection to, or isolation from, other aquifer systems. Transmission losses in semiarid watersheds raise important distinctions about the spatial and temporal nature of surface water–groundwater interactions compared to humid basins. Transmission losses can be limited to brief periods during runoff events and to specific areas associated with the runoff production and downstream routing (Boughton and Stone, 1985). Walters (1990) and Jordan (1977) provided the evidence that the rate of loss is linearly related to the volume of surface discharge. Andersen et al. (1998) showed that losses are high

when the alluvial aquifer is fully saturated, but are small once the water table drops below the surface. Sorman and Abdulrazzak (1993) provided an analysis of groundwater rise due to transmission loss for an experimental reach in wadi Tabalah, South west of Saudi Arabia and they stated that about average 75% of bed infiltration reaches the water table.

Much high quality research is needed, particularly to investigate processes such as spatial rainfall, and infiltration and groundwater recharge from ephemeral flows. New approaches to flood simulation and management are required because it represents the most important characteristics of arid areas. Also, effective water management, utilization of wadi surface flow and appropriate decision support systems, including modeling tools based on the availability of the data, as well as of their analysis are urgently needed.

With regard to the aforementioned problems of arid and semi-arid regions, the objectives of this work are as follows:

1) To develop a physically-based distributed hydrological model to overcome the prescribed struggles for wadi runoff and flash flood simulation
2) This study aims to propose a homogenization method of upscaling hydrological parameters related to a distributed runoff model from microscopic aspects up to macroscopic ones. Homogenization is a mathematical method that allows us to upscale differential Equations. The essential idea of homogenization is to average inhomogeneous media in some way in order to capture global properties of the medium.
3) To present a consistency of empirical and physical methodology to estimate the initial and transmission loss in wadi basins, throughout the empirical approaches with the physical approaches have been connected to develop a new methodology for this purpose
4) To evaluate the initial and transmission loss and its effect on both surface and subsurface water due to its importance in the hydrological processes in arid

regions because it is considered one effective factor on the interaction between surface and subsurface water.

5) To understand distributed wadi runoff behaviors in space and time throughout a comparative study between some Arabian wadi basins. The comparison between such wadi basins is focusing on the effect of topographical conditions of the catchments, the difference of degree of urbanization, the difference of basin's scales or shapes, the difference of total amounts of rainfall or rainfall duration in the upstream and mountainous areas, the difference of soil permeability on the river channels, and the difference of mitigation strategies for flash floods in wadi basins.
6) To simulate flash floods using Satellite Remote Sensing Data to overcome the paucity of data in such regions and its threat on the human life and their properties.
7) To assess and evaluate the contribution of wadi basins to the Nile River which is representing the main water resource for Egypt and the other sharing countries, so the advantage of this research is considering additional water resources from flash flood in wadi basins.

1.3. THESIS STRUCTURE AND ORGANIZATION

The thesis consists of six chapters concerning wadi system runoff modeling and flash flood simulation and it contains a detailed description of analytical approaches of numerical simulation of wadi runoff and flash flood as well as their applications on different arid and semi-arid regions as summarized in the flow chart (**Figure 1.3**).

The first chapter is an introduction about wadi basins and their problems, it consists of three categories, the first is motivation and background of the current research, the second one is discussing the problem of wadi system as well as the

objectives which are needed to be accomplished, the last part is the thesis organization.

The second chapter presents some important features of wadi basin in arid and semi-arid regions which play a vital role in the formation of surface flow and subsurface. Moreover, it contains outcome of field survey for wadi basins in Egypt. Some of the geomorphologic features take part in the estimation of surface runoff discharge that results after each storm rainfall. It is well known that surface vegetation and forest cover are so rare but the geological features such as rock outcrops and geomorphologic characteristics are characterized to wadi basins and they are so important for the hydrological process and water resources there.

In the third chapter, the developed physically-based hydrological approaches which have been used in this research are introduced and discussed, the Hydrological River Basin Environmental Assessment Model (Hydro-BEAM), a homogenization method of upscaling hydrological parameters related to a distributed runoff model from microscopic aspects up to macroscopic ones, and developing a physically based approach to estimate initial and transmission loss in wadi basin are presented and discussed.

In the forth chapter, the numerical simulation of wadi runoff is carried out as well as discussion of its results. The hydrological approaches are applied on some Arabian wadi basins to understand the flow characteristics and the factors affecting on its behaviors. Moreover, the target wadi basins of wadi Alkhoud in Oman, wadi Ghat in Saudi Arabia, and wadi Assiut in Egypt are discussed as examples of application due to their importance not only as water resources but also as vulnerable wadis for flash flood occurrence.

The fifth chapter is devoted to explain the flash floods simulation using remote sensing data. The availability of data and the feasibility of use satellite remote sensing data have been discussed. The Global Satellite Mapping of Precipitation (GSMaP) is validated and compared with the Global Precipitation Climatology Center (GPCC) as gauge-based gridded monthly precipitation data sets for the

global land surface for the purpose of evaluate the possibility of use the near real time data of GSMaP product to predict the flash flood in arid regions. Furthermore, the simulation of flash flood for different events is performed in the Nile River and wadi El-Arish, Sinai Peninsula, Egypt as the target basins of application.

The sixth chapter summarizes the overall results and the major conclusions drawn from the present research, presents some recommendations for future research and discusses the advantages and findings from this study.

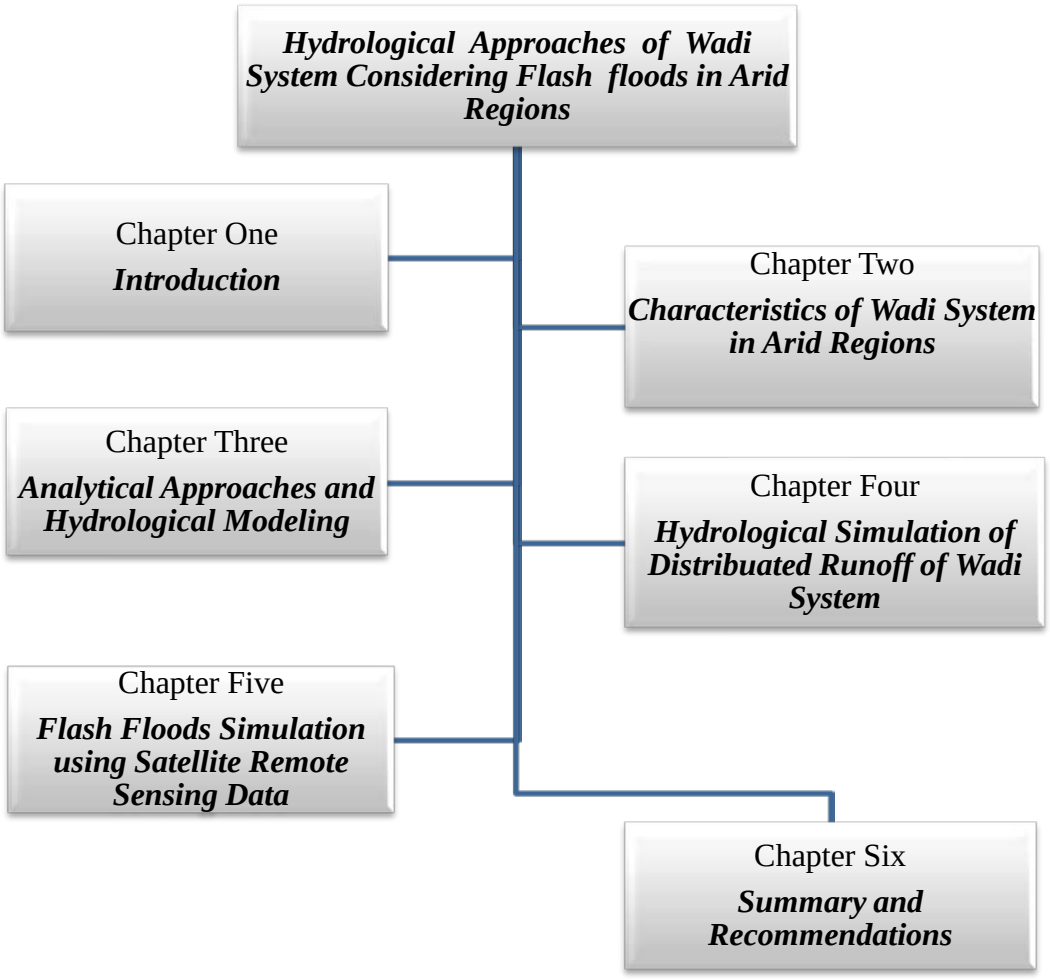

Figure 1.3 Flow chart showing framework of thesis organization

Chapter Two

Characteristics of Wadi System in Arid Regions

2.1. Introduction

The geomorphologic features take part in estimation of surface runoff discharge that results after each storm rainfall. It is well known that surface vegetation and forest cover are so rare but the geological features such as rock outcrops, and geomorphologies are characterized to wadi basins and they are so important for the hydrological process and water resources.

In arid regions, water is one of the most challenging current and future natural-resources issues. The importance of water in arid regions is self-evident indeed obviously. Water is not only the most precious natural resource in arid regions but also the most important environmental factor of the ecosystem. Arid and semi-arid regions of the world are characterized by the expanding populations, increasing per capita water use, and limited water resources as well as draught and flash flood thread. The most obvious characteristics in the ephemeral streams in arid areas are the initial and transmission losses in addition to discontinuous occurrence of flow in both space and time.

Desert is an alternative term can be used to describe arid or dry lands. Many deserts are formed by rain shadows that are mountains blocking the path of precipitation to the desert (on the lee side of the mountain). Deserts contain valuable mineral deposits that were formed in arid environment or that were exposed by erosion. Due to extreme and consistent dryness, some deserts are ideal places for natural preservation of artifacts and fossils. The largest ten deserts are

listed in **Table 2.1** (web link: **http://en.wikipedia.org/wiki/Desert#cite_note-usgs-0**). Antarctica is the world's largest cold desert (composed of about 98 percent thick continental ice sheet and 2 percent barren rock). The largest hot desert is the Sahara in northern Africa, covering 9 million square kilometers and 12 countries.

Table 2.1 The 10 largest deserts of the world

The 10 largest deserts			
Rank	Desert	Area (km^2)	Area (mi^2)
1	Antarctic Desert (Antarctica)	13,829,430	5,339,573
2	Arctic	13,700,000	5,300,000
3	Sahara (Africa)	9,100,000	3,320,000
4	Arabian Desert (Middle East)	2,330,000	900,000
5	Gobi Desert (Asia)	1,300,000	500,000
6	Kalahari Desert (Africa)	900,000	360,000
7	Patagonian Desert (South America)	670,000	260,000
8	Great Victoria Desert (Australia)	647,000	250,000
9	Syrian Desert (Middle East)	520,000	200,000
10	Great Basin Desert (North America)	492,000	190,000

2.2. Geomorphology

A significant fraction of the Earth's land surface can be described as arid. This is primarily a climatic term, implying lower rainfall and distinctive vegetation adapted to the scarcity of water. Much of the arid terrains can also be called deserts. Deserts do not necessarily consist mainly of sand; some are mountainous but with usually well exposed rocks and thinner soils (**Figure 2.1**) (http://geology.com/records/sahara-desert-map.shtml).

Many landforms characterize arid regions and the major types of dunes are as follows: a) Crescentic dune; b) linear or longitudinal dune; c) star dune; d) parabolic dune; e) dome dune.

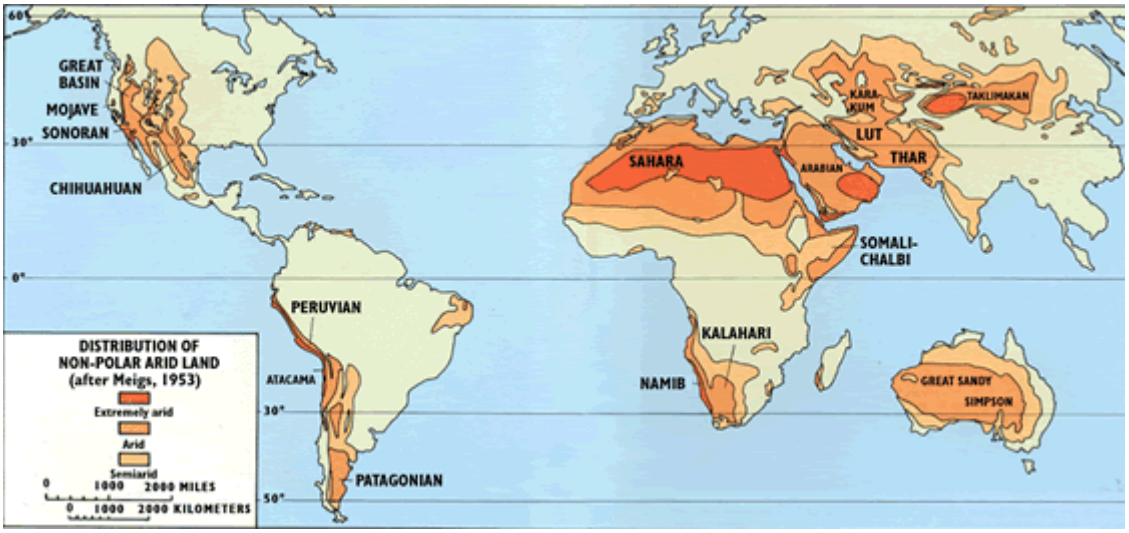

Figure 2.1 World desert map (http://geology.com/records/sahara-desert-map.shtml).

2.3. Climatic Conditions

2.3.1 Rainfall Patterns

Rainfall is the primary hydrological input, but rainfall in arid and semi-arid areas is commonly characterized by extremely high spatial and temporal variability. The temporal variability of point rainfall is well known. Annual variability is marked and observed daily maxima can exceed annual rainfall totals (Wheater et al., 2008). Rainfalls can be summarized as follows: Where rainfall is very variable in space and time. One storm event can be very high where, in many cases, the single storm rainfall exceeds the mean annual rainfall. Most of sediment yield could be greatly formed and increased during the high rainfall intensity. Due to the scarcity of vegetation the formation of sediment transportation is so high during the rainfall event. Spatial variability is directly related to the local and regional topography. At high elevations topographic rainfall occurs, and this happens especially if surface water and nearby escarpments, cliffs, or high hills extend within 150 to 200 km (i.e. distribution or horizontal extension). The

rainfall initiation and intensity is augmented due to windy storms prior to rainfall, which makes the nucleus of condensation. At times, even though the moist air is available, in the absence of winds the rainfall does not occur. This is one of the main reasons for spatial and temporal variation of rainfall in arid regions. On the other hand, summer monsoon rainfalls, primarily from tropical storms and convectional thunderstorms, represent about 20 to 30% of the total annual rainfall in the coastal plains. Over the highlands (more than 1,000 m elevation), it represents only 80% of the total rainfall (Zen, 2008)

The rainfall that falls from the atmosphere at a particular location is either intercepted by trees, shrubs, and other vegetation, or it strikes the ground surface and becomes overland flow, subsurface flow, and groundwater flow. Regardless of its deposition, much of the rainfall eventually is returned to the atmosphere by evapotranspiration processes from the vegetation or by evaporation from streams and other bodies of water into which overland, subsurface, and groundwater flow move (FAO, 1989).

The mountains have elevations of up to 3000 m a.s.l., hence the basins encompass a wide range of altitude, which is matched by a marked gradient in annual rainfall, from 30 to 100mm on the Red Sea coastal plain to up to 450mm at elevations in excess of 2000 m a.s.l. (Wheater et. al, 2008)

Unlike conditions in temperate regions, the rainfall distribution in arid zones varies between summer and winter. For example, in some Arabian countries as Morocco and Egypt, receives rain during the cold winter period, while the warm summer months are almost devoid of rainfall. On the other hand, some others like Sudan, has a long dry season during the winter, while the rains fall during the summer months (FAO 1989).

Rainfall also varies from one year to another in arid zones; this can easily be confirmed by looking at rainfall statistics over time for a particular place. The difference between the lowest and highest rainfall recorded in different years can be substantial, although it is usually within a range of ± 50 percent of the mean

annual rainfall (FAO 1989).

For other arid or semi-arid areas, rainfall patterns may be very different. For example, data from arid New South Wales, Australia have indicated spatially extensive, low intensity rainfalls (Cordery et al., 1983), and recent research in the Sahelian zone of Africa has also indicated a predominance of widespread rainfall. This was motivated by concern to develop improved understanding of land-surface processes for climate studies and modeling, which led to a detailed (but relatively short-term) international experimental program of the HAPEX-Sahel project based on Niamey, Niger (Goutorbe et al., 1997). Although designed to study land surface/atmosphere interactions, rather than as an integrated hydrological study, it has given important information. For example, Lebel et al. (1997) and Lebel and Le Barbe (1997) note that a 100 rain gauge network was installed and reported the information on the classification of storm types, spatial and temporal variability of seasonal and event rainfall, and storm movement. Of total seasonal rainfall, 80 % was found to fall as widespread events which covered at least 70%of the network.

The Arabian Peninsula, in keeping with its location in one of the greatest desert belts of the world, has a low and irregular rainfall, typically less than 150 mm/yr. It can be as low as 50 mm in the northern and central parts of the Arabian Gulf area. As the region receives little benefit from barometric depressions during the summer months, it is not surprising that large areas have low rainfall, in the range of 100-300 mm/year. The lower the precipitation, the greater its variability, in Bahrain, for example, the average annual rainfall is 76 mm, but ranges between 10 mm and 170 mm. Only the Arabian Sea coast benefits to even a limited extent from the passage of the monsoon. Climate is modified by regional factors including the distribution of land/water, the local topography, particularly the location of mountains. The Oman Mountains and the A1 Hijaz Mountains of Yemen and Saudi Arabia provide a good example. Rainfall is less than 100 mm in Saudi Arabia, but sometimes exceeds 200 mm in Oman, where ice may be

expected in the higher elevations during winter (Alsharhan et.al, 2001).

2.3.2 Temperature and Evaporations

The climatic pattern in arid zones is frequently characterized by a relatively "cool" dry season, followed by a relatively "hot" dry season, and ultimately by a "moderate" rainy season. In general, there are significant diurnal temperature fluctuations within these seasons. Quite often, during the "cool" dry season, daytime temperatures peak between 35 and 45 centigrade and fall to 10 to 15 centigrade at night. Daytime temperatures can approach 45 centigrade during the "hot" dry season and drop to 15 centigrade during the night. During the rainy season, temperatures can range from 35 centigrade in the daytime to 20 centigrade at night. In many situations, these diurnal temperature fluctuations restrict the growth of plant species. Growth of plants can take place only between certain maximum and minimum temperatures. Extremely high or low temperatures can be damaging to plants. Plants might survive high temperatures, as long as they can compensate for these high temperatures by transpiration, but growth will be affected negatively. High temperatures in the surface layer of the soil result in rapid loss of soil moisture due to the high levels of evaporation and transpiration (FAO, 1989).

2.3.3 Atmospheric Humidity

Although rainfall and temperature are the primary factors upon which aridity is based, other factors have an influence. The moisture in the air has importance for the water balance in the soil. When the moisture content in the soil is higher than in the air, there is a tendency for water to evaporate into the air. When the opposite is the case, water will condense into the soil. Humidity is generally low in arid zones. In many areas, the occurrence of dew and mist is necessary for the

survival of plants. Dew is the result of condensation of water vapor from the air onto surfaces during the night, while mist is a suspension of microscopic water droplets in the air. Water that is collected on the leaves of plants in the form of dew or mist can, at times, be imbibed through the open stomata, or alternatively, fall onto the ground and contribute to soil moisture. The presence of dew and mist leads to higher humidity in the air and, therefore, reduced evapotranspiration and conservation of soil moisture (FAO, 1989).

Low humidities increase the atmospheric demand for moisture and have been found to cause partial to full stomatal closure in plants, resulting in reduced transpiration, photosynthesis and plant productivity (Korner and Bannister, 1985; Choudhury and Monteith, 1986). Over longer temporal scales, humidities may influence plant evolutionary adaptations such as leaf area and cuticle thickness (Grantz, 1990). These factors influence soil moisture and runoff at local scales and may influence precipitation and atmospheric circulation patterns at regional to global scales (Hansen et al., 1984).

2.3.4 Wind

Because of the scarcity of vegetation that can reduce air movements, arid regions typically are windy. Winds remove the moist air around the plants and soil and, as a result, increase evapotranspiration. Soil erosion by wind will occur wherever soil, vegetative, and climatic conditions are conducive to this kind of erosion. These conditions (loose, dry, or fine soil, smooth ground surface, sparse vegetative cover, and wind sufficiently strong to initiate soil movement) are frequently encountered in arid zones. Depletion of vegetative cover on the land is the basic cause of soil erosion by wind. The most serious damage from wind-blown soil particles is the sorting of soil material; wind erosion gradually removes silt, clay, and organic matter from the surface soil. The remaining materials may be sandy and infertile. Often, sand piles up in dunes and present a serious threat to

surrounding lands.

2.3.5 Aridity Index

Arid environments are extremely diverse in terms of their land forms, soils, fauna, flora, water balances, and human activities. Because of this diversity, no practical definition of arid environments can be derived. However, the one binding element to all arid regions is aridity. Aridity is usually expressed as a function of rainfall and temperature. A useful "representation" of aridity is the following climatic aridity index: p/ETP, where P = precipitation and ETP = potential evapotranspiration, calculated by method of Penman, taking into account atmospheric humidity, solar radiation, and wind (FAO 1989).

Three arid zones can be delineated by this index: namely, hyper-arid, arid and semi-arid. Of the total land area of the world, the hyper-arid zone covers 4.2 percent, the arid zone 14.6 percent, and the semiarid zone 12.2 percent. Therefore, almost one-third of the total area of the world is arid land. The hyper-arid zone (arid index 0.03) comprises dryland areas without vegetation, with the exception of a few scattered shrubs. Annual rainfall is low, rarely exceeding 100 millimeters. The rains are infrequent and irregular, sometimes with no rain during long periods of several years. The arid zone (arid index 0.03-0.20) is characterized by no farming except with irrigation. For the most part, the native vegetation is sparse, being comprised of annual and perennial grasses and other herbaceous vegetation, and shrubs and small trees. There is high rainfall variability, with annual amounts ranging between 100 and 300 millimeters (FAO 1989).

The semi-arid zone (arid index 0.20-0.50) can support rain-fed agriculture with more or less sustained levels of production. Native vegetation is represented by a variety of species, such as grasses and grass-like plants, fortes and half-shrubs, and shrubs and trees. Annual precipitation varies from 300-600 to 700-800

millimeters, with summer rains, and from 200-250 to 450-500 millimeters with winter rains. Arid conditions also are found in the sub-humid zone (arid index 0.50-0.75). The term "arid zone" is used here to collectively represent the hyper-arid, arid, semi-arid, and sub-humid zones (FAO, 1989).

Also, a drought is a departure from average or normal conditions in which shortage of water adversely impacts on the functioning of ecosystems, and the resident population of people, whereas aridity refers to the average conditions of limited rainfall and water supplies, not to the departures there from. In general, arid zones are characterized by pastoralism and little farming but there are always exceptions (Malhotra, 1984).

Many aridity and semi-aridity definitions appeared in the literature but none can be entirely satisfactory, and the terms of arid and semi-arid remain somewhat imprecise and vague. Generally, the aridity implies that rainfall does not support regular rainfed farming. According to Walton (1969) this definition encompasses all the seasonally hot arid and semi-arid zones classified by means of rainfall, temperature, and evaporation indices. Among the aridity indices, those based on rainfall only state that any duration without rainfall for 15 consecutive days is considered a dry period. In some regions, 21 days or more with rainfall less than one-third of normal is considered as a dry period. There are also percentage-dependent indices such as in the case of annual rainfall less than 75% and monthly rainfall less than 60% of normal (normal rainfall on any given day is typically taken to mean the average of all the observed rainfall events on a particular date.) . However, in an individual case, any rainfall less than 85% is also considered a dry case (Zen, 2008).

A simple quantitative aridity index, A_i, measure of a region is defined as the rainfall amount per temperature degree.

$$A_i = \frac{\overline{R}}{\overline{T}} \tag{2.1}$$

where, $\overline{R}$ and $\overline{T}$ are the average monthly rainfall and temperature values, respectively. Generally, it takes values around 1. The greater the aridity index, the higher the rainfall amount associated with low temperatures. Hence, big aridity indices correspond to better groundwater recharge possibilities.

An aridity index (AI) is a numerical indicator of the degree of dryness of the climate at a given location. A number of aridity indices have been proposed in Table 2.2; these indicators serve to identify, locate or delimit regions that suffer from a deficit of available water, a condition that can severely affect the effective use of the land for such activities as agriculture or stock-farming. More recently, the UNEP has adopted yet another index of aridity (UNEP, 1992), defined as:

$$AI_U = \frac{P}{PET} \tag{2.1}$$

where, *PET*, is the potential evapotranspiration, and *P* is the average annual precipitation. Here also, *PET* and *P* must be expressed in the same units, *e.g.*, in millimeters. In this latter case, the boundaries that define various degrees of aridity and the approximate areas involved are as described in **Table 2.2**:

Table 2.2 Classification of dry lands based on Aridity index

Classification	Aridity Index	Global land area
Hyper-arid	AI < 0.05	7.5%
Arid	0.05 < AI < 0.20	12.1%
Semi-arid	0.20 < AI < 0.50	17.7%
Dry sub-humid	0.50 < AI < 0.65	9.9%

2.4. Arid Zone Soils and Importance of Soil Properties

Soils are formed over time as climate and vegetation act on parent rock

material. Important aspects of soil formation in an arid climate: 1- Significant diurnal changes in temperature, causing mechanical or physical disintegration of rocks. 2- Wind-blown sands that score and abrade exposed rock surfaces. The physical disintegration of rocks leaves relatively large fragments. It is only chemical weathering which can break up these fragments. The process of chemical weathering in arid zones is slow because of the characteristic water deficit. Also, extended periods of water deficiencies are important in the elimination or leaching of soluble salts, for which the accumulation is enhanced by the high evaporation. Short periods of water runoff do not permit deep penetration of salts (only short-distance transport), often resulting in accumulation of salts in closed depressions. Vegetation plays a fundamental role in the process of soil formation by breaking up the rock particles and enriching the soil with organic matter from aerial and subterranean parts. However, this role of the vegetation is diminished in arid zones because of the sparse canopy cover and the limited development of aerial parts. Nevertheless, the root systems often exhibit exceptional development and have the greatest influence on the soil.

2.5. Vegetation in arid zone

The vegetation cover in arid zones is scarce as shown in **photo 2.1.** Its growth is restricted to a short wet period. In general, the vegetation cover is small in size, has shallow roots, and their physiological adaptation consists of their active growth.

The dynamics of vegetation in regions of drifting sand have been studied primarily on the coastal dunes of temperate regions (Willis et al., 1959). The literature related to the adaptation of plants to the movement of sand in arid regions is much less abundant. For instance, Bowers (1982) has indicated adaptations of species to the dune environment in the U.S.A., especially the elongation of stems and roots. Dittmer (1959) also noted such adaptations in roots.

2.6. Initial and transmission losses

Initial losses occur in the sub-basins before runoff reaches the stream networks, whereas transmission losses occur as water is channeled through the valley network. Initial losses are related largely to infiltration, surface soil type, land use activities, evapotranspiration, interception, and surface depression storage. Transmission losses are important not only with respect to their effect on stage flow reduction, but also to their effect as recharge to groundwater of alluvial aquifers. It was suggested that two sources of transmission losses could be occurring, direct losses to the wadi channel bed, limited by available storage, and losses through the banks during flood events as shown in **Figure 2.2**.

The rate of transmission loss from a river reach is a function of the characteristics of the channel alluvium, channel geometry, wetted perimeter, flow characteristics, and depth to groundwater. In ephemeral streams, factors influencing transmission losses include antecedent moisture of the channel alluvium, duration of flow, storage capacity of the channel bed and bank, and the content and nature of sediment in the stream flow. The total effect of each of these factors on the magnitude of the transmission loss depends on the nature of the stream, river, irrigation canal, or even rill being studied (Vivarelli and Perera, 2002).

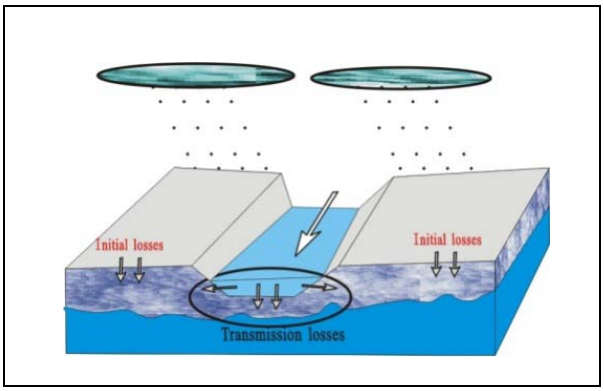

Figure 2.2 Conceptual model showing transmission and initial losses in the Wadi System

Transmission losses in semiarid watersheds raise important distinctions about the spatial and temporal nature of surface water–groundwater interactions compared to humid basins. Because of transmission losses, the nature of surface water–groundwater interactions can be limited to brief periods during runoff events and to specific areas associated with the runoff production and downstream routing (Boughton and Stone, 1985). Walters (1990) and Jordan (1977) provided evidence that the rate of loss is linearly related to the volume of surface discharge. Andersen et al. (1998) showed that losses are high when the alluvial aquifer is fully saturated, but are small once the water table drops below the surface.

Sorman and Abdulrazzak (1993) provided an analysis of groundwater rise due to transmission loss for an experimental reach in Wadi Tabalah, S.W. Saudi Arabia and they stated that about average 75% of bed infiltration reaches the water table.

Surface water–groundwater interactions in arid and semi-arid drainages are controlled by transmission losses. In contrast to humid basins, the coupling between stream channels and underlying aquifers in semiarid regions often promotes infiltration of water through the channel bed, i.e. channel transmission losses (Boughton and Stone, 1985; Stephens, 1996; Goodrich et al., 1997). The relationship between the wadi flow transmission losses and groundwater recharge depend on the underlying geology. The alluvium underlying the wadi bed is effective in minimizing evaporation loss through capillary rise (the coarse structure of alluvial deposits minimizes capillary effects). Wheater et al. (1997) and Telvari et al. (1998) stated that surface water and groundwater interactions depend strongly on the local characteristics of the underlying alluvium and the extent of their connection to, or isolation from, other aquifer systems. Sorey and Matlock (1969) reported that measured evaporation rates from streambed sand were lower than those reported for irrigated soils.

2.6.1. Water Resources in the Arid Regions.

Water resources in the arid and semi-arid regions are limited. For instance, groundwater is the most important resource, desalinated water, and some perennial streams in some regions. However, the quality and quantity of them are inadequate to cover the current needs for domestic, agricultural, manufacturing and economic use in such arid areas. In the Arabian countries as Saudi Arabia, Oman, and Egypt, they depend mainly on the ground water as the main water resources, it is likely that the groundwater aquifers be contaminated and affected by the sea water intrusion.

In the Arabian Peninsula, groundwater accounts for 40-98% of the total freshwater resource. Of the meagre rainfall 1-10% becomes available as soil moisture and ends up nourishing economic crops (Rogers and Lydon, 1994; Abdel Magid, 1995). Thus, in a region where water is in short supply, it is imperative that a coherent policy be established through a system of permits, regulations and standards to ensure supplies for sustainable development as a basis from which water supplies can be successfully managed.

The purpose of such policy is not only to provide an adequate supply of water both in quality and quantity to meet current needs, but one which is adaptable to, and anticipates future needs. It has to be recognized that freshwater is a finite resource as the average yield from the hydrological cycle, a natural capital asset requiring maintenance to sustain the desired services, but one which cannot meet the demands placed upon it. Human activities can reduce the availability and quality through the mining of groundwater, and the pollution of surface and groundwater, changing land use (deforestation, afforestation, urbanization), the temporal and spatial variability of flow and the planned re-use of return flow (Alsharhan et.al, 2001).

2.6.2. Water Resources in Saudi Arabia

The agriculture in Saudi Arabia depends mainly on groundwater for rain-supported agriculture which is limited to parts of the southwestern part of the country. The water sources in Saudi Arabia summarized in the following: The rainfall in Saudi Arabia exhibits a wide variation in space and time. Occasional heavy and short rainstorms cause floods in soil-rich wadi channels. To control floodwater the Ministry of Agriculture and Water has constructed more than 190 dams of variable sizes and storage capacities. The total storage capacity of dams in Saudi Arabia is 850 Mm^3. These dams are intended to retain floodwater for irrigation and recharging aquifers. After proper treatment, floodwater can be also used for domestic and drinking purposes (Alsharhan et.al, 2001).

Spring waters are used for irrigation in areas such as A1 Hofuf, A1 Qatif and A1 Aflaj. A small number of springs exist in the western region of Saudi Arabia and their water is mainly used for drinking. Both shallow (5 to 50 m) and deep (50-2000 m) aquifers are utilized in Saudi Arabia. Groundwater in the shallow aquifers seems to be renewable as parts of rainwater and occasional floods may recharge them. Groundwater satisfies about 70% of water needs in Saudi Arabia and the number of drilled wells has reached over 78,000m in 1995.

The Saudi Arabia is the largest producer of desalinated water in the world. This is attributed to the steadily rising demands for water in the country as a result of population growth and rising standard of living. The industrial and urban development also need additional water resources. Several recent desalination plants were constructed and pipelines from these plants were extended to areas of use. Twenty-three desalination plants built by 1995 supply the water needs of 40 cities and villages along the eastern and western coasts of Saudi Arabia (Alsharhan et.al, 2001).

2.6.3. Water Resources in Oman

Oman realized the importance of water and initiated the Ministry of Water Resources in 1994. The ministry responsibilities include research studies, evaluation and quality of water in Oman and the producing aquifers. Groundwater is the main source of water used for irrigation, domestic purposes and drinking in Oman. The total number of wells tapping both shallow and deep groundwater in Oman is more than 167,000. These wells produce about 56% of water used for irrigation. Falajes represent one of the oldest irrigation technologies developed by Omani people hundreds of years ago.

The falaj waters meet 40% of the irrigation needs. The individuals who have constructed them or their families own the falajes. The falaj water is distributed among owners on an accurate time-share basis. The Ministry of Agriculture and Fisheries fix and maintain falaj systems all over the country. The falajes of Oman are classified into two main types; Daudi and Gheli. The Daudi falajes represent 80% of the falajes used for irrigation in Oman. These falajes are subsurface tunnels constructed to transfer groundwater from the foothills of mountains, where the water table is usually shallow, to farms further away from the mountains. Retention dams are very important in Oman. Dams are constructed to retain rainwater before it reaches the Gulf of Oman. Oman constructed 4 dams of a total storage capacity of 46 Mm^3. Oman is the least dependent on desalinated water of the Gulf States.

The production of the water desalination plants in Oman reached 5 Mm^3 in 1995. Sewage treated water is used for irrigation of green areas, gardens, parks and roundabouts. The sewage treatment plants in Oman produce 60,000 gallons/day (Alsharhan et.al, 2001).

2.6.4. Water Resources in Egypt

Egypt lies in an arid belt of North Africa, where annual rainfall reduces from 200 mm/year near the Mediterranean coasts, to zero at near Cairo. It is also the most downstream country in the Nile River Basin and does not contribute to its water. The Nile runs as a single channel with no tributaries when it enters the Egyptian borders up to the north of Cairo where it divides into two branches. Since, ancient times the Egyptians have realized the need to control the Nile as a single source of water. Socio-economic development and increases in water demand over the past century mandated the search for other water resources and better management of the Nile water. Currently the balance between the available and required water in Egypt is fragile. Any movement away from the balancing point means either less ambitious economic development or depletion of the resources and degradation of the environment. Water resources of Egypt are classified into two major categories: (a) conventional; and (b) non-conventional. Conventional water resources are further classified into renewable water (Nile water and groundwater in the Nile Delta and the Nile Valley) and non renewable (deep or fossil groundwater). Non-conventional water resources include treated waste water, desalinated water, and recycled drainage water. The other side of the water resources system is water use. The agricultural sector is the major water consumer in Egypt; it uses approximately 85% of the total consumption. The other 15% is distributed between domestic and industrial sectors while the navigation and hydropower sectors are considered as non-consumptive uses of water.

2.6.5. Water Resource Assessment

In the arid region, the water supply cannot be maintained by the uncontrolled extraction of groundwater, even with the use of all other available water resources, such as desalination and treated wastewater. In the absence of an established

policy, water shortage will be expected, which can largely be attributed to the agricultural demands, as stated above. Over much of the region, the seasonal rainfall is small in quantity, so that water harvesting is seldom a viable option. In the absence of running water, except on the rare occasions of floods following rainstorms, the assessment of available supplies, requires a basin study, of both the natural discharge and recharge areas. Technically, the geological setting, basin and aquifer extent and their hydrological properties, are required on an "ongoing" basis, since some factors may change with time and in space. The basic hydrological data cover precipitation, evaporation, surface runoff drainage patterns, topography and soil studies, groundwater flow and the hydraulic conditions of groundwater flow, transmission storage and leakage.

The assessment of water resources can be considered in four phases as summarized by (Alsharhan et.al, 2001): i) The first phase is an inventory of all wells with the relevant technical data as depth, movement of the groundwater, water composition (covering both quality and quantity), and aquifer characteristics, ii) The second phase will cover conservation techniques, which include control of drilling and extraction rates, the potential of water harvesting, and the construction of underground and surface dams, iii) The third phase will be based on the knowledge derived from the water inventory to determine the cost, and some projection of present needs, and future demand, based upon an accepted growth rate, v) The final phase is the methods of increasing supply by importing water, which range from towing icebergs or water filled plastic pods to diverting river water long distances. The other means of importing water in the form of importing food, especially grain since a ton of grain requires a thousand tons of water to produce it.

2.8. Field Survey of Wadi System

Most of the arid regions are occupied with desert. Field trip of Japan Egypt

HydroNET Project under the activity of GCOE Project of Kyoto University, Disaster Prevention Research Institute has been implemented from March 23th to March 29th, 2010. During the trip, wadi basins have been surveyed along the Nile River in both Eastern and Western Deserts. The most important characteristic have been studied such as wadi channel geomorphology, vegetation, soil types, and some structures along wadis.

During our investigation at this stop of downstream of wadi, some sparse trees which is characterized by its concentration along wadi channel where the flash flood water accumulated but they are not so dense in their distribution as shown in **Photos 2.1 and 2.2**. The sediment of downstream of wadi is clay or silty-clay showing mud cracks phenomena which happen due to the dryness of deposited sediments especially mud as depicted in **Photo 2.3**. Another investigation characteristics is the sediment transportation with the flash flood water and final deposition at the outlet of wadi, for instance, last two flood events can be detected based on the sediment accumulation where two consequence thin layers of clay have been investigated imply to occurring of two events of flash flood at that wadi as shown in **Photo 2.3**.

Also, the constructed high way is built as dam for the purpose of flash flood prevention and water retention to protect the high way and recharge flash flood water to subsurface water at this region. But we think that the flow volume water should be evaluated because the vertical height of it is about 18 m (**Photo 2.4**) and may be the coming water during the strong flash flood events may be threat and damage the high way construction. Moreover, they set up small tunnels to pass the flash flood water to the other side of the wadi channel as shown in **Photo 2.5**. It is clear that in the other side the effect of water passing toward this side creating a land depression illustrated in **Photo 2.6**. In some parts in the desert, people are depending on some subsurface water by extracting some boreholes to find some water to be used for cultivation some crops or fruits as shown in **Photos 2.7 and 2.8**.

Photo 2.1 Sparse distribution of vegetation at the downstream mouth of one wadi along the Eastern Desert High Way, Egypt

Photo 2.2 Mud cracks due to the dryness of land after flash flood event at the downstream plain area of wadi, exactly in front of high way which is working as dam for flood prevention.

Photo 2.3 Two thin clay layers showing the last flash flood events at downstream area of wadi

Photo 2.4 Eastern desert High way Dam is built at the mouth of the wadi in the Eastern Desert, Egypt.

Photo 2.5 Highway as constructed Dam with small tunnels to overpass the flash flood water to the other side.

Photo 2.6 Land hall or depression which is formed due to passing of flash flood water from the upstream side of the High Way

Photo 2.7 Cultivated farms are developed in the desert depending on the available of subsurface water extraction.

Photo 2.8 Cultivated farms of Date Fruit in the Eastern Desert of Egypt; it is very famous and dominant in the Arabian countries.

Photo 2.9 Construction of new cities in the desert, Minia New City along the Eastern Desert High way, Egypt

Nowadays, the Egyptian government has started a big project for constructing and developing new cities in the desert due to the ever-increasing of population along the Nile River and Nile Delta, for example, Assiut new city, Minia New City (**Photo 2.9**), Fayoum New City, Helwan New City, etc. Those new constructed cities need new water resources and they need urgently quick and valuable water resources management and flash flood control to be comfortable for residents to live there. With that regard, hydrological modeling of wadi system considering water resources management and flash flood control in arid regions is the most optimal choice to develop such new urbanized regions and protect the human life and their properties by save the minimum base of water resources for their demand as well as from the flash flood threat which become horrible and dangerous in wadi system due to the climate change.

Further field surveying is needed for more evaluation of wadi basins hydrology considering geomorphologic, topographic, geologic properties as well as land use

and soil types to get a comprehensive view of its actual circumstances and behaviors which might be useful for developing the physical based hydrological modeling for flash flood warning system and water resources management at wadi environment not only in Egypt but also in other arid regions all over the world.

Chapter Three

Analytical Approaches and Hydrological Modeling

3.1. Introduction

As prescribed before, different modeling techniques and tools have been widely used for a variety of purposes, but almost all have been primarily developed for humid area applications. However, arid and semi-arid regions have particular challenges that have received little attention however their very severe situation of scarcity of water resources and flash flood threat. So, developing the powerful hydrological models and physical based approaches to be applied in arid regions for a variety of purposes particularly to investigate processes such as spatial rainfall, and infiltration and groundwater recharge from ephemeral flows as well as new approaches to flood simulation and management are required.

In this chapter, an attempt is made to introduce, develop and discuss different approaches which could be applied in this study at some of wadi basins. Basically, the developed and discussed methodologies are mainly relying on the physically-based hydrological conditions. A homogenization method of upscaling hydrological parameters related to a distributed runoff model from microscopic aspects up to macroscopic ones is introduced and discussed, the Hydrological River Basin Environmental Assessment Model (Hydro-BEAM) has been adopted to be applied in arid environment, and developing a physically based approach to estimate initial and transmission loss in wadi basins are presented.

3.2. Upscaling of hydrological parameters based on homogenization theory

3.2.1. Outline of homogenization

Homogenization is a mathematical method that allows us to upscale differential equations (i.e. it is a mathematical method which provides a means for upscaling of differential equations). The essential idea of homogenization is to average inhomogeneous media in some way in order to capture global properties of the medium. Also, the homogenization, instead of working with one functions u (as in the representative elementary volume), one consider a whole family of functions u^{ε} where $\varepsilon > 0$ is the spatial (length) scalar parameter (the typical size of pore). The work with homogenization consists of determining the limit and considering this limit as the result of the upscaling procedure (**Figure 3.1**). On other words, it consists of finding the differential equations in which the limit u satisfies this formula (3.1) (Hornung. 1997).

$$u = \lim_{\varepsilon \to 0} u^{\varepsilon} \tag{3.1}$$

The scale at which the properties can be considered as homogeneous is called Representative Elementary Volume (REV). The representative elementary volume (REV) means that for any function u describe a domain which describes a certain physical quantity such as cell length (x is small) and the point x is one of several hundred of cells in REV, if this function reflect the behavior of a physical quantity as ‘’microscale’’ (pore scale), the averaged function is supposed to describe its properties on a larger scale ‘macroscale’). The basic difference between the two methodologies: the REV approach uses smoothing and spatial averaging formulas, but homogenization does the upscaling by letting the microscale tend to zero (**Figure 3.1**), this figure show that the microscale described as length parameter x and y is total length and the scalar parameter ε =x/y (Hornung, 1997).

This study proposes a homogenization method for upscaling hydrological parameters related to a distributed runoff model from microscopic aspects up to

macroscopic ones. These parameters are equivalently derived from the mathematically formulated descriptions based on the conservation of surface and subsurface water quantities. A surface flow direction through a flow direction/routing map is significant to calculate the homogenized values of upscaling hydrological parameters. It will be proven that equivalently homogenized parameters stem just from the macroscopic-modeled parameters and the numbers of longitudinal and its transverse cells, and that a conventional way of equivalent parameters by weighted arithmetic mean is simple and easy but inadequate to figure out.

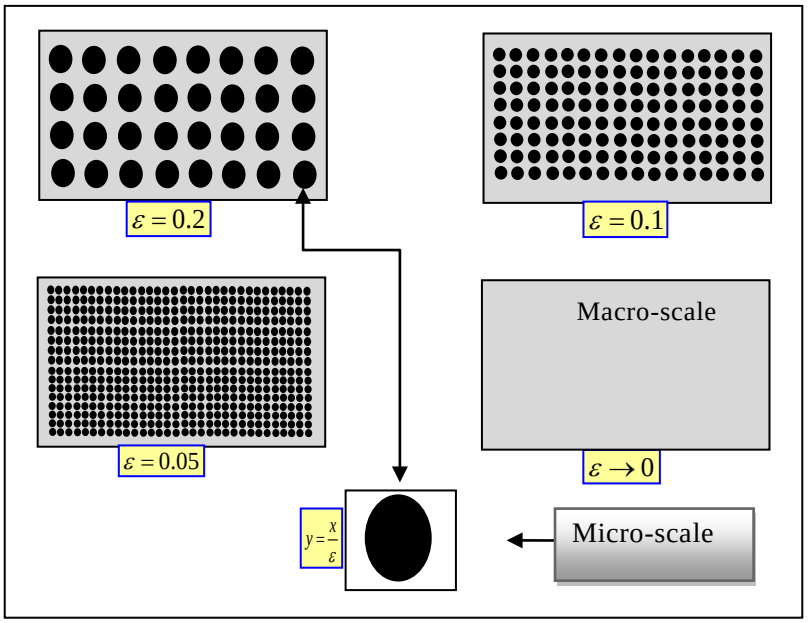

Figure 3.1 Schematic diagram shows the homogenization limit (Hornung, 1997).

3.2.2. Homogenization of two dimensional domain

Homogenization method of two dimensional cells to estimate the equivalent parameters of hydraulic conductivity of ground water $k*$ and coefficient roughness $n*$ is applied with considering the number of longitude and transverse cells and the direction of flow as well as length and width of cells. The following

way in our calculation of the target parameters is used.

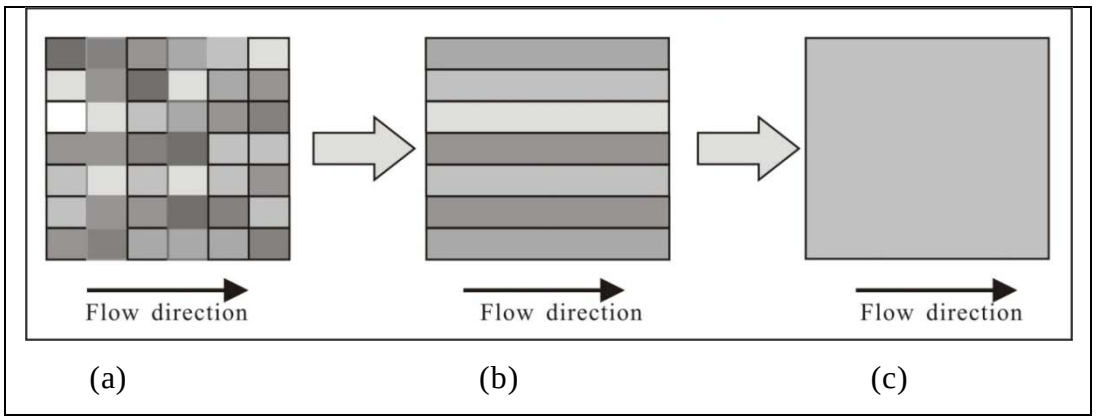

Figure 3.2 Schematic diagram shows the upscasling technique of homogenization theory.

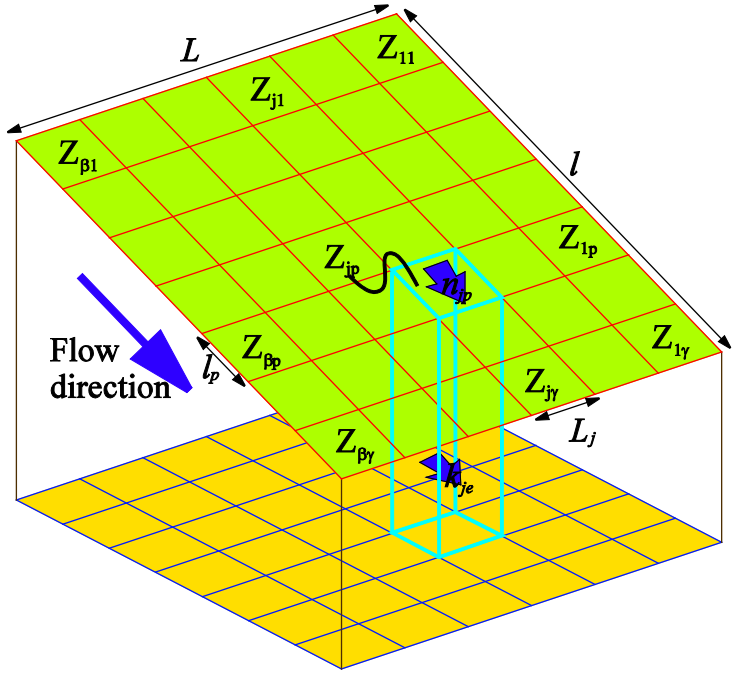

Figure 3.3 Schematic diagram shows distribution of the slope direction cells and the transverse cells (as two dimensional domain), where γ is slope direction, β is vertical direction, l(m) is slope length, L(m) is slope width, Z_{jp} is modeled cell, L_j(m)×l_p (m) is the mesh area, n_{jp}(m-1/3.s) is coefficient of roughness, and k_{jp}(m/s) is coefficient of permeability.

The equivalent parameters ($k*$ and $n*$) is calculated of two dimensional

cells (**Figures. 3.2a and 3.3**) where we started by the longitudinal direction (slope direction), on other words in the direction of flow (**Figures. 3.2b and 3.3**), then estimating of the equivalent parameters of the transverse cells to get the final homogenized parameters (**Figures. 3.2c and 3.3**).

3.2.3. Hydrology application on surface flow

Application of homogenization theory on surface flow and subsurface flow (seepage flow) will obey to Manning's law and Darcy's law respectively. The formula of Manning's law is derived from the kinematic wave equation which is depicted in the following equations (3.2), (3.3), and (3.4), where n^* is the equivalent homogenized model parameter of roughness coefficient.

$$\frac{\partial h}{\partial t}+\frac{\partial q}{\partial x}=r\left(x,t\right) \tag{3.2}$$

$$q=\alpha A h^{m},\quad where,\quad \alpha=\frac{\sqrt{\sin\theta}}{n} \tag{3.3}$$

where, h is the water depth (m), q is the discharge per unit length of flow [m^3/m.s], r is the effective rainfall intensity [m/s], t is the time [s], x is the distance from the upstream edge, A is cross sectional area, and α, m is constant concerning frictions.

Calculation of coefficient roughness is independent of time t, so the equation (3.2) will be simplified into equation (3.4).

$$\frac{\partial q}{\partial x}=r_e, or, \frac{\Delta q}{l}=r_e \tag{3.4}$$

where, l is the mesh length in the slope direction (m).

The homogenized parameters of coefficient roughness on the direction of slope (the flow direction) have been calculated. Then, it is estimated on the transverse direction of cells. Finally, the equivalent parameters for two dimensional domain as homogenized values are obtained. Calculation of the homogenized equivalent parameters in case of supposing length and width of cells

are different in addition to the numbers of longitude and transverse cells also unequal. The equations (3.5) and (3.6) can be obtained in which the homogenized coefficient roughness (n^*) depend on length, breadth and number of cells.

$$n_j^* = \frac{1}{\ell}\sum_{p=1}^{\gamma} \ell_p n_{jp} \tag{3.5}$$

$$n^* = \frac{L}{\sum_{j=1}^{\beta} \frac{L_j}{n_j^*}} = \frac{L}{\ell} \cdot \frac{1}{\sum_{j=1}^{\beta} \frac{L_j}{\sum_{p=1}^{\gamma} \ell_p n_{jp}}} \tag{3.6}$$

On the other hand, if a regular grid with even longitude and transverse intervals (i.e. the length and the breadth of the cells are the same) is considered in the calculation of the homogenized equivalent parameters, the details of calculation process can be shown as follows:

3.2.3.1. Calculation of coefficient roughness from cell Z1 to Zp

In this case the maximum number of cells is expressed by γ and n is coefficient roughness for each cell, q is the flow rate, and h is the flow head. So, the target is to calculate the equivalent parameters from cell n_1 to n_p (Figure 3.4) which is corresponding to the cells Z_1 to Z_p (**Figure 3.3**).

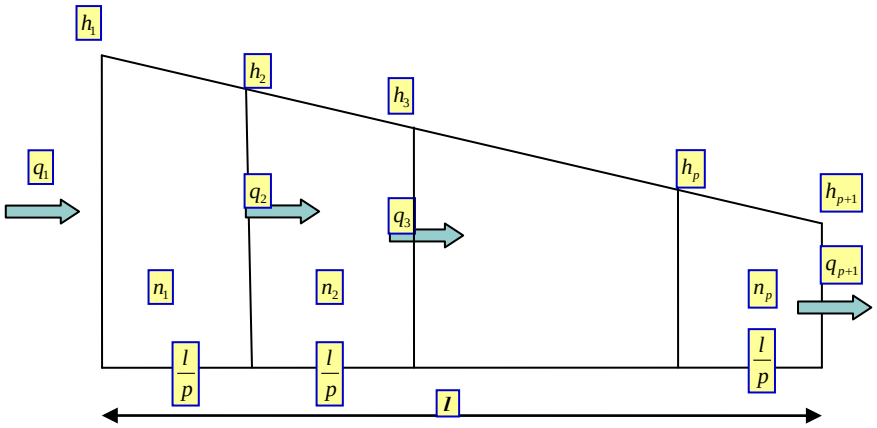

Figure 3.4 Schematic diagram shows the slope direction cell n_1~ n_p, which is corresponding to cells z_1 to z_p.

By following up the same way of obtaining coefficient roughness, equation (3.7) can be deduced from equations (3.2), (3.3), and (3.4).

$$\frac{\partial q}{\partial x} = \frac{\Delta q}{l} = \frac{q_1 - q_p}{l} = re \tag{3.7}$$

From equation (3.3) and (3.7), the following equations (3.8), (3.9), (3.10), (3.11), and (3.12) can be expressed as follow.

$$(h_1^{\,m} - h_{p+1}^{\,m}) = \frac{re.l}{\alpha^*} \tag{3.8}$$

$$\frac{\Delta q_1}{\frac{l}{p}} = \frac{q_1 - q_2'}{\frac{l}{p}} = \frac{\alpha_1 (h_1^{\,m} - h_2^{\,m})}{\frac{l}{p}} = re \tag{3.9}$$

$$(h_1^{\,m} - h_2^{\,m}) = \frac{re.\frac{l}{p}}{\alpha_1} \tag{3.10}$$

$$(h_2^{\,m} - h_3^{\,m}) = \frac{re.\frac{l}{p}}{\alpha_2} \tag{3.11}$$

$$(h_p^{\,m} - h_{p+1}^{\,m}) = \frac{re.\frac{l}{p}}{\alpha_p} \tag{3.12}$$

By summation of the upper equations with each other (3.8), (3.9), (3.10), (3.11), and (3.12) as follow, the equations (3.13) and (3.14) can be done.

$$(h_1^{\,m} - h_2^{\,m}) + (h_2^{\,m} - h_3^{\,m}) + ... + (h_{p-1}^{\,m} - h_p^{\,m}) + (h_p^{\,m} - h_{p+1}^{\,m}) = (h_1^{\,m} - h_{p+1}^{\,m}) = \frac{re.l}{\alpha^*} = \frac{re.\frac{l}{2}}{\alpha_1} + \frac{re.\frac{l}{2}}{\alpha_2} + ... + \frac{re.\frac{l}{p}}{\alpha_{p-1}} + \frac{re.\frac{l}{p}}{\alpha_p} \tag{3.13}$$

$$n^* = \frac{n_1}{p} + \frac{n_2}{p} + ... + \frac{n_{p-1}}{p} + \frac{n_p}{p} = \frac{1}{p}(n_1 + n_2 + ... + n_p) = \frac{1}{p}\sum n_p \tag{3.14}$$

The final equation in which the target parameter n^* calculated is equation (3.15) which corresponds with the cells Z_1 *to* Z_p (Figure 3.3), where the maximum

number of cells is γ, also, the equivalent parameter is assumed as independent of length and width of cells.

$$n_j^* = \frac{1}{\gamma}\sum_{p=1}^{\gamma} n_{jp} \tag{3.15}$$

3.2.3.2. Calculation of coefficient roughness from cell Z to Zj

In this case the maximum number of cells is expressed by β , and n is coefficient roughness for each cell, q is the flow rate, and h is the flow head. The necessary target in this study is to calculate the equivalent parameter along the transverse direction of cell n_1 *to* n_j (Figure 3.5) which is corresponding to the cells Z_1 *to* Z_j (Figure 3.3). In the transverse direction, the following conditions have been considered. The flow rate is variable from one cell to the other, and the water head is constant, so the calculation will be as follow:

From equation (3.3) and (3.4), the equations are deduced (3.16) and (3.17).

$$q = \alpha A h^m = \frac{\sqrt{\sin\theta}}{n} h^m \tag{3.16}$$

$$\frac{\partial q}{\partial x} = \frac{\Delta q}{l} = re = \frac{q - q'}{A.l} \tag{3.17}$$

where the flow rate is variable, the following equation (3.18) can be expressed as follow.

$$\Delta q = \Delta q_1 + \Delta q_2 + ... + \Delta q_j \tag{3.18}$$

Also by substituting the equations (3.16) and (3.17) on equation (3.18), the following equations (3.19), (3.20), (3.21), and (3.22) are obtained.

$$\Delta q = \frac{A.l\sqrt{\sin\theta}}{n^*}(h^m - h'^m) = re.l \tag{3.19}$$

$$\Delta q_1 = \frac{A.l\sqrt{\sin\theta}}{j.n_1}(h^m - h'^m) = re.l \tag{3.20}$$

$$\Delta q_2 = \frac{A.l\sqrt{\sin\theta}}{j.n_2}(h^m - h'^m) = re.l \tag{3.21}$$

$$\Delta q_j = \frac{A.l\sqrt{\sin\theta}}{j.n_j}(h^m - h'^m) = re.l \tag{3.22}$$

Also, by substituting the equations (3.19), (3.20), (3.21), and (3.22) on the equation (3.18), the equation (3.23) also is expressed.

$$\Delta q = \frac{A.l\sqrt{\sin\theta}}{n^*}(h^m - h'^m) = \frac{A.l\sqrt{\sin\theta}}{j.n_1}(h^m - h'^m) + \frac{A.l\sqrt{\sin\theta}}{j.n_2}(h^m - h'^m) + ...+ \frac{A.l\sqrt{\sin\theta}}{j.n_j}(h^m - h'^m) \tag{3.23}$$

$$n^* = \frac{j}{(\frac{1}{n_1} + \frac{1}{n_2} + ... + \frac{1}{n_j})} = \frac{j}{\sum \frac{1}{n_j^*}}$$

So, the final equation in which the target parameter $n*$ is calculated represented as equation (3.24) of the transverse direction concerning cell n_1 to n_j (**Figure 3.5**) and the corresponding cells Z_1~ Z_j (Figure 3.3), where the maximum number of cells is β, and it is proposed that the equivalent parameter is independent of length and width of cells.

$$n^* = \frac{\beta}{\sum_{j=1}^{\beta} \frac{1}{n_j^*}} \tag{3.24}$$

In the upper description of the mathematical calculation of the homogenized parameters, two equations are obtained, the first to calculate $n*$ in the longitude direction (slope direction), and the second one is to calculate $n*$ in the transverse directions. Therefore, the equivalent homogenized parameter of coefficient roughness for the two-dimensional cell is expressed in equation (3.25) by substituting the equation (3.15) in the equation (3.24).

$$n^* = \frac{\beta}{\gamma} \cdot \frac{1}{\sum_{j=1}^{\beta} \frac{1}{\sum_{p=1}^{\gamma} n_{jp}}} \tag{3.25}$$

On the other hand, in case of the same number of partitions (the grid

intervals, $\beta = \gamma\ (= \mu)$), the equivalent homogenized parameter of coefficient roughness n^* is represented in equation (3.26). From this equation, the equivalent parameter n^* is independent of the number of cells and the length and breadth of cells.

$$n^* = \frac{1}{\sum_{j=1}^{\mu} \frac{1}{\sum_{p=1}^{\mu} n_{jp}}} \tag{3.26}$$

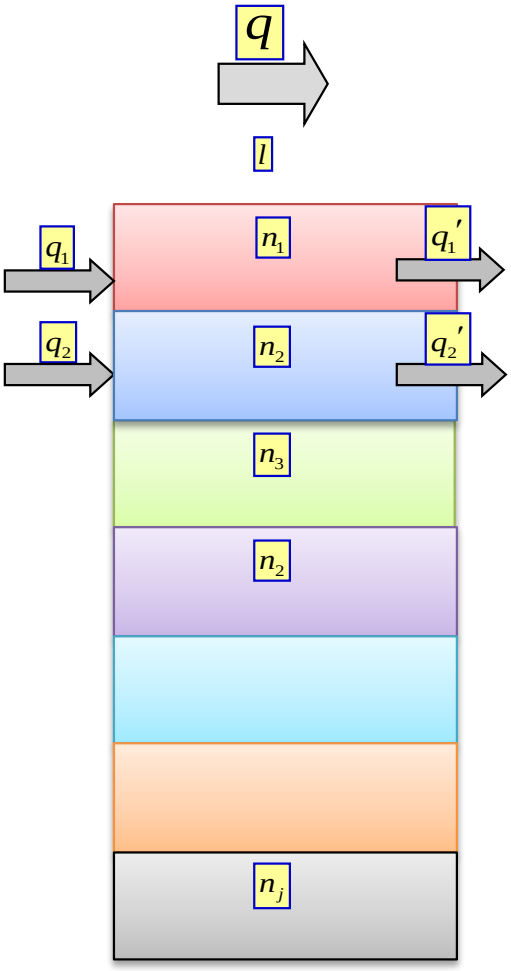

Figure 3.5 Schematic diagram shows the transverse direction concerning cell n_1 *to* n_j and the corresponding cells Z_1~ Z_j of Figure 3.3

3.2.4. Hydrology application on subsurface flow

The homogenization method is applied on the groundwater flow to calculate the homogenized parameter of hydraulic conductivity of two dimensional domain. It is represented by Darcy's Law (steady seepage), where k^* is the homogenization model parameter, and its formula is represented in the equation (3.27):

$$q = -kA\frac{\partial h}{\partial x} \tag{3.27}$$

where, q: Darcy's velocity or specific discharge [m^3/s], K: hydraulic conductivity (m/s), $\partial h / \partial x$ is the hydraulic gradient, and A: cross-sectional area of flow (m^2)

The homogenized parameter of hydraulic conductivity on the two-dimensional domain with considering the same mathematical process of calculation of coefficient roughness has been followed up. Firstly, the longitude and the transverse direction are calculated considering the flow direction and length and width as well as number of cells of the grid intervals. The equivalent parameters are calculated considering length and width of cells are different in addition to numbers of longitude and transverse cells also are unequal. In this case, the equations (3.28) and (3.29) are obtained in which the homogenized hydraulic conductivity k^* depends on length, breadth and number of cells.

$$k^* = \frac{\ell}{\sum_{p=1}^{\gamma}\frac{\ell_p}{k_{jp}}} \tag{3.28}$$

$$k^* = \frac{1}{L}\sum_{j=1}^{\beta} L_j k_j \quad = \frac{\ell}{L}\sum_{j=1}^{\beta}\frac{L_j}{\sum_{p=1}^{\gamma}\frac{\ell_p}{k_{jp}}} \tag{3.29}$$

On the other hand, if the modeled mesh is assumed to be with even longitude and transverse intervals (i.e. length and breadth of cells are same), the calculation process under these assumptions has been done in the following two items:

3.2.4.1. Calculation of hydraulic conductivity from cell Z1 to Zp

In this case the maximum number of cells is expressed by γ and k is hydraulic conductivity of each cell and q is the flow rate. So, the target is to calculate the equivalent parameters of cell k_1 to k_p (**Figure 3.6**) which is corresponding to the cells Z_1 to Z_p) (**Figure 3.3**).

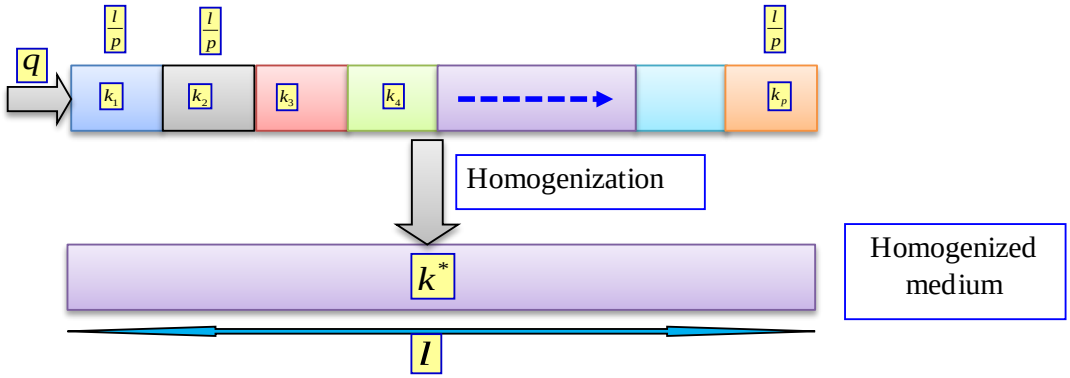

Figure 3.6 Schematic diagram shows the slope direction cells from k_1 *to* k_p.

From Darcy's law (3.27), the following equations are deduced as expressed in equation (3.30)

$$q = kA\frac{\Delta h}{l} \rightarrow \Delta h = \frac{q.l}{k*},\ \Delta h_1 = \frac{q.l/p}{k_1},\ \Delta h_2 = \frac{q.l/p}{k_2},\ \Delta h_p = \frac{q.l/p}{k_p} \qquad (3.30)$$

With the assumptions of the flow rate is constant and the hydraulic head is variable, the equation is expressed (3.31).

$$\Delta h = \Delta h_1 + \Delta h_2 + ... + \Delta h_p \qquad (3.31)$$

By substituting the equations (3.30) in the equation (3.31), we got the following equation (3.32).

$$\frac{q.l}{k^*} = \frac{q.l/p}{k_1} + \frac{q.l/p}{k_2} + ... + \frac{q.l/p}{k_p}, \qquad \rightarrow \qquad k^* = \frac{p}{\sum \frac{1}{k_p}} \tag{3.32}$$

The final equation in which the homogenized parameter $k*$ is expressed in the equation (3.33) of cell k_1 *to* k_p which corresponds with the cells Z_1 *to* Z_p (**Figure 3.3**), where the maximum number of cells is γ, and the equivalent parameter is independent of length and width of cells.

$$k_j^* = \frac{\gamma}{\sum_{P=1}^{\gamma} \frac{1}{k_{jP}}} \tag{3.33}$$

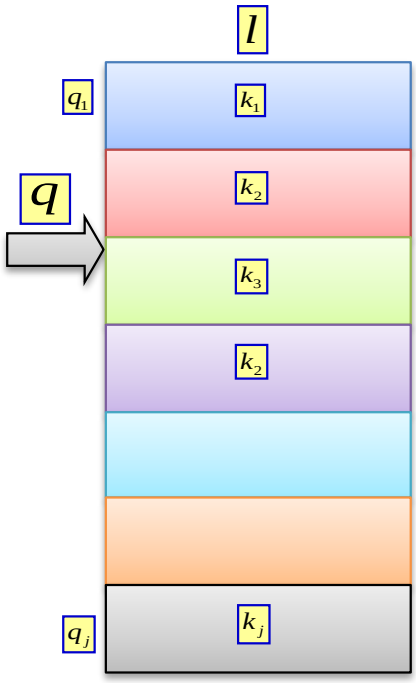

Figure 3.7 Schematic diagram shows the transverse direction of cell k_1 *to* k_p which is corresponding to the cells Z_1 *to* Z_j (Figure 3.3).

3.2.4.2. Calculation of hydraulic conductivity from cell Z1 to Zj

In this case the maximum number of cells is expressed by β and k is hydraulic conductivity for each cell and q is the flow rate. So, the target is to calculate the equivalent parameter along the transverse direction of cell k_1 *to* k_p (**Figure 3.7**) which is corresponding to the cells Z_1 *to* Z_j (**Figure 3.3**).

In the transverse directions, the flow rate is variable from one cell to the other, and the hydraulic head is constant, so the calculation process will be as follow:

$$\Delta h = \Delta h_1 = \Delta h_2 = ... = \Delta h_j \quad (cons.), \quad and \qquad q = q_1 + q_2 + ... + q_j \qquad (3.34)$$

From Darcy's law (the equation (3.27)), the formula (3.34) is expressed.

So, $$q_1 = k_1 A\frac{\Delta h_1}{j.l}, \qquad q_2 = k_2 A\frac{\Delta h_2}{j.l}, \qquad q_j = k_j A\frac{\Delta h_2}{j.l}, \qquad q = k^* A\frac{\Delta h}{l} \qquad (3.35)$$

By substituting of the equation (3.35) into the equation (3.34), the following equation (3.36) is obtained.

$$k^* A\frac{\Delta h}{l} = k_1 A\frac{\Delta h_1}{j.l} + k_2 A\frac{\Delta h_2}{j.l} + ... + k_j A\frac{\Delta h_j}{j.l} \rightarrow k^* = \frac{1}{j}(k_1 + ... + k_j) = \frac{1}{j}\sum k_j \qquad (3.36)$$

The homogenized parameter $k*$ is calculated and expressed in equation (3.37) of the transverse direction concerning cell k_1 *to* k_p (**Figure 3.7**) and the corresponding cells Z_1 *to*Z_j (**Figure 3.3**), where the maximum number of cells is β, and the equivalent parameter is independent of length and width of cells.

$$k^* = \frac{1}{\beta}\sum_{j=1}^{\beta} k_j^* \qquad (3.37)$$

In the upper description of the mathematical calculation of the homogenized parameters, two equations have been expressed, the first one to calculate $k*$ in the longitude direction (flow direction), and the second one is to calculate $k*$ in the transverse directions. Therefore, the equivalent homogenized parameter of hydraulic conductivity for the two-dimensional cell is expressed in equation (3.38) of the two-dimensional cell is obtained by substituting the

equation (3.33) to the equation (3.37).

$$k^* = \frac{\gamma}{\beta} \sum_{j=1}^{\beta} \frac{1}{\sum_{p=1}^{\gamma} \frac{1}{k_{jp}}} \tag{3.38}$$

On the other hand, if the number of partitions (the grid intervals, $\beta = \gamma\ (= \mu)$) is the same, the equivalent homogenized parameter of hydraulic conductivity is obtained in the equation (3.39).

$$k^* = \sum_{j=1}^{\mu} \frac{1}{\sum_{p=1}^{\mu} \frac{1}{k_{jp}}} \tag{3.39}$$

3.2.5. Hypothetical examples of homogenization theory application for roughness coefficient

The equation 3.26 of homogenized roughness coefficient has been applied to ensure the applicability of this methodology in upscaling the hydrological parameters. The hypothetical mesh is assumed about 1 km by 1 km and it is divided into 100 meshes (100m by 100m) as shown in **Figures 3.7a, 3.7b, 3.8a, and 3.8b.** Land use types of examples 1 and 2 are distributed randomly but examples 3 and 4 are distributed as banded zones of different land use types.

Standard Roughness coefficients in Nagara River are: rice field =0.3; field=0.3 m exponent (-1/3).S; forest=0.7; city=0.03; and water = 0.04

Example 1

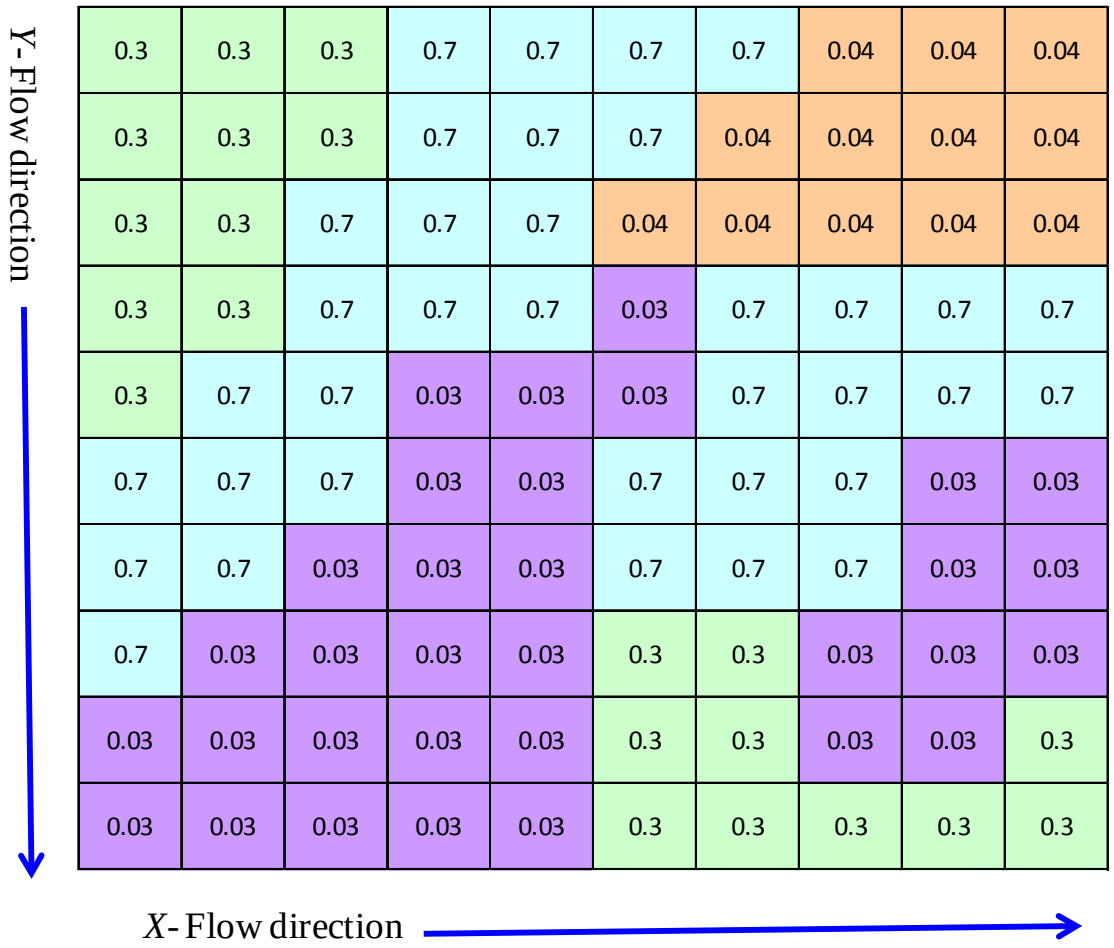

Figure 3.7a the modeled mesh showing the random distribution of land use types

The conventional method of averaging of roughness coefficients is 0. 3224. If the flow direction (slope direction) is parallel to Y-direction, the equivalent homogenized value is 0. 250223, but if the flow direction is parallel to X-direction, the equivalent homogenized value is 0. 304632.

Example 2

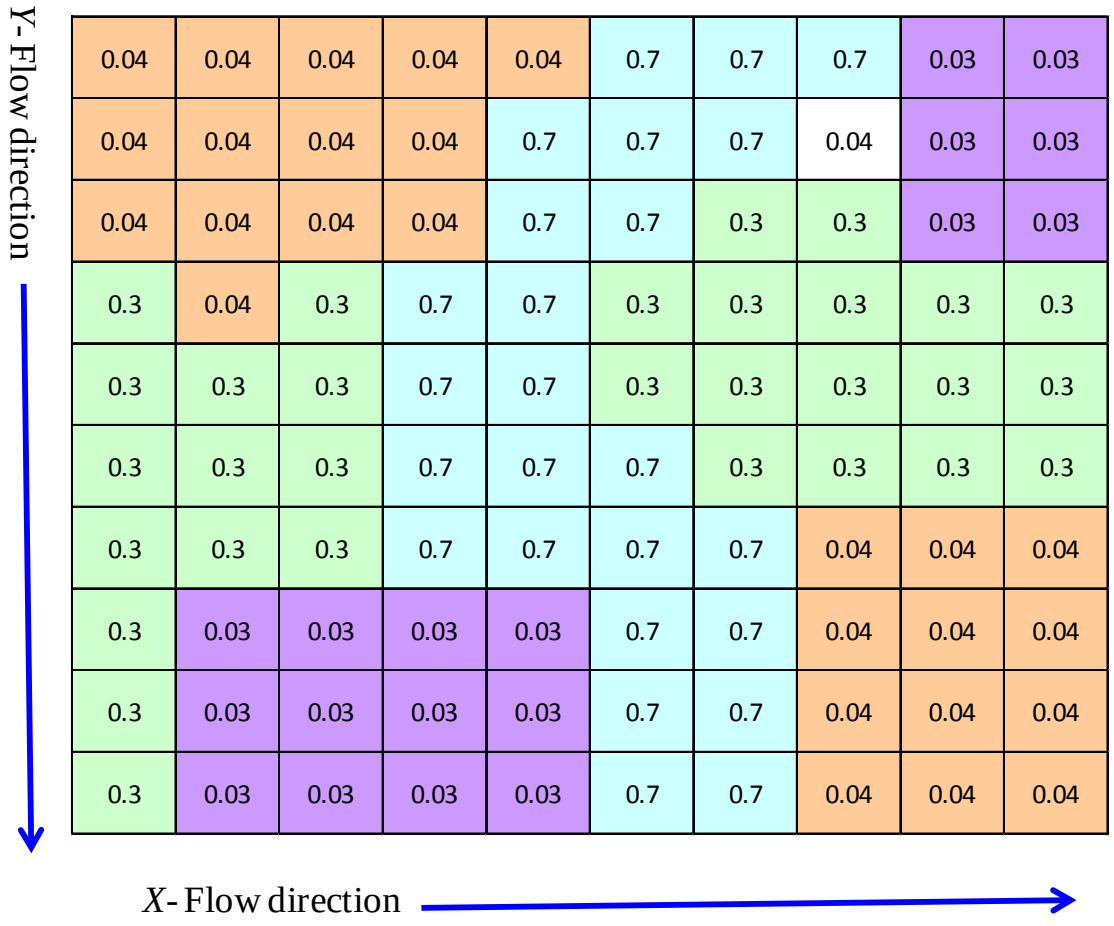

Figure 3.7b the modeled mesh showing the random distribution of land use types

The conventional method of averaging of roughness coefficients is 0.2812. If the flow direction (slope direction) is parallel to Y-direction, the equivalent homogenized value is 0.257081, but if the flow direction is parallel to X-direction, the equivalent homogenized value is 0.194016.

Example.3

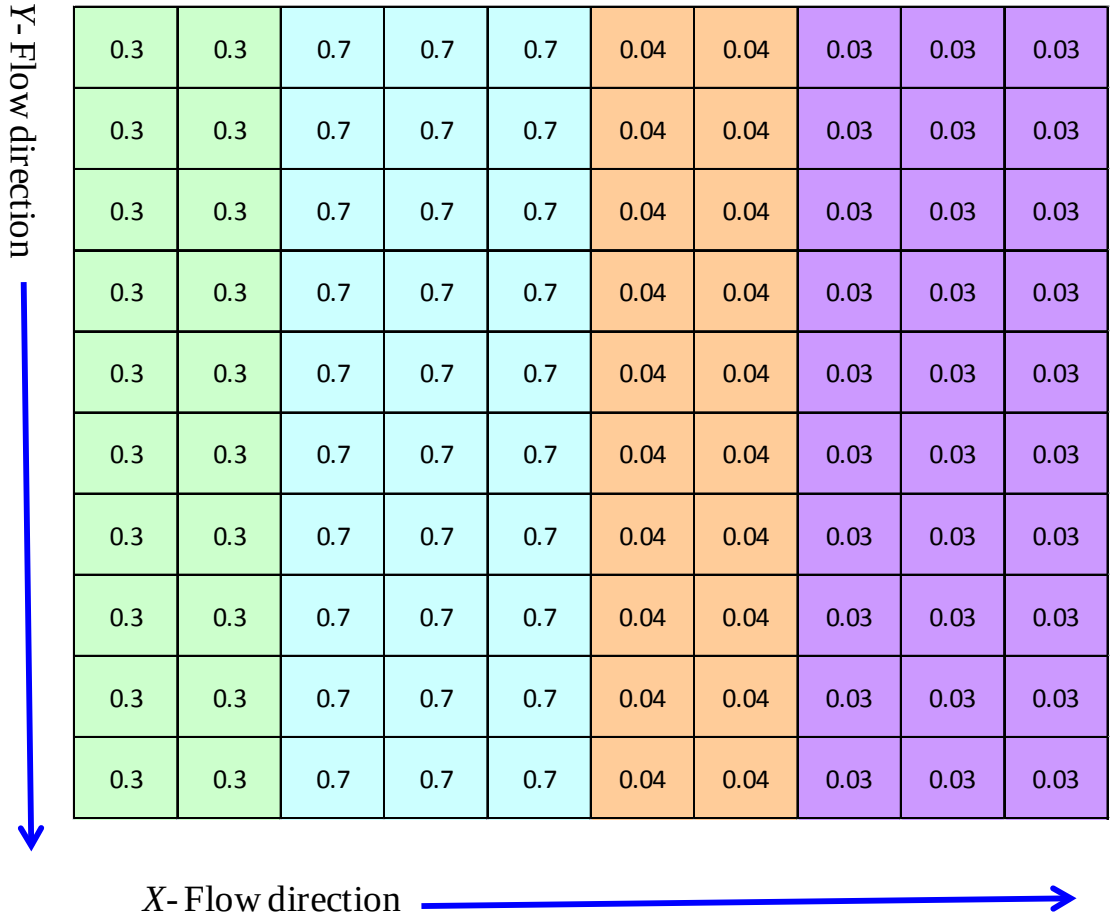

Figure 3.8a the modeled mesh showing the banded distribution of land use types

The conventional method of averaging of roughness coefficients is 0. 287. If the flow direction (slope direction) is parallel to Y-direction, the equivalent homogenized value is 0. 287, but if the flow direction is parallel to X-direction, the equivalent homogenized value is 0. 06213.

Example.4

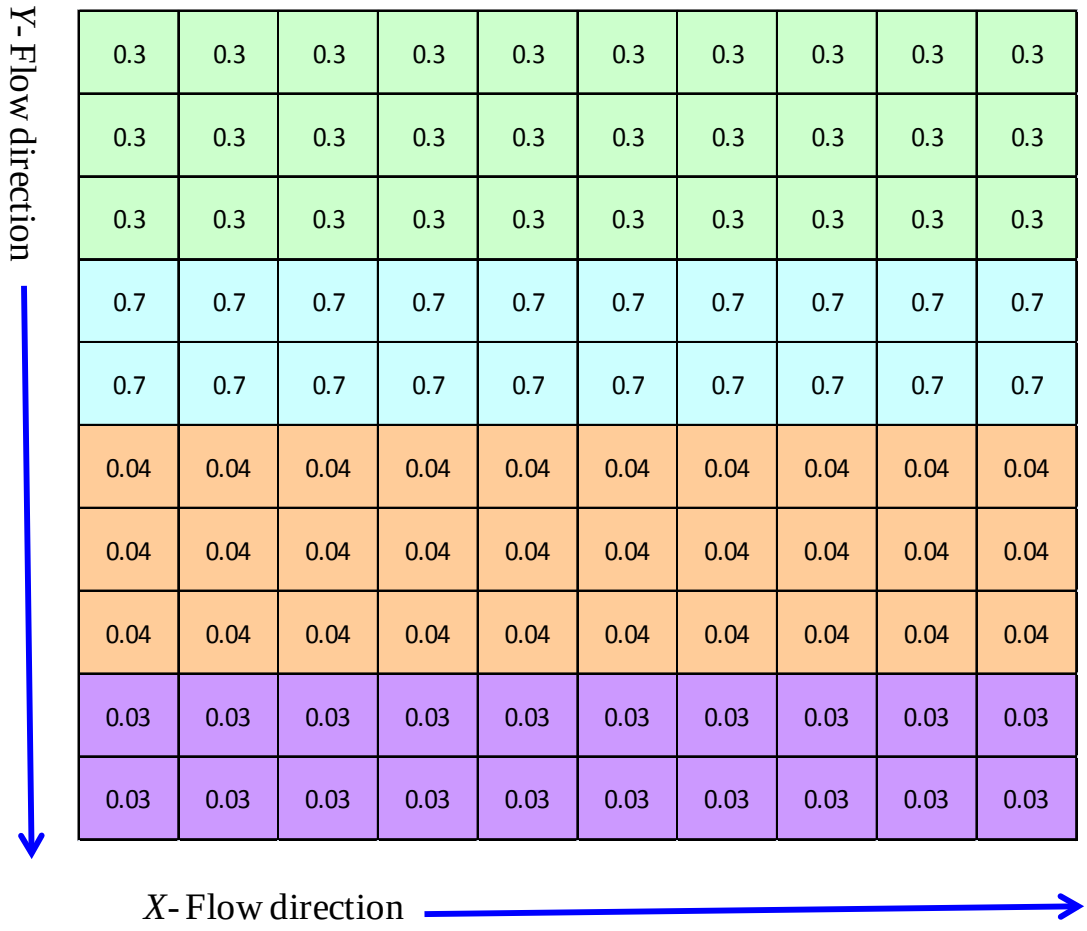

Figure 3.8b the modeled mesh showing the banded distribution of land use types

The conventional method of averaging of roughness coefficients is 0. 248. If the flow direction (slope direction) is parallel to Y-direction, the equivalent homogenized value is 0. 064715, but if the flow direction is parallel to X-direction, the equivalent homogenized value is 0. 248.

It is noticed from these examples of hypothetical homogenized meshes that there are remarkable differences between the conventional method and the homogenized parameter of roughness coefficient. For instance in **Figure 3.7b**, the

averaged value of roughness coefficient is 0.2812. If the flow direction (slope direction) is parallel to Y-direction, the equivalent homogenized value is 0.257081, but if the flow direction is parallel to X-direction, the equivalent homogenized value is 0.194016. This difference indicates to the effect of using the homogenization method in upscaling the hydrological parameters with considering the flow direction of flow as a physical based consideration in the hydrological modeling of hydrological parameters. Furthermore, it is also founded that the distribution of land use in the same mesh show a difference in the equivalent of homogenized parameter in either random or banded distribution as represented in **Figures 3.8a and 3.8b**.

It is deduced that the homogenized parameters k^* and n^* are equivalently derived from the mathematically formulated descriptions based on the conservation of surface and subsurface water quantities, these parameters are relied on Darcy's law and Manning's law. The obtained equations of the equivalent parameters are different considering the cell conditions, for instances, when we have a regular grid with even longitude and transverse intervals (i.e. the length and the breadth of the cells are the same), it is noted that the parameters are only depending on number of cells and independent of the length and breadth of cells. On the other hand, if we have uneven longitude and transverse intervals, the parameters are depending on them. Moreover, when we have the same number of longitude and transverse intervals, the result are independent of number of them.

The proposed methodology of Upscaling the hydrological parameters based on homogenization theory could be more applicable and effective in the hydrological modeling because it is developed based on the physical conditions considering the flow direction in each mesh.

3.3. Hydro-BEAM incorporating Wadi system (Hydro-BEAM-WaS)

Due to the severe problems in wadi system in arid areas, it is recommended to develop distributed hydrological models to understand the runoff characteristics and surface water/groundwater interactions in arid regions. These are challenging studies, with particularly challenging logistical problems, and require the full range of advanced hydrological experimental methods and approaches to be applied. A distributed hydrological model in wadi system is proposed. This model is based on the modification of Hydro-BEAM (Hydrological Basin Environmental Assessment Model) which has been chosen for simulation the surface runoff model and estimation of the transmission losses.

Hydro-BEAM was first developed by Kojiri *et al.* (1998) as a tool to assist in simulating long-term fluctuations in water quantity and quality in rivers through an understanding of the hydrological processes that occur within a watershed. It has since been used in a pioneering work on comparative hydrology, where a methodology for assessing the similarity between watersheds was proposed (Park *et al.*, 2000), to investigate sediment transport processes in the large watershed of the Yellow River, China (Tamura and Kojiri, 2002), and to investigate pesticide levels in rivers and their effects on hormone levels in fish (Tokai *et al.*, 2002).

The proposed approach is a physically-based numerical model and it can be summarized as following in this study; the watershed modeling using GIS technique is processed, surface runoff and stream routing modeling based on using the kinematic wave approximation is applied, the initial and transmission losses modeling is estimated by using SCS (1997) method (an empirical model for rainfall abstractions suggested by the U.S Soil conservation Service) and Walter's equation (1990) respectively, groundwater modeling based on the linear storage model is used.

3.3.1. Model Components

Rainfall-runoff modeling is the process of transforming a rainfall hyetograph into a runoff hydrograph. This can be achieved through the use of data-driven or statistical mathematical techniques, through developing physical descriptions of the rainfall-runoff process, or through various combinations of these approaches. Hydro-BEAM has been chosen for simulation the surface runoff in arid zones due to its flexibility of application to accomplish many purposes of hydrological simulation.

The watershed is modeled as a uniform array of multi-layered mesh cells, each mesh containing information regarding surface land use characteristics, ground surface slope direction, runoff, and the presence/absence of a channel. The original Hydro-BEAM model that was used for the humid conditions can be adopted for simulation in the arid areas in wadi system as described in the following sections. Initial and transmission losses are evaluated as subroutine model in Hydro-BEAM, as crucial resource for the subsurface water in such areas as shown in **Figure 3.9**.

The watershed to be investigated is divided into an array of unit mesh cells. A mesh cell can be arranged as a combination of a surface layer and several subsurface layers. The following description considers Hydro-BEAM calibrated with four subsurface layers, labeled A, B, C and D. A-Layer is calibrated using kinematic wave model for the overland flow evaluation and the other C-D layers (subsurface layers) are calculated by the linear storage model.

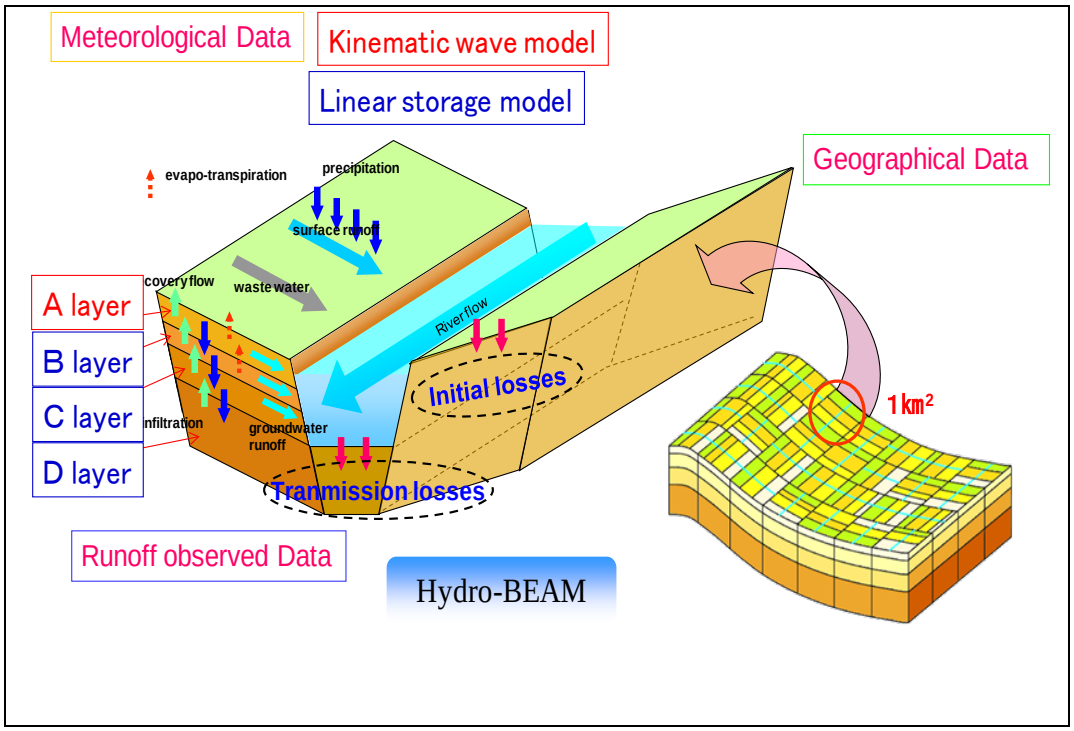

Figure 3.9 Conceptual representation of Hydro-BEAM

3.3.2.1. Watershed Modeling

Remote sensing and GIS techniques were used to assist in the modeling process as watershed modeling. Data of a watershed are usually spatial in nature. Spatial data such as elevation, land use, soil, and geology could be linked directly or indirectly with the hydrological processes occurring inside the watershed. In the distributed models, major input parameters are based on the spatial information of the watershed such as rainfall, land use, soils, topography etc. Therefore, based on the characteristics of constructed database, appropriate analysis techniques could be adopted to accomplish the overall goals of watershed modeling. GIS as powerful tool for the spatial data and more understanding for the watershed characteristics is used in this study for processing the Digital Elevation Model (DEM) so that delineate and determine the watershed and sub catchments as well as the stream networks of the drainage pattern.

The data of digital elevation model (DEM); (Shuttle Radar Topography

Mission), 90 m spatial resolution has been used to delineate and determine the watershed and stream networks in the studied wadi basins. The data are distributed free of charge by USGS and are available for download from the USGS server at http://dds.cr.usgs.gov/srtm/. Data are also available through the USGS seamless server at http://seamless.usgs.gov/. By processing DEM using Global Mapper and Golden Surfer software, then importing the data into Arcview GIS tool, the watershed basin, sub-basin watersheds were delineated and stream networks were determined for the target wadi catchments (Wadi Al-Khoud, Oman (A), Wadi Ghat, Saudi Arabia (B), Wadi Assiut, Egypt (C)).

Some geomorphologic information such as watershed area, perimeter, and main channel length were calculated. The following processes in the watershed modeling must be taken in consideration such as:

- Determination of the watershed boundary location,
- Division of the watershed into a regular grid of mesh cells (1 km or 2 km, etc.),
- Determination of a flow routing network based on mesh cell elevation as given by a DEM and checked against topographical maps.

(a) Flow routing map

As well known, there are two types of flow routing system; 4 directions and 8 directions to determine drainage of flow water direction of drainage basin. Hydro-BEAM was originally developed to use a 4-direction flow routing map.

The function of a flow routing map is to define a downstream destination for the discharge resulting from every cell in the watershed, with the exception of the furthest downstream mesh cell located at the watershed mouth. Flow direction from any given mesh cell can be estimated using the DEM elevations of the corners of each mesh cell as declared in **Figure 3.10**.

Where the flow path of each mesh is decided based on the elevation values of each corner. On the other hand, the perpendicular direction of slope of the two

half of the mesh is estimated based on dividing of each mesh into subdivisions. The flow direction in each mesh depends on the direction of its slope, then manually the opposite and paradox flow directions can be corrected based on the elevation and topographic maps.

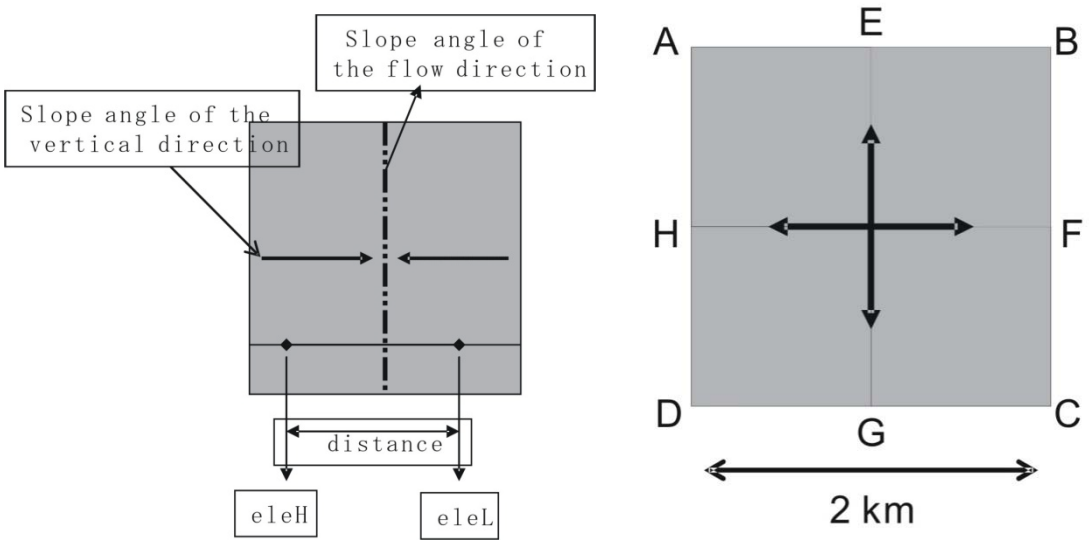

Figure 3.10 Schematic diagram of the flow direction determination

(b) Setting of river channel cross section

The river channel section inside the drainage basin which is dealt with is needed to be set. For this purpose, the hydraulic geometry (Leopold and Maddock, 1953) of regime formality is used. As shown below, the Regime formality which applies the theoretical value of Leopold-Maddock to factor *f* and *b*.

$$H \propto Q^{f}, \qquad f = 0.36 \tag{3.40}$$

$$B \propto Q^{b}, \qquad b = 0.55 \tag{3.41}$$

where, H is depth of water (m), Q is flow (m^3s^{-1}) and B: is flowing water width (m).

The cross section of the optional position is set from flowing water width, By

applying the above-mentioned regime formality. It can define the next formula from regime formality at the datum point and the optional position.

$$H_{std} = \beta Q_{std}{}^{f}, \qquad B_{std} = \alpha Q_{std}{}^{b} \tag{3.42}$$

$$H_i = \beta Q_i^{f}, \qquad B_i = \alpha Q_i^{b} \tag{3.43}$$

wher, *std* is the subscript which displays the datum point, i is the subscript which displays the optional position. It can define the legal surface slope m_{ri} of the cross section from the above-mentioned formula in the optional position as follows.

$$m_{ri} = \frac{B_i}{H_i} \tag{3.44}$$

$$H_i = H_{std}\left(\frac{Q_i}{Q_{std}}\right)^{f}, \qquad B_i = B_{std}\left(\frac{Q_i}{Q_{std}}\right)^{b} \tag{3.45}$$

$$Q_i = \frac{Q_{std}}{A_{std}} A_i \tag{3.46}$$

where, A is the catchment area, m^2.

(c) Land use classification

Land use information is used to specify the structure of each mesh, its infiltration and runoff characteristics. Hydro-BEAM is set to use five categories of land use types, where they are grouped and represented as a percentage land cover of the total area of the mesh cell.

The land use distribution data (GLCC; Global Land Cover Characterization and ECOCLIMAP Data; a global database of land and surface parameters at 1km resolution in meteorological and climate models) are used for identify and extract the land use distribution of the studied wadi basins.

Land use data of GLCC is divided into 24 land use types. For the reason of hydro-BEAM using five land use categories, those types 24 are reclassified into 5 types to be compatible. The five categories of land use types are; forests, paddy field (rice field), desert, urban or city, water as given in **Table 3.1**.

Table 3.1 Land use types of modified Hydro-BEAM

Category	Description
Forests	Densely-vegetated regions (forests)
Field+ Paddy field	Agricultural regions including farms
Desert	Most of wadi areas are desert
Urban area	Paved or impervious urban regions
Water body	Bodies of water

3.3.2.2. Climatic data

The metrological data (**Table 3.2**) are needed for each mesh in hydro-BEAM as input data to calculate evapotranspiration. The climatic data of NCDC (National Climatic Data Center), Global Hourly data can be used in this work. Due to the lacking of many kinds of data, we adopted Thornthwaite method to calculate daily mean potential evapotranspiration as given in the equations (3.47), (3.48), (3.49), and (3.50). The mean air temperature and duration of possible sunshine of each mesh are needed as meteorological data for the model.

$$E_p = 0.553 D_0 (10 T_i / J)^a \tag{3.47}$$

$$a = 0.000000675 J^3 - 0.0000771 J^2 + 0.01792 J + 0.049293 \tag{3.48}$$

$$J = \sum_{i=1}^{12} (T_i / 5)^{1.514} \tag{3.49}$$

$$E_a = M \cdot E_p \tag{3.50}$$

where, E_a, *and* E_p *(mm/d)* are the actual and the potential evapotranspiration; *Ti* (^0C) is the monthly average temperature, *J*: Heat index, D_0 *(h/12h)* is the potential day length and *M* is the reduction coefficient, vapor effective parameter.

Table 3.2 Types of input data and its resources

Type of data	Description
Digital Elevation Model	SRTM (Shuttle Radar Topography Mission). CGIAR-CSI (Consortium for Spatial Information)
Land use	GLCC (Global Land Cover Characterization) And ECOCLIMAP data (1 km resolution) USGS (U.S. Geological Survey)
Climatic Data (Rainfall, Temperature)	Global Surface Data, Hourly , NCDC (National Climatic Data Center)

3.3.2.3. Kinematic wave model

Kinematic wave model are derived from the St. Venant equations by preserving conservation of mass and approximately satisfying conservation of momentum. The momentum of the flow can be approximated with a uniform flow assumption as described by Manning's equation. In this study, kinematic wave approach is applied for surface runoff and stream routing modeling based on using the kinematic wave approximation with the assumption of the river channel cross section as a triangle shape (**Figure 3.11**).

A finite difference approximation of the kinematic wave model can be used to model watershed runoff on the surface and layer A in Hydro-BEAM. The various features of the irregular surface geometry of the basin are generally approximated by either of two types of basic flow elements: an overland flow element, or a stream- or channel flow element. In the modeling process, overland flow elements are combined with channel-flow elements to represent the subbasin.

In Hydro-BEAM, the integrated model of kinematic wave is used for overland flow and A-layer flow as expressed in the equations (3.51), (3.52), (3.53) and (3.54).

$$\frac{\partial h}{\partial t}+\frac{\partial q}{\partial x}=r\left(x,t\right) \tag{3.51}$$

$$q=\begin{pmatrix}\alpha\left(h-d\right)^{m}+ah\\ ah\end{pmatrix},\quad when\begin{pmatrix}h\geq d\\ h<d\end{pmatrix},d=\lambda D \tag{3.52}$$

$$\alpha=\frac{\sqrt{\sin\theta}}{n}\quad\left(Manning\quad formula\right) \tag{3.53}$$

$$a=\frac{k\sin\theta}{\lambda}\quad\left(Darcy\quad formula\right) \tag{3.54}$$

where, h is the water depth (m), q is the discharge per unit length of flow [m^3/m.s], r is the effective rainfall intensity [m/s], t is the time [s], x is the distance from the upstream edge, and α, m is constant concerning frictions, λ is the porosity, D is the thickness (m), and d is the saturation pondage (m),

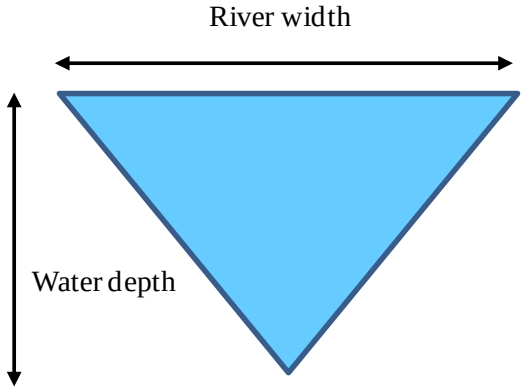

Figure 3.11 Triangle River channel cross section.

In Hydro-BEAM, the integrated model of kinematic wave is used for surface flow and A-layer (**Figure 3.12**), where the paddy field is formulated as the double Tanks Model where the upper tank is recognized as the surface zone. The upper hole in the tank means the overflow discharge from the surrounding paddy path, the lower hole does the runoff discharge from normal release gate and the infiltration rate through paddy path, and the bottom hole does the vertical infiltration. The water demand to be supplied is calculated as the difference

between water depth of the surface tank and the desired pounding depth as expressed in equations (3.55) and (3.56).

$$\frac{dh}{dt} = r(x,t) - q \tag{3.55}$$

$$q = \sum_j a_{P_j} \max\left(h - Z_{AP_j}, 0\right) \tag{3.56}$$

where, h is storage height (m), and A_P is subscription of compound tank model constant (s^{-1}) and Z_{Ap} is compound tank model constant (m).

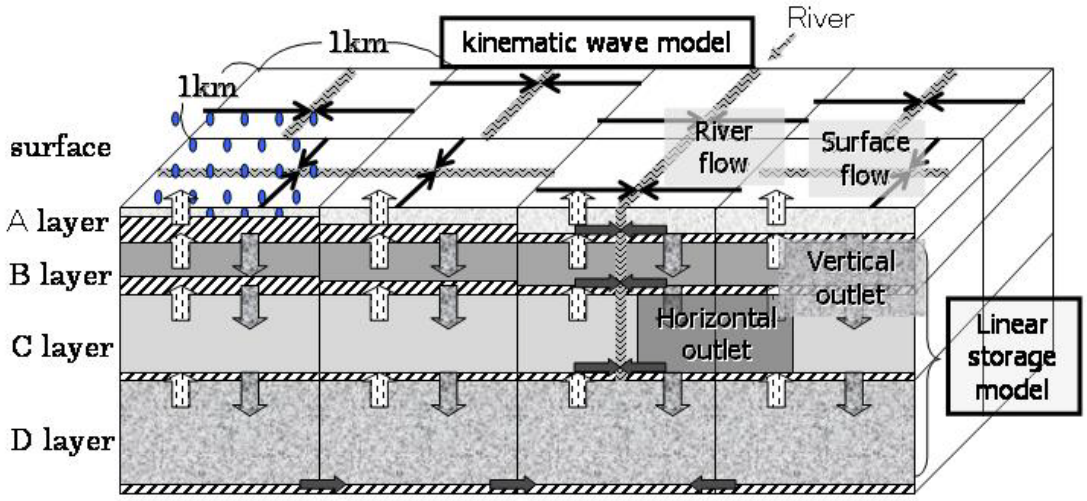

Figure 3.12 Schematic of Kinematic wave and linear storage model

3.3.2.4. Linear storage model

Linear storage model as given in equations (3.57) and (3.58) is used for modeling of groundwater in layers B, C, and D layers in each mesh of catchment area, thus the ground water storage can be evaluated in the proposed model.

$$\frac{dS}{dt} = I - O, \text{ where, } \quad O = (k_1 + k_2) \cdot S \tag{3.57}$$

where S: is storage amount [m], I: is inflow [ms^{-1}], O: is outflow [ms^{-1}], k_1, k_2: are outlet coefficients.

Details of calculation processes as follow:

i)- B-layer

$$\frac{dh_B}{dt} = I_B - q_B, \qquad q_B = q_{h_B} + q_{v_B} \tag{3.58}$$

$$I_B = r\left(1 - \overline{f}_{Al}\right) + u_C, \qquad \overline{f}_{Al} = \frac{\sum_l f_{Al} A_l}{\sum_l A_l}, \tag{3.59}$$

$$q_{h_B} = k_{h_B} \max\left(h_B - Z_B, 0\right), \qquad q_{v_B} = k_{v_B} h_B, \qquad Z_B = D_B\left(\lambda_B - \lambda_w\right) \tag{3.60}$$

$$u_B = \begin{pmatrix} h_B - d_B \\ 0 \end{pmatrix}, \quad when \begin{pmatrix} h_B - d_B \geq 0 \\ h_B - d_B < 0 \end{pmatrix}, \qquad d_B = \lambda_B D_B \tag{3.61}$$

where, f_{AL} is the runoff, h is storage high (m), k_{v_B} is vertical permeability, I is inflow (ms^{-1}) and q is outflow (ms^{-1}) and u *is* return quantity from c-layer, (ms^{-1}), k_h and k_v is horizontality and vertical related constant (s^{-1}) of soil, λ is percentage of void -, D is thickness m, d is saturation pondage m, B is the subscript which displays B layer, λ_w is the percentage of void which contributes to outflow . However, when storage high h exceeds saturation pondage d, the water content u returns to higher stratum of society.

ii)- C-layer

$$\frac{dh_C}{dt} = I_C - q_C, \qquad q_c = q_{h_c} + q_{v_c} \tag{3.62}$$

$$I_C = q_{v_B} + u_D \tag{3.63}$$

$$q_{h_C} = k_{h_C} \max\left(h_C - Z_C, 0\right), \qquad q_{v_C} = k_{v_C} h_C, \qquad Z_C = D_C\left(\lambda_C - \lambda_w\right) \tag{3.64}$$

$$u_C = \begin{pmatrix} h_C - d_C \\ 0 \end{pmatrix}, \quad when \begin{pmatrix} h_C - d_C \geq 0 \\ h_C - d_C < 0 \end{pmatrix}, \qquad d_C = \lambda_C D_C \tag{3.65}$$

iii）D-layer

$$\frac{dh_D}{dt} = I_D - q_D, \qquad q_D = q_{h_D} \tag{3.66}$$

$$I_D = q_{v_C} \tag{3.67}$$

$$q_{h_D} = k_{h_D} \max\left(h_D - Z_D, 0\right), \qquad Z_D = D_D\left(\lambda_D - \lambda_w\right) \tag{3.68}$$

$$u_D = \begin{pmatrix} h_D - d_D \\ 0 \end{pmatrix}, \quad when \begin{pmatrix} h_D - d_D \geq 0 \\ h_D - d_D < 0 \end{pmatrix}, \qquad d_D = \lambda_D D_D \tag{3.69}$$

where, h is storage high m, I is inflow (ms^{-1}) and q is outflow (ms^{-1}) and u is return quantity (ms^{-1}), k_h and k_v is horizontality and vertical related constant (s^{-1}) of soil, λ is percentage of void -, D is thickness m, d: saturation pondage m and C is the subscript which displays C layer and D is the subscript which displays D layer, λ_w is the percentage of void which contributes to outflow. However, when storage high h exceeds saturation pondage d, the water content u returns to higher stratum of society.

3.3.2.5. Initial and transmission losses model

Due to the importance of the losses in the arid areas, one subroutine is added to Hydro-BEAM to calculate the initial and transmission losses in each mesh.

(a) Initial Losses

Initial losses occur in the sub-basins before runoff reaches the stream networks. It is largely related to infiltration, surface soil type, land use activities, evapotranspiration, interception, and surface depression storage. In other words, the initial abstraction I_a, which is equal to the accumulated rainfall from the beginning of the storm to the time when direct runoff started.

The NRCS method (Soil Conservation Service (SCS):1997) is adopted to calculate initial losses in the target catchments where it has been successfully applied to ephemeral watersheds in South West of United States (Osterkamp et al. 1994), which resembles the desert of Oman, Saudi Arabia and Egypt, climate conditions, topographical and land use characteristics. Runoff in sub basins occurs after rainfall exceeds an initial abstraction (I_a) value. Rainfall excess, P_e, in NRCS method is related to the effective potential retention value, S, as given in equation (3.70).

The curve number (CN) method uses the following equations (3.71), (3.72) and (3.73):

$$P_e = \frac{(P - I_a)^2}{(P - I_a) + S} \tag{3.70}$$

$$CN = \frac{25400}{254 + S} \tag{3.71}$$

$$I_a = \lambda S \tag{3.72}$$

where: P is the depth of rainfall (mm), P_e is the depth of runoff or excess rainfall (mm), I_a is the initial abstraction (mm), S is the maximum potential retention after runoff begins (mm), is a dimensionless parameter varying from 0 to 1, CN is the curve number.

The initial abstraction λ is suggested by NRCS to be approximately 20 % of the maximum potential retention value. It consists mainly of interception, infiltration prior to runoff, and surface storage, and it is related to potential maximum retention (Empirical relationship of I_a and S) as given in equation (3.72).

The optimum values of λ obtained in the least squares fitting procedure were around 0.05 for most experimental plots which was observed by Hawkins *et al.* (2002). Therefore, it was decided to set it as 0.05 in this research. In some other studies similar low initial abstraction ratio are close to the suggested ratio of 0.05 (Hawkins *et al.*, 2002) have been reported (Mishra and Singh, 2004; Jiang, 2001).

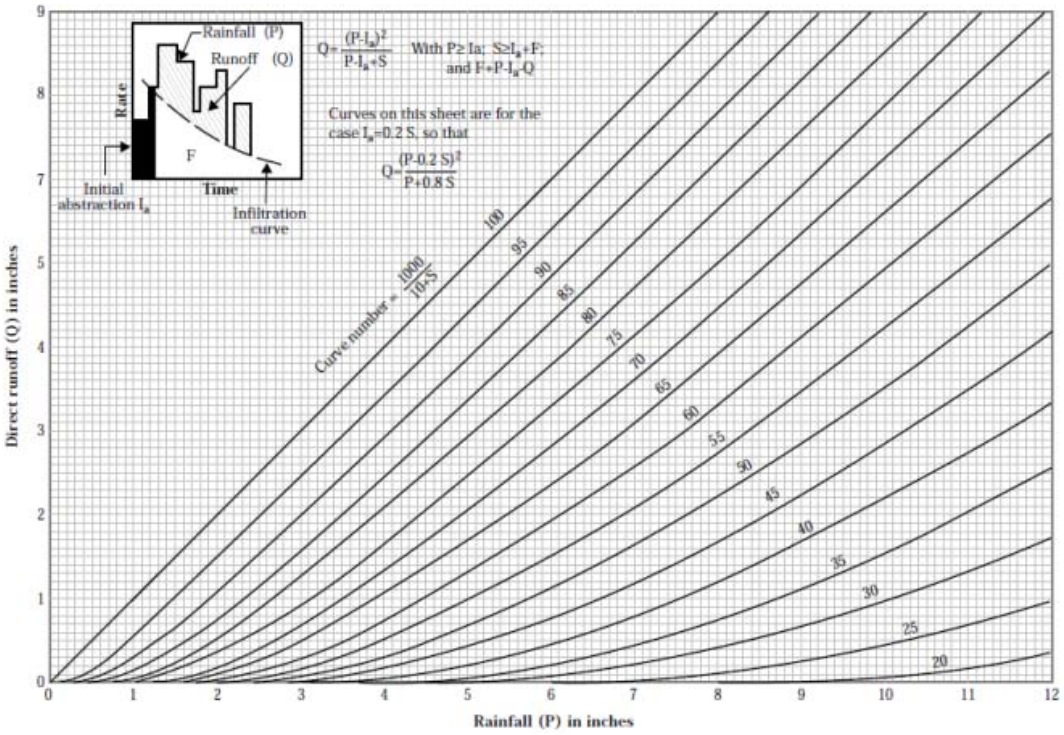

Figure 3.13 Curve number values based on SCS method to estimate initial abstractions.

The catchment's capability for rainfall abstraction is inversely proportional to the runoff curve number. For *CN* = 100, no abstraction is possible, with runoff being equal to total rainfall. On the other hand, for *CN* = 1 practically all rainfall would be abstracted, with runoff being reduced to zero as declared in **Figure 3.13**) (SCS, 1997).

The curve number *CN* value depends on hydrologic soil group and land use cover complex. The hydrologic soil groups are A, B, C, and D. They are classified based on the soil type and infiltration rate. So, based on the land use, soil type and infiltration rate, the curve number of the land use can be estimated as given in **Table 3.3**.

Table 3.3 Curve number values of the land use type

Land use	Soil group	Curve number
Forests	A	45
Field	B	71
Desert	A	63
Urban	B	86

(b) Transmission losses

Transmission losses are important not only for their obvious effect on flow reduction, but also as a source of ground water recharge to underlying alluvial aquifers. The variables that are considered useful in estimating the variation in the transmission loss included; 1-the flow volume at the upstream end of the reach, 2-channel antecedent condition, 3-chaneel slope, 4-channel bed material, the duration of the flow, 5-channel width. A regression model form was developed by Walter (1990) to assess transmission losses as given in Equation (3.73). Unit of the equation was converted from its original unit (acre-ft) into metric unit (cubic meter) as follows;

$$V_1 = 0.0257 V_A^{0.872} \tag{3.73}$$

where V_1 is the transmission loss for the first kilometer (m^3), V_A is the upstream flow volume (m^3).

The equation was adopted in this study to estimate transmission loss in each mesh based on the flow direction from the upstream to the downstream point.

A trial is made to develop a physical based model of transmission losses, we introduce this model as a combination between physical and empirical one as follow"

As well known, Taylor expansion of the function $f(x) = x^a \quad (a \neq 0) \quad around \quad x = 1$ is expressed as follow:

$$f(x) = f(1) + f'(1)(x-1)^2 + \frac{f''(1)}{2}(x-1)^2 + ... \\ \Leftrightarrow \quad x^a = 1 + a(x-1) + \frac{1}{2}a(a-1)(x-1)^2 + ... \tag{3.74}$$

We herein substitute x into $1+\varepsilon$ we get the following equation as:

$$(1+\varepsilon)^a = 1 + a\varepsilon + \frac{1}{2}a(a-1)\varepsilon^2 + ... \tag{3.75}$$

When we consider the condition of $\varepsilon \approx 0$, the above equation is approximately formulated as:

$$(1+\varepsilon)^a \approx 1 + a\varepsilon \tag{3.76}$$

Because the 2nd and higher order power ε^n is approximately recognized as a zero based on 1st order power ε.

The transmission loss ΔV subject to physical condition is calculated as:

$$\Delta V = \int_0^l kWTdx = kWTl \tag{3.77}$$

where, k is hydraulic conductivity, W is a river channel width, T is a travelling time and l is a travelling distance. The relationship between the transmission loss and the corresponding distance derived from the empirical data is expressed as:

$$\frac{dv}{dx} = -C_1 V^{C2} \tag{3.78}$$

The differential equation can be solved via a definite integration as:

$$\int_{V_0}^{V_1} V^{-C_2} dV = -C_1 \int_0^l dx \quad \Leftrightarrow \quad \frac{1}{1-C_2}\left(V_1^{1-C_2} - V_0^{1-C_2}\right) = -C_1 l \tag{3.79}$$

The solution is arranged as:

$$V_1 = \left\{V_0^{1-C_2} - (1-C_2)C_1 l\right\}^{\frac{1}{1-C_2}} \tag{3.80}$$

The transmission loss based on empirical aspects is obtained as expressed in equation (3.81).

$$\Delta V = V_0 - V_1 = V_0 - \left\{V_0^{1-C_2} - (1-C_2)C_1 l\right\}^{\frac{1}{1-C_2}} \tag{3.81}$$

Secondly, we reform the above equation as:

$$\Delta V = V_0 - \left[V_0^{1-C_2} \left\{ 1-\left(1-C_2\right) C_1 l V_0^{C_2-1} \right\} \right]^{\frac{1}{1-C_2}} = V_0 - V_0 \left\{ 1-\left(1-C_2\right) C_1 l V_0^{C_2-1} \right\}^{\frac{1}{1-C_2}} \quad (3.82)$$

We can approximately arrange the above equation subject to $1 >> \left(1-C_2\right) C_1 l V_0^{C_2-1}$ as:

$$\Delta V \approx V_0 - V_0 \left(1 - C_1 l V_0^{C_2-1}\right) = C_1 l V_0^{C_2} \quad (3.83)$$

The compatibility condition between physical-based and empirical-based approaches can originally be developed based on equations, (3.77) and (3.83) as follow:

$$kWTl = C_1 l V_0^{C_2} \quad \Leftrightarrow \quad k = \frac{C_1 V_0^{C_2}}{WT} \quad or \quad V_0 = \left(\frac{kWT}{C_1} \right)^{\frac{1}{C_2}} \quad (3.84)$$

Flow rate up to distance l can be calculated as represented in equation (3.83) as:

$$Q = \frac{V_l}{T} = \frac{1}{T} \left\{ V_0^{1-C_2} - \left(1-C_2\right) C_1 l \right\}^{\frac{1}{1-C_2}} \quad (3.85)$$

where, Q is a river flow rate.

From this equation, the value of the upstream and downstream points are claculated as:

$$Q_0 = \frac{V_0}{T} \quad (3.86)$$

$$Q_1 = \frac{1}{T} \left\{ V_0^{1-C_2} - \left(1-C_2\right) C_1 l \right\}^{\frac{1}{1-C_2}} \quad (3.87)$$

The abovementioned value of T is a traveling time of water transmission from upstream to downstream points. The approximation of T with the assumption of kinematic wave model is given as:

$$T = \frac{l}{v} = \frac{lhW}{Q_R} \quad \Leftrightarrow \quad lhW = Q_R T \quad (3.88)$$

where, v is a velocity, Q_R is a river flow rate. The motion equation of the kinematic wave model in river channels is used into equation (3.88). A depth of the wadi river is much small compared with W. Tthe following equation is obtained

as:

$$Q_R = \frac{\sqrt{I}}{n} W h^{\frac{5}{3}} \tag{3.89}$$

The continuum equation of the kinematic wave model in river channel is expressed as:

$$\frac{d(hW)}{dt} + \frac{dQ_R}{dx} = r(x,t).W \tag{3.90}$$

where $r(x,t)$ is an areal source term per unit time. The coupling equations (3.89) and (3.90) are equivalently transformed as follows:

$$\frac{dx}{dt} = \frac{d}{dh}\left(\frac{\sqrt{I}}{n} h^{\frac{5}{3}}\right) = \frac{\sqrt{I}}{n} h^{\frac{2}{3}} \tag{3.91}$$

$$\frac{dh}{dt} = r(x,t) \tag{3.92}$$

Let us suppose that $r(x,t)$ is uniformly constant as $p-1$, where p is a rainfall rate and i is an infiltration rate. From equation (3.92),

$$h - h_0 = (p-i).t \tag{3.93}$$

where h_0 is a river depth at a starting point of transmission losses, Substituting equation (3.93) into equation (3.91),

$$\frac{dx}{dt} = \frac{\sqrt{I}}{n}\left\{h_0 + (p-i).t\right\}^{\frac{2}{3}} \tag{3.94}$$

The equation (3.94) is calculated by integrals as expressed in equation (3.95).

$$x = \frac{3\sqrt{I}}{5n(p-i)}\left\{h_0 + (p-i).t\right\}^{\frac{5}{3}} \tag{3.95}$$

Under the condition $x = l$ and $t = T$, equation (3.95) is rewritten as:

$$l = \frac{3\sqrt{I}}{5n(p-i)}\left\{h_0 + (p-i).T\right\}^{\frac{5}{3}} \tag{3.96}$$

Therefore, the following solution is founded as:

$$T = \frac{1}{p-i}\left[\left\{\frac{5n(p-i)l}{3\sqrt{I}}\right\}^{\frac{3}{5}} - h_0\right] \tag{3.97}$$

And

$$h_1 = h_0 + (p-i).T = \left\{\frac{5n(p-i)l}{3\sqrt{I}}\right\}^{\frac{3}{5}} \tag{3.98}$$

Lets go back to the consideration of V and substitute equation (3.98) into equation (3.86).

$$V_0 = Q_0 T = \frac{\sqrt{I}}{n} W h_0^{\frac{5}{3}} . \frac{1}{p-i}\left[\left\{\frac{5n(p-i)l}{3\sqrt{I}}\right\}^{\frac{3}{5}} - h_0\right] = \frac{W\sqrt{I}h_0^{\frac{3}{5}}}{n(p-i)}\left[\left\{\frac{5n(p-i)l}{3\sqrt{I}}\right\}^{\frac{3}{5}} - h_0\right] \tag{3.99}$$

In the same way as:

$$V_1 = Q_1 T = \frac{5Wl}{3} . \left[\left\{\frac{5n(p-i)l}{3\sqrt{I}}\right\}^{\frac{3}{5}} - h_0\right] \tag{3.100}$$

Therefore,

$$\begin{aligned}\Delta V = V_0 - V_1 &= \frac{W\sqrt{I}h_0^{\frac{3}{5}}}{n(p-i)}\left[\left\{\frac{5n(p-i)l}{3\sqrt{I}}\right\}^{\frac{3}{5}} - h_0\right] - \frac{5Wl}{3} . \left[\left\{\frac{5n(p-i)l}{3\sqrt{I}}\right\}^{\frac{3}{5}} - h_0\right] \\ &= W\left\{\frac{\sqrt{I}h_0^{\frac{3}{5}}}{n(p-i)} - \frac{5}{3}l\right\} . \left[\left\{\frac{5n(p-i)l}{3\sqrt{I}}\right\}^{\frac{3}{5}} - h_0\right]\end{aligned} \tag{3.101}$$

When the infiltration rate, i, is equivalent to $\Delta V / lWT$ which indicates an averaged value in space and time as i_0,

$$\begin{aligned}&i_0 lT = \left\{\frac{\sqrt{I}h_0^{\frac{5}{3}}}{n(p-i_0)} - \frac{5}{3}l\right\} . \left[\left\{\frac{5n(p-i_0)l}{3\sqrt{I}}\right\}^{\frac{3}{5}} - h_0\right] \Leftrightarrow \frac{i_0}{p-i_0} l = \frac{\sqrt{I}h_0^{\frac{5}{3}}}{n(p-i_0)} - \frac{5}{3}l \Leftrightarrow \\ &i_0 = \frac{5}{2}p - \frac{3\sqrt{I}h_0^{\frac{5}{3}}}{2nl}\end{aligned} \tag{3.101}$$

If this resulting value of i_0 is conditioned before numerical simulations, the consistency and compatibility between empirical and theoretical models are then established. The value i_0 equals to the hydraulic conductivity k. Without observed data, the coefficient C1 and C2 can be identified from i_0 using equation (3.101). As a next consideration, substituting equation (3.101) into equation (3.83),

$$\begin{aligned} C_1 l V_0^{C_2} &= W\left\{\frac{\sqrt{I}h_0^{\frac{5}{3}}}{n(p-i_0)}-\frac{5}{3}l\right\}\cdot\left[\left\{\frac{5n(p-i_0)l}{3\sqrt{I}}\right\}^{\frac{3}{5}}-h_0\right] \\ &= Wl\frac{5npl-3\sqrt{I}h_0^{\frac{5}{3}}}{3\left(\sqrt{I}h_0^{\frac{5}{3}}-npl\right)}\cdot\left[\left(\frac{5}{2\sqrt{I}}\right)^{\frac{3}{5}}\left(\sqrt{I}h_0^{\frac{5}{3}}-npl\right)^{\frac{3}{5}}-h_0\right] \end{aligned} \tag{3.102}$$

Thus,

$$C_1 V_0^{C_2} = W\frac{5npl-3\sqrt{I}h_0^{\frac{5}{3}}}{3\left(\sqrt{I}h_0^{\frac{5}{3}}-npl\right)}\cdot\left[\left(\frac{5}{2\sqrt{I}}\right)^{\frac{3}{5}}\left(\sqrt{I}h_0^{\frac{5}{3}}-npl\right)^{\frac{3}{5}}-h_0\right] \tag{3.102}$$

The value of h_0 is the solution as the physical-based compatibility condition between surface runoff model and the empirical one given as equation (3.78).

$$\begin{aligned} i_0 = k = \frac{C_1 V_0^{C_2}}{WT} &= C_1\left(\frac{\sqrt{I}h_0^{\frac{5}{3}}}{n}\right)^{C_2}\cdot\left(\frac{W}{p-i}\right)^{C_2-1}\cdot\left[\left\{\frac{5n(p-i)l}{3\sqrt{I}}\right\}^{\frac{3}{5}}-h_0\right]^{C_2-1} \\ &= C_1\left(\frac{\sqrt{I}h_0^{\frac{5}{3}}}{n}\right)^{C_2}\cdot\left\{\frac{Wnl}{3\left(\sqrt{I}h_0^{\frac{5}{3}}-npl\right)}\right\}^{C_2-1}\cdot\left[\left(\frac{5}{2\sqrt{I}}\right)^{\frac{3}{5}}\left(\sqrt{I}h_0^{\frac{5}{3}}-npl\right)^{\frac{3}{5}}-h_0\right]^{C_2-1} \end{aligned} \tag{3.103}$$

The above equation denotes the physical-based compatibility condition between subsurface runoff model and the empirical one. The exact condition of equation (3.101) is presented below as:

$$C_1\left(\frac{\sqrt{I}h_0^{\frac{5}{3}}}{n}\right)^{C_2}\cdot\left\{\frac{Wnl}{3\left(\sqrt{I}h_0^{\frac{5}{3}}-npl\right)}\right\}^{C_2-1}\cdot\left[\left(\frac{5}{2\sqrt{I}}\right)^{\frac{3}{5}}\left(\sqrt{I}h_0^{\frac{5}{3}}-npl\right)^{\frac{3}{5}}-h_0\right]^{C_2-1} \quad (3.104)$$

$$=\frac{5}{2}p-\frac{3\sqrt{I}h_0^{\frac{5}{3}}}{n}$$

The coefficients of C1 and C2 are identified from equation (3.104), and then this result can give us a smooth simulation with hydrological backgrounds.

It is concluded that a physical based model for the consistency and compatibility between empirical (empirically proposed transmission losses) and theoretical (kinematic wave) models has been developed.

So, we can summarize the structure of modified hydro-BEAM as shown in **Figure 3.14**.

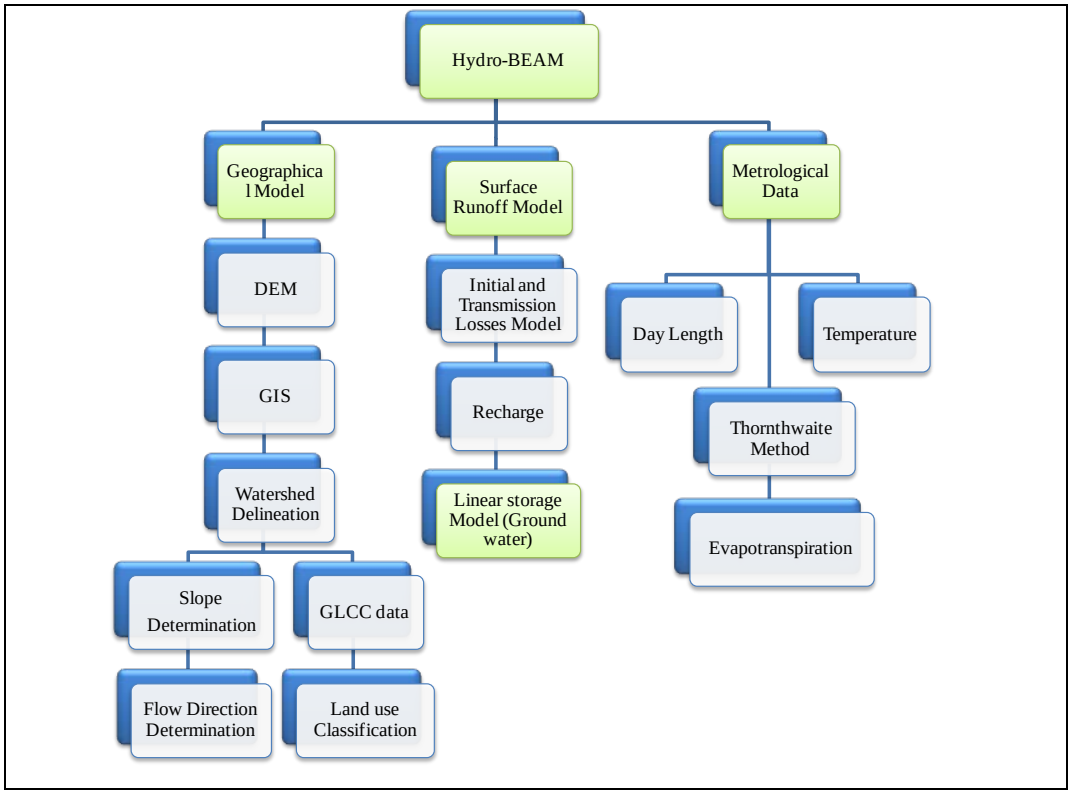

Figure 3.14 Flow chart of the modified Hydro-BEAM Structure.

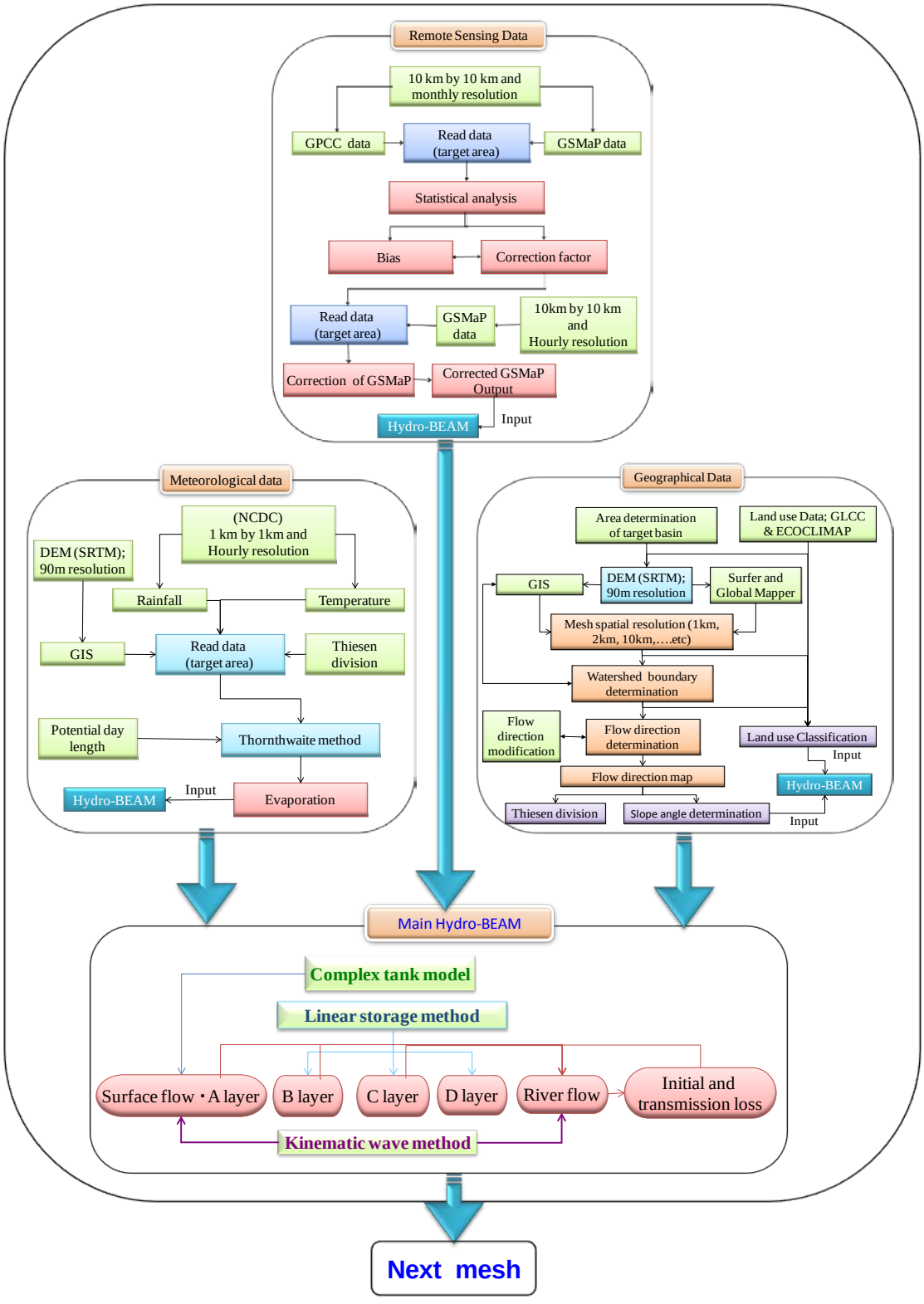

Figure 3.15 Flow chart of calculation processes of the modified Hydro-BEAM in wadi system.

The main constituents of Hydro-Beam are watershed modeling, climatic modeling, and the main program as shown in Figure 3.14. The calculation processes of Hydro-BEAM have been linked as depicted in the flow chart (**Figure 3.15)**. The first part is a flow chart of Satellite Remote Sensing Data (GSMaP Product) analysis. It is linking with Hydro-BEAM while the modelled mesh resolution about 1okm × 10km as in the Nile River, Egypt, 1km×1km as in wadi Elkhoud, Oman, or 2km×2km as in wadi Assiut, Egypt, etc. The second part is a flow chart of geographical data process to determine flow direction map, slope angle, and land use types. The third part is a flow chart of calculation of evaporation by Thornthwaite method using meteorological data of National Climatic Data Center (NCDC).

Chapter Four

Hydrological Simulation of Distributed Runoff of Wadi System

4.1. Introduction

Hydrological modeling and approaches are so important and desperately needed in the wadi system in the arid and semi-arid regions due to the difficulty of data acquisition as well as the difficulty of hydrological modeling of surface and sub surface flow at the wadi system due to the high variability of rainfall and flow in both time and space. In this work a trial is made to simulate and evaluate surface and subsurface runoff in the wadi system, in addition to understand the flow characteristics and the factors affecting on its behaviors. Throughout this study, a comparative study has been done between some wadi basins in the Arabian regions such as Egypt, Oman, and Saudi Arabia.

4.2. The Target Wadi Basins

Due to the aforementioned characteristics and problems of the wadi system, some wadi catchments were selected from the Arabian countries for application such as wadi Alkhoud in Oman, wadi Ghat in Saudi Arabia, and wadi Assiut in Egypt. They were nominated due to their importance not only as water resources for their habitants but also as suffering regions for flash flood threat as well as the spreading of urbanization towards the deserts to find new developed areas for the increasing of population. In other words, due to the direct and major impact on the

wadi system on security of life of urban and rural populations in such regions.

4.2.1. Wadi Al-Khoud in Oman.

Oman is one of several countries located in an arid zone which is subjected to infrequent and unexpected flash floods events. Wadi Al-Khoud in Oman is located in the northern part of Oman and at the western-north part of Muscat, the capital of Oman. The downstream of catchment is towards northeast Gulf of Oman. It is occupied between Long. 57° 58′ W & 58° 02 E ′ and Lat. 24° 00′ N & 23° 00 S ′ as shown in the location map **Figure 4.1**.

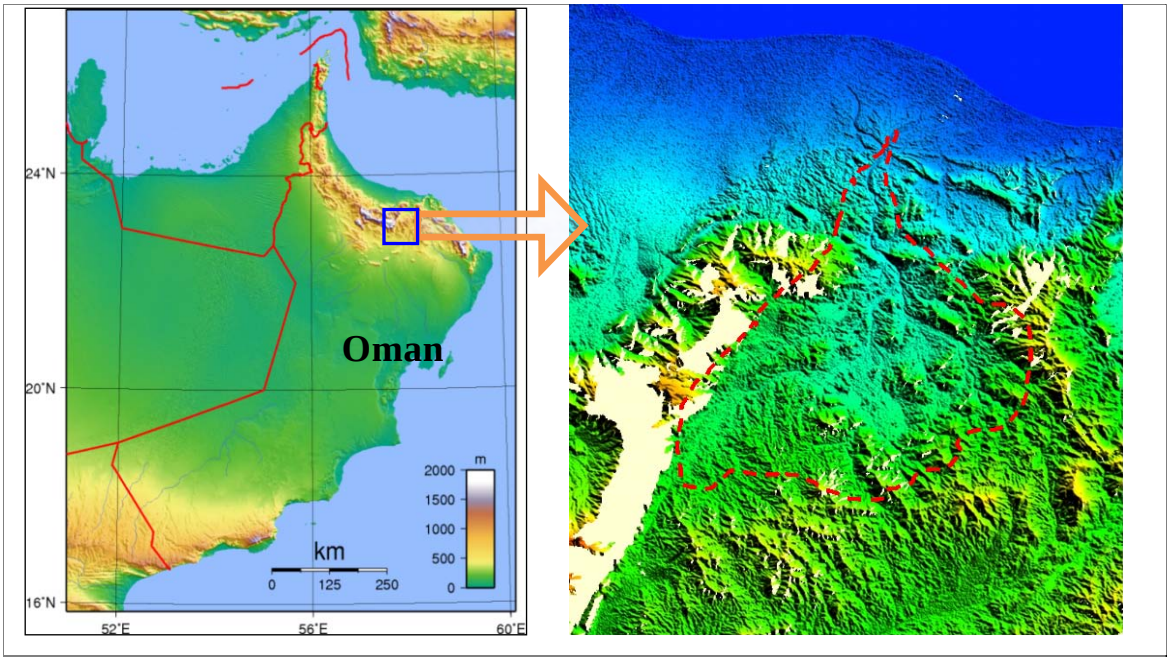

Figure 4.1 Location map and DEM of W. Al-Khoud watershed, Oman.

The total area of its catchment is 1874.84 Km^2 as calculated from SRTM DEM, 100 m resolution through ArcView GIS. It is characterized by arid zone characteristics and its importance as the main water resources for use in this area, especially for agriculture and domestic purposes. The topographical conditions of it show that the general slope is from south to the north with the maximum

elevation more than 2000m which imply the steepness of the catchment slope.

4.2.2. Wadi Ghat in Saudi Arabia.

Wadi Ghat watershed is a sub-catchment of Wadi Yiba, one of the Saudi Arabian basins in the south-western part of the kingdom, and drains from the Asir Mountain Range towards the Red Sea as shown in **Figures (4.2a, 4.2b)**. It is located between Long. 41° 46′ W & 42° 10 E ′ and Lat. 19° 20′ N & 19° 00 S ′. The total area of its catchment is 649.55 km2 as calculated from DEM through GIS. It is characterized by arid zone characteristics, and approximately 90 percent of the catchment comprises of rock outcrop and shallow soils. Annual precipitation is 322 mm. Intensive convectional rain storms produce typical flash floods with steep rising limbs and rapid recession to zero base flow.

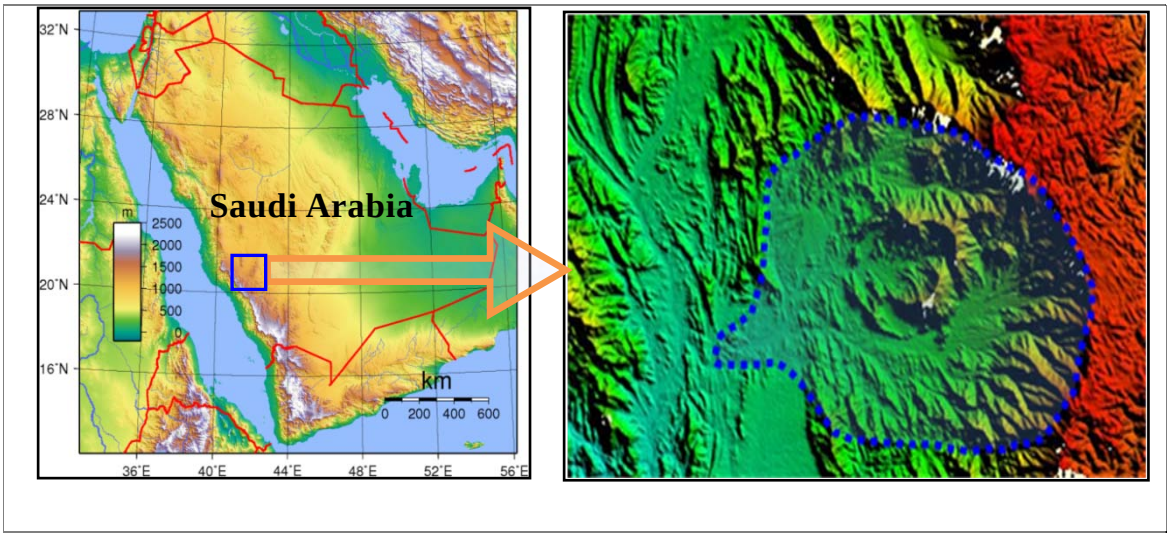

Figure 4.2a Location map and DEM of Wadi Ghat Watershed, Saudia Arabia.

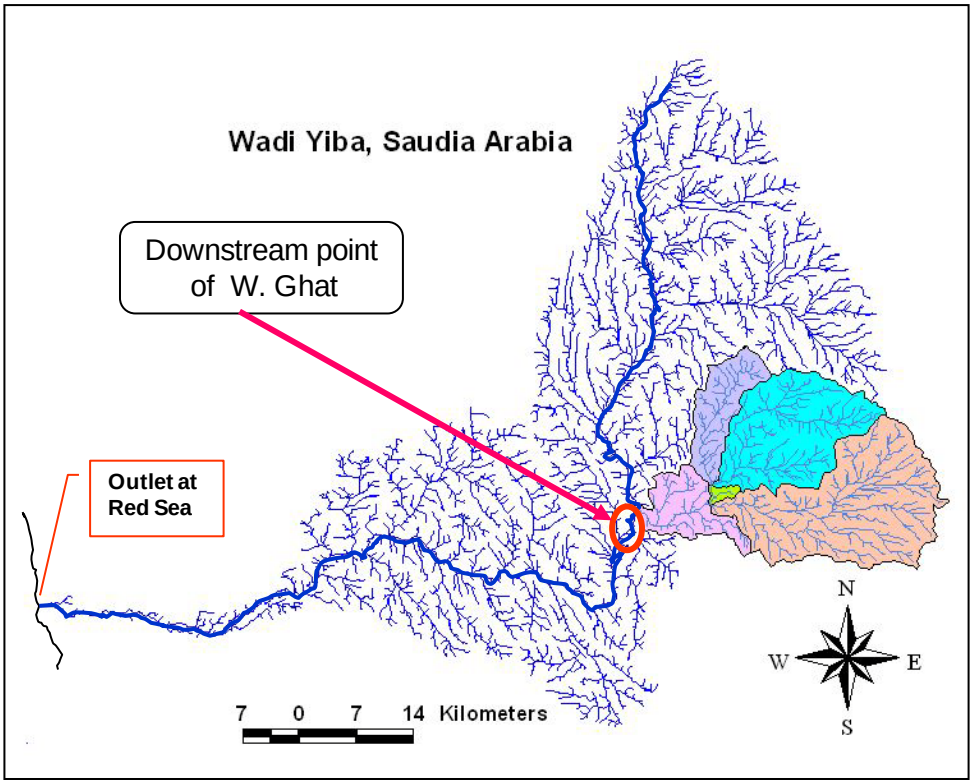

Figure 4.2b Drainage pattern and catchment of wadi Ghat watershed as sub-catchment of wadi Yiba, Saudia Arabia.

Rainfall in Saudi Arabia varies with place and time. Sporadic rainfall, sometimes with very heavy precipitation, may occur during short unpredictable intervals in limited areas, followed by long dry periods. Precipitation during such storms may equal the annual precipitation for the region. Precipitation of 109.2 mm was recorded during a twenty-four hour period in Sharjah where the average rainfall is 107 mm. The principal rainfall occurs between November and March/April, with the greatest frequency of rain being during February and March. There are two sources of rain, the most important being winter cyclones which traverse the eastern Mediterranean.

4.2.3. Wadi Assiut in Egypt

Wadi Assiut watershed (**Figure 4.3**) is located in the Eastern Desert of Egypt. It is one of the most populous countries in Africa. The great majority of people estimated 80 million people live near the banks of the Nile River and in the Nile Delta, in an area of about 40,000 square kilometers, where the only arable agricultural land is found. Thus finding and proposing new and appropriate regions to overcome the ever-increasing of population is urgently needed. Wadi Assiut watershed is located between Long. 32°30′ E & 31°12′ W and Lat. 27°48′ N & 27°00′ S, and it is one of sub-basins of the Nile River.

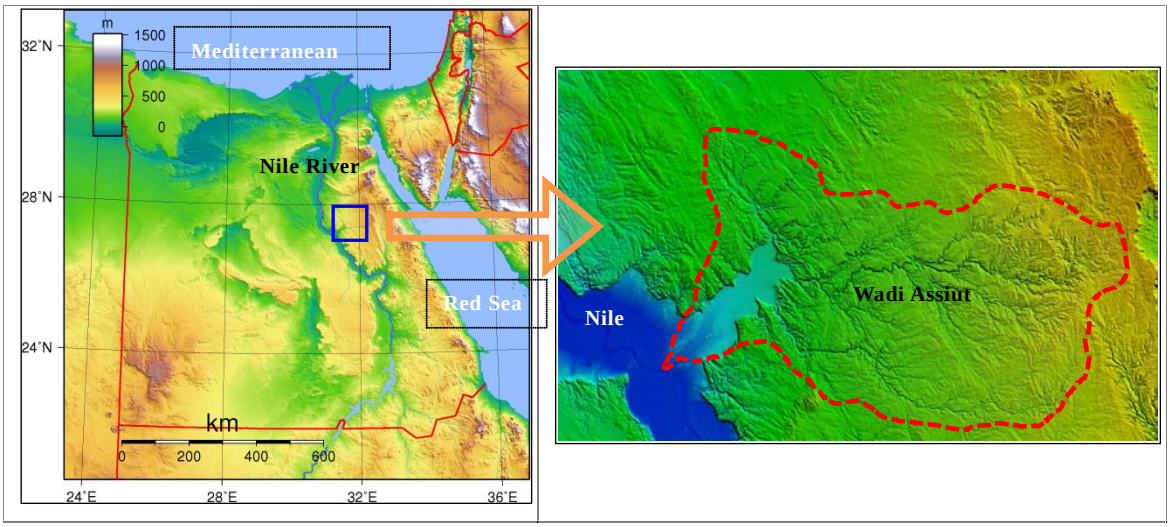

Figure 4.3 Location map and DEM of W. Assiut

The total area of Wadi Assiut catchment is 7,109 km^2, the perimeter is 496.91 Km and the length of the main channel is 165.09 km. Most of its area is a desert except some part of urbanization, and very small areas of agriculture which are closed to Assiut city along the Nile River Basin. Study area is important due to the propagation of populations and consequently the demand of water resources for agricultural, domestic, social and industrial activities.

Wadi Assiut catchment has undergone a number of improvements over the past centuries, where many of the past studies were applied and many of projects established there due to its importance. Presently, the establishment of new town, which will be in the near future crowded by populations and consequently the importance of hydrological modeling for water resources management and flood threat control, is so essential.

4.3. Numerical Simulation and Discussions

Hydro-BEAM is a multilayer hydrological model, four layers (A-D); A-Layer is composed of the surface and soil surface layer. Kinematic wave model and Manning equation are used to estimate the surface runoff and roughness coefficient in each mesh of the watershed basin. B-D-Layers are subsurface layers, which are evaluated using linear storage model, with the assumption of that the flow in both of B and C layers is toward the river, but D-layer is considered as groundwater storage. It makes the ground-water zone which does not exert influence in river flow. When storage water content reaches to thickness and becomes saturated state, water content flows into the upper layer of model as returned style.

Modeling processes and programming were accomplished using programming language of FORTRAN. Hydro-BEAM consists mainly of three main modeling parts; climatic modeling, watershed modeling and the main program modeling. The simulation periods are chosen based on the availability of observed data in the target basins where the geographical and climatic data of 2007 (two rainfall events) are used in wadi Al-Khoud. Also, the simulation have been done for one event of 1982 (one rainfall event) in wadi Ghat and one event of 1994 (one rainfall event) in wadi Assiut.

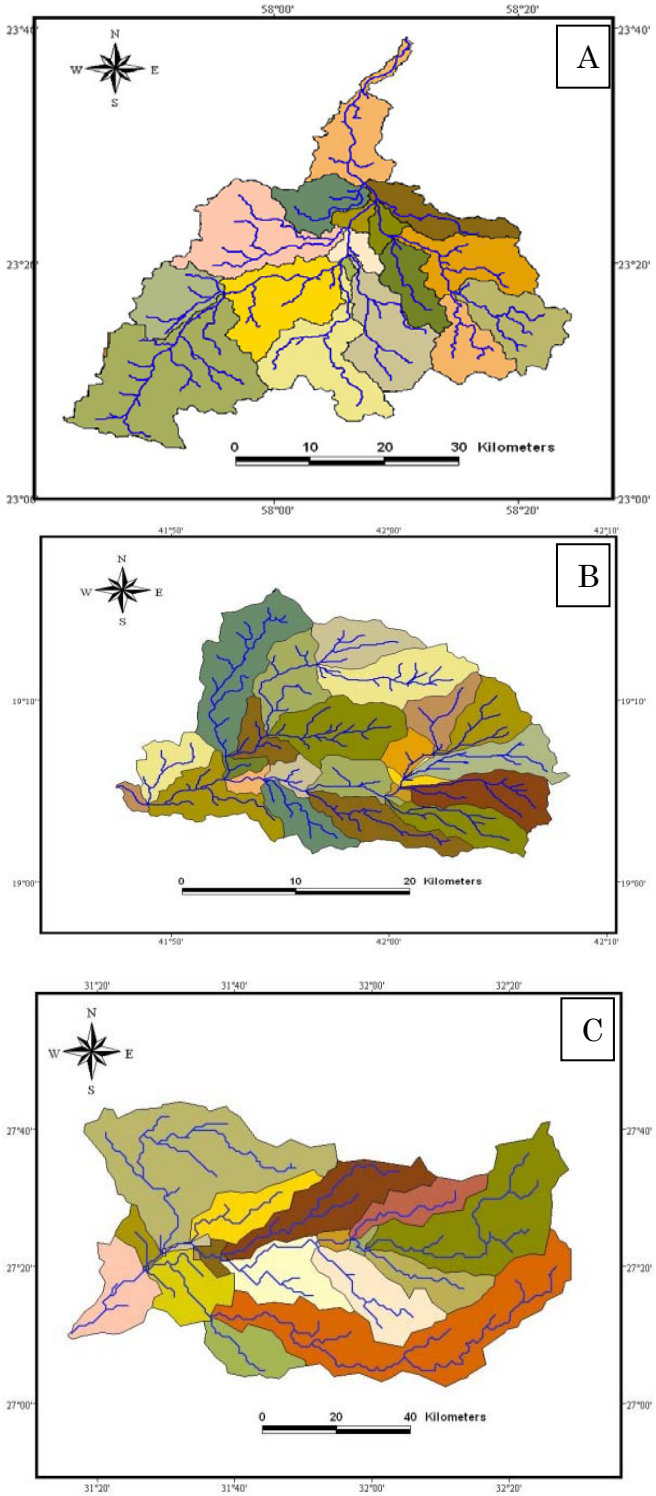

Figure 4.4 Watershed delineation and stream network determination of wadi Al-Khoud (A), wadi Ghat (B), wadi Assiut (C).

4.3.1. Watershed Modeling

The watershed modeling of the selected Wadis is achieved based on DEM (SRTM, 100 m resolution) by processing it using ArcView GIS. Watershed delineation and network determination of Wadi Al-khoud, Wadi Ghat, and Wadi Assiut are processed as depicted in **Figures (4.4A, 4.4B, and 4.4C)**. It is founded that the maximum elevation in W. Al-Khoud and W. Ghat is more than 2000 m elevation but in W. Assiut is approximately 900 m, on other words; they are steeper than W. Assiut.

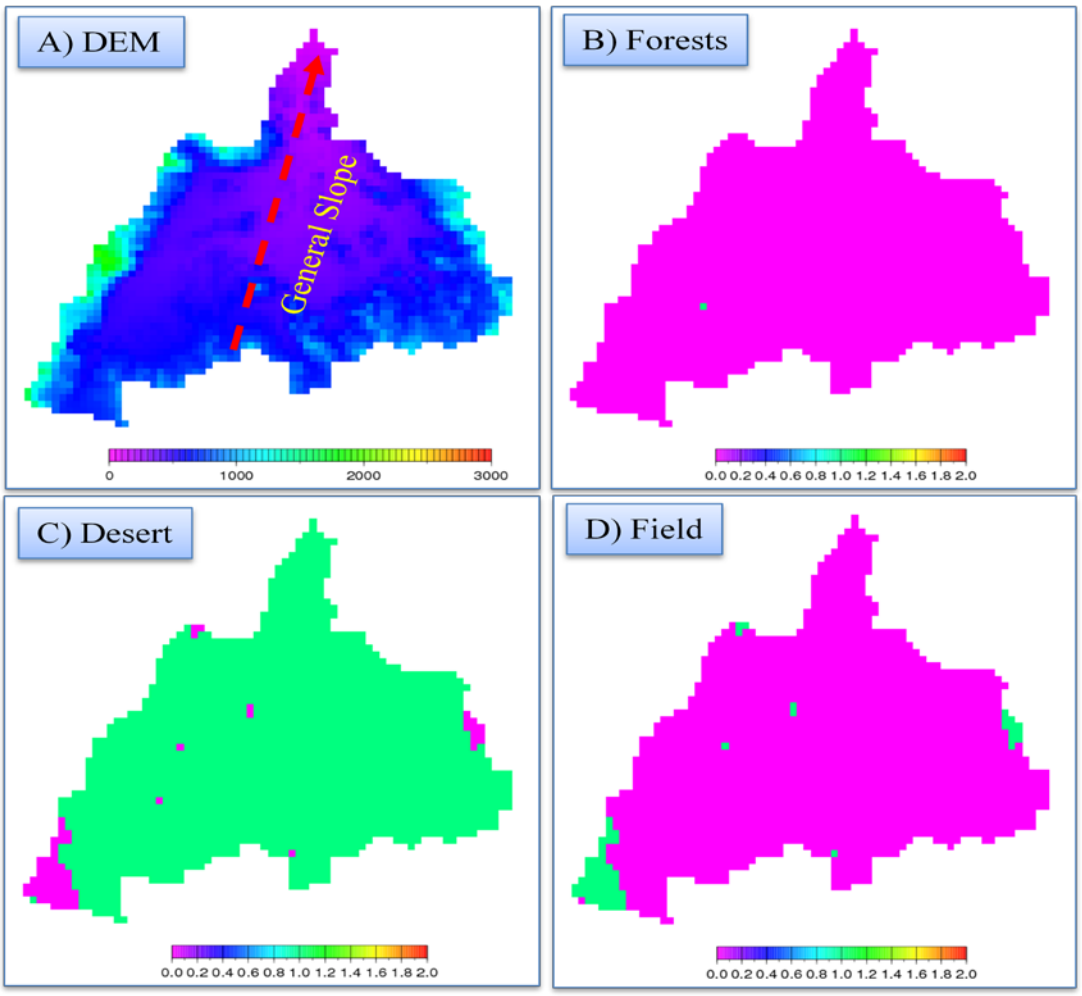

Figure 4.5 Digital elevation model (DEM) (A), and distribution maps of forests (B), field (C), desert (D) of Wadi Al-Khoud

4.3.2. Land use classification

Land use types can be reclassified from using GLCC (http://edc2.usgs.gov/glcc/glcc.php) data or ECOCLIMAP (http://www.cnrm.meteo.fr/gmme/PROJETS/ECOCLIMAP/frame_text_ecoclimap.html#licence) data into five categories. Land use types in the arid regions were distinguished into the flowing five categories as follow; forests, field (paddy field & field), desert, city or urban areas and Water. The results of land use distribution in the target basins were depicted as Forests, field, desert, city, and water for W. AL-Khoud, W. Ghat, and W. Assiut as shown in **Figures (4.5, 4.6, and 4.7)**.

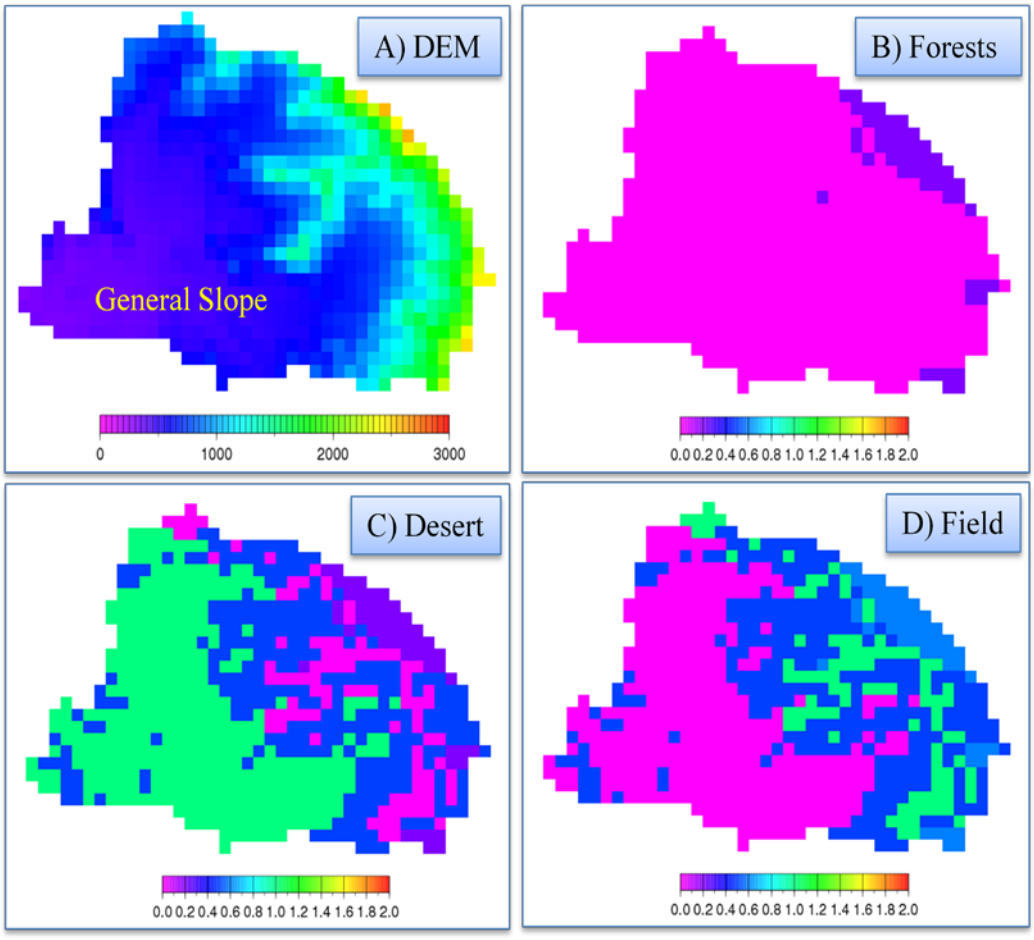

Figure 4.6 Digital elevation model (DEM) (A), and distribution maps of forests (B), field (C), desert (D) of Wadi Ghat

From the distribution maps of land use types, it was found that the forests, urban and water are limited in the target wadi basins except in some small parts. Field land use type is distributed in some parts in the wadis especially at the vicinity of downstream. On the other hand, the majority of wadis are desert which reveal the aridity conditions of these regions.

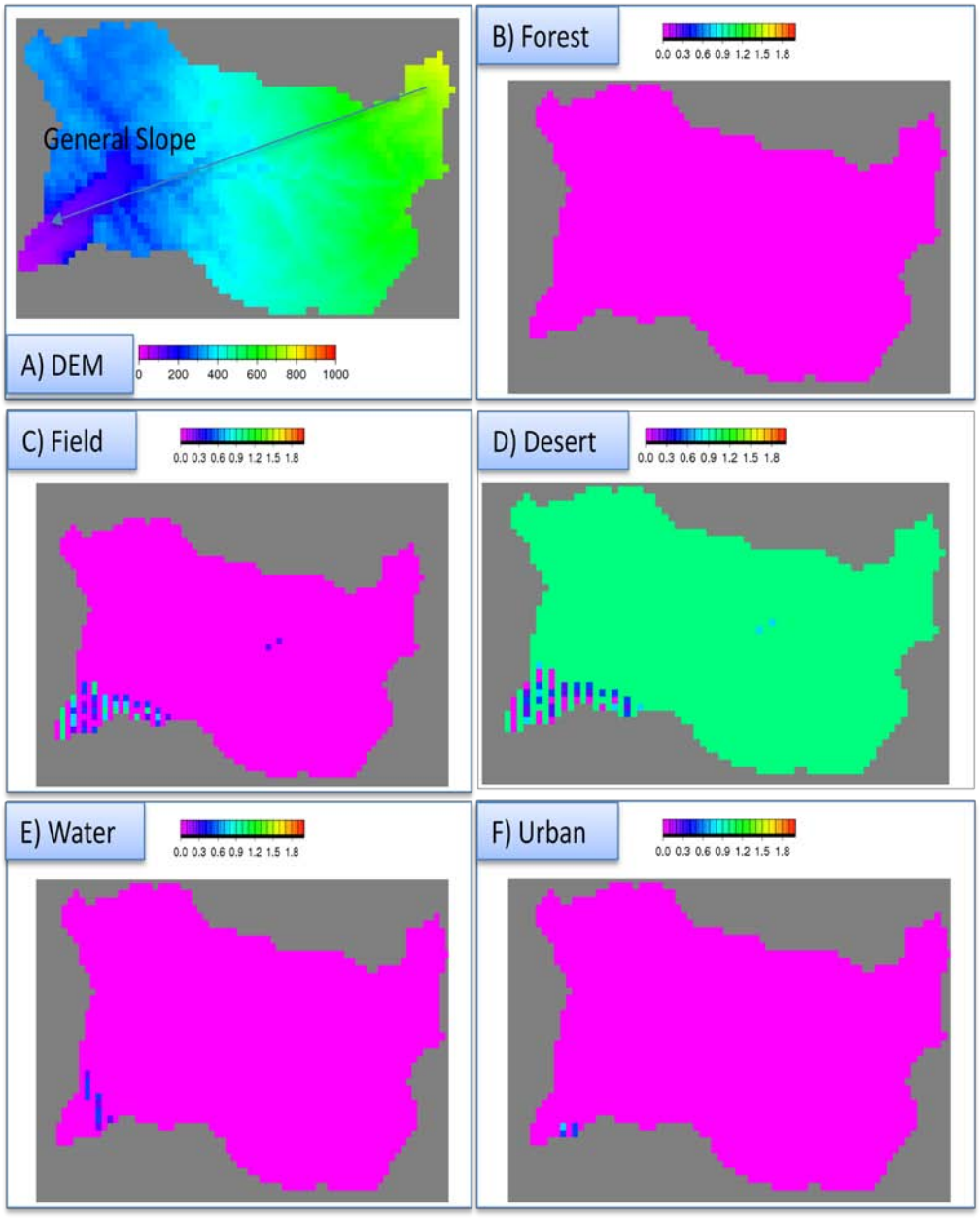

Figure 4.7 Digital elevation model (DEM) (A), and distribution maps of forests (B), field (C), desert (D), city (E), water (F) of Wadi Assiut

4.3.3. Climatic Data

The climatic data of the three catchment areas from NCDC (National Climatic Data Center) have been used as input data to Hydro-BEAM. Temperature data and day length are used in Thowrnthwaite method to estimate evaporation. Rainfall events are showing the high variability in space and time in the studied regions. As well known, rainfall is the main input in the hydrological models of runoff and it has the largest effect on the conditions of runoff hydrographs. The more frequent events the highest discharge peaks with longer duration of flow.

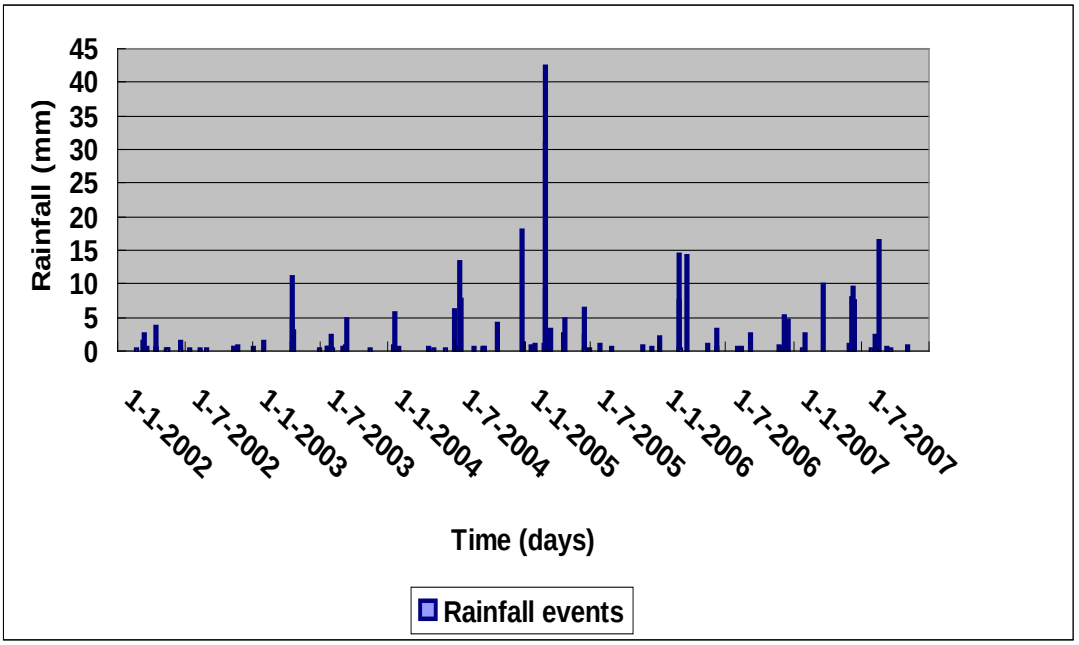

Figure 4.8 Hydrograph of rainfall events of W. Al-Khoud (2002- 2007)

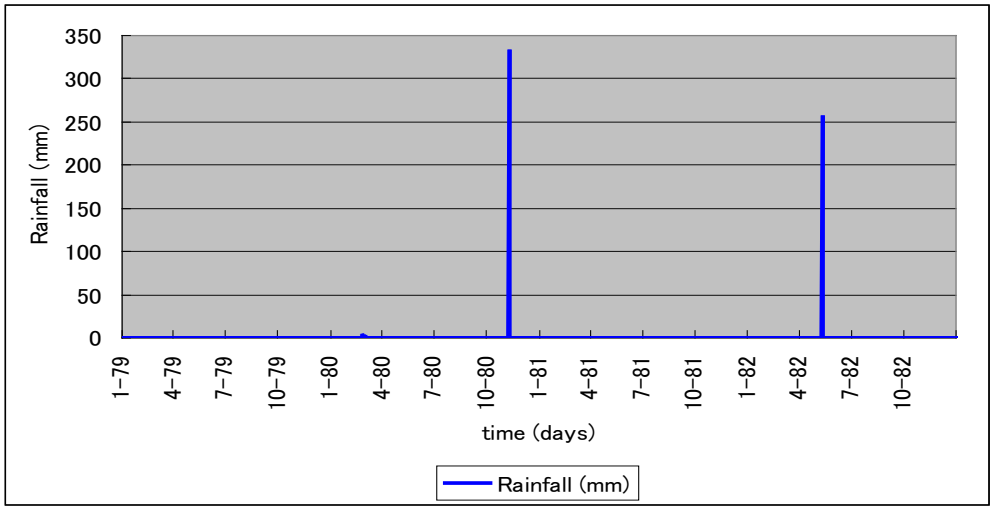

Figure 4.9 Hydrograph of rainfall events of W. Ghat from 1979-1982

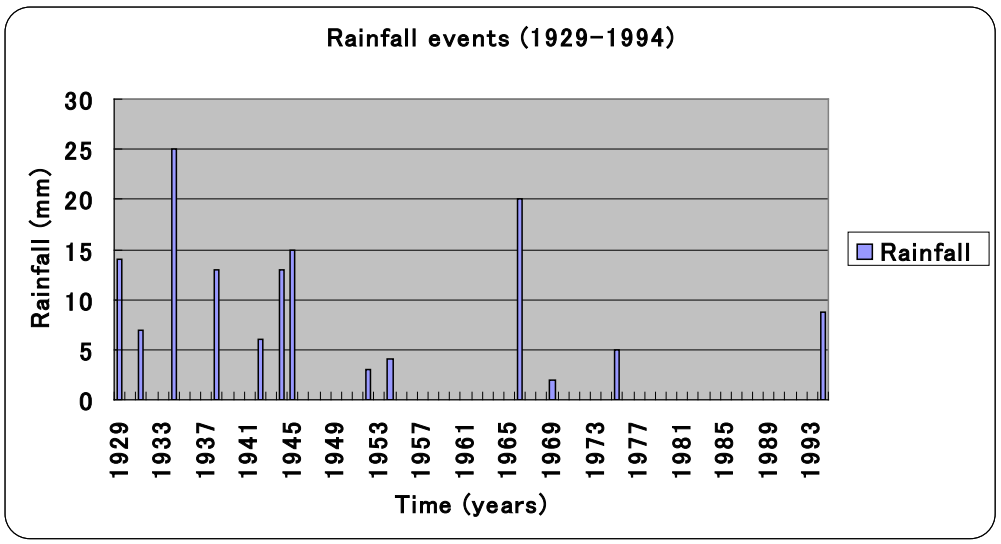

Figure 4.10 Hydrograph of rainfall events in wadi Assiut from 1929-1994, where the average of events one event every five years

The rainfall events charts showed that the average of rainfall events in W. Al-Khoud are multiple events every year which are more frequent than W. Ghat where it is one event every two years. But in W. Assiut is one event every five years as shown in **Figures 4.8, 4.9, and 4.10**.

The aforementioned analysis is based on the available data and these conditions might be different if another historical data is considered. Rainfall

events reflect the degree of aridity where W. Assiut more arid than the other two wadis.

4.4. Wadi Al-Khoud Simulation and Calibration

The surface flow discharge in arid regions is characterized by behaviors which are different from the humid areas. It is showing short time for starting and finishing the flood event, in other words, it is extremely steep rising and rapid recessing during the same event. In addition to, there is a lag time between the rainfall hyetographs and runoff hydrographs but it is very short.

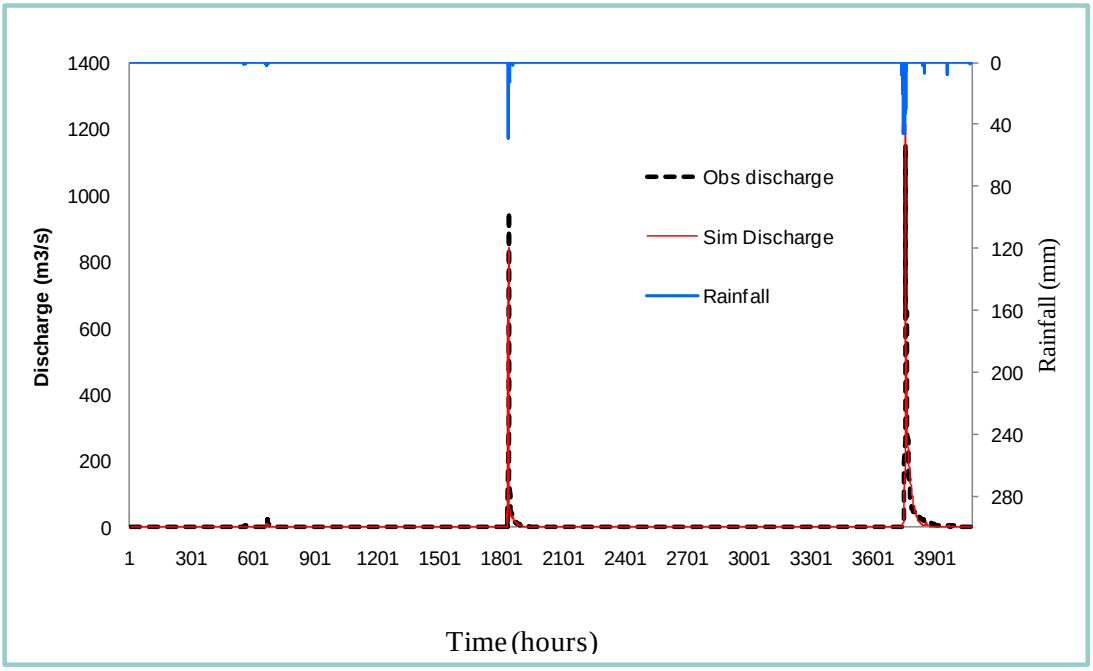

Figure 4.11 Hourly hydrographs of simulated and observed discharges in wadi Al-Khoud during three infrequent events of rainfall.

In this work, surface runoff was estimated in wadi Al-Khoud using the climatic and topographical data of one year (2007) due to the availability of observed runoff data; however they include some missing data. The simulated

results of discharge are showing a reasonable fitting with the observed ones. One of the most important merits of this work is evaluating multiple consequent storm events in spite of their including long no rainy periods as well as the time difference between the events is almost big. The simulated hydrographs of the strong rainfall events were carried out illustrating the characteristics of runoff in wadi basins very well as depicted in **Figure 4.11.**

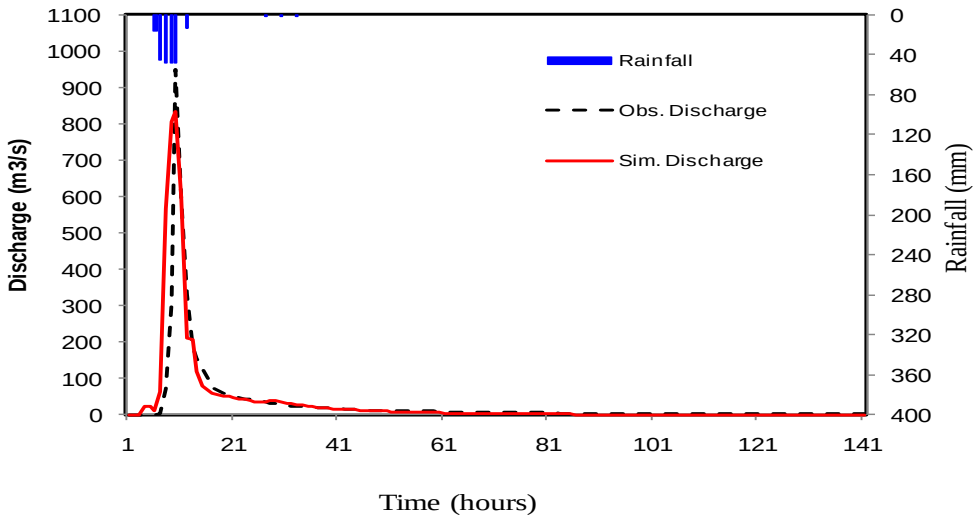

Figure 4.12 Hourly hydrographs of simulated and observed discharges in wadi Al-Khoud during the event (Mar. 18- 2007)

The first event is strong storm during (Mar. 18- 2007), where the maximum peak of the observed runoff is 950 m^3/s and the maximum peak of the simulated runoff is 838 m^3/s indicating satisfied fitting between both of them however there is underestimate in the peak value of simulated discharge as shown in **Figure 4.12**.

The third event is also strong storm during (Jun. 6- 2007). The maximum peaks of the observed and simulated hydrographs are 1185 m3/s and 1200 m^3/s respectively as declared in **Figure 4.13**.

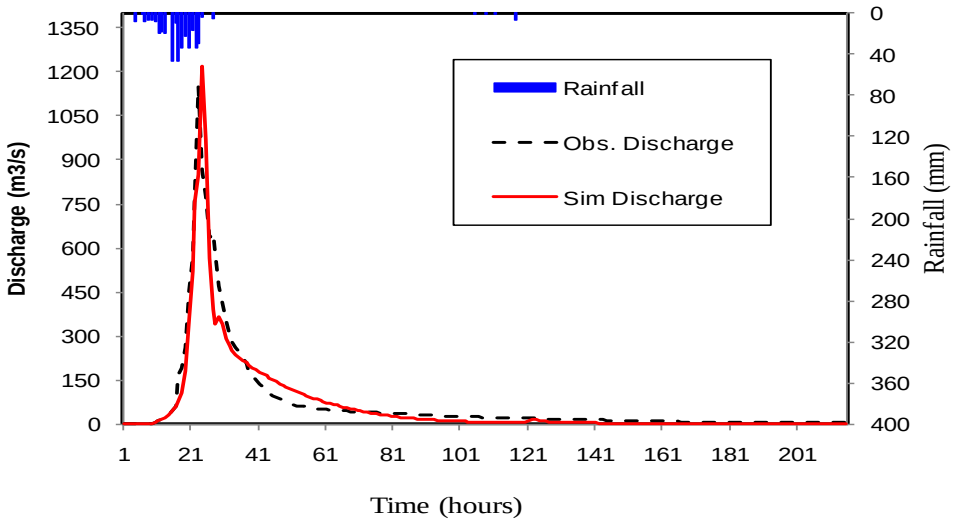

Figure 4.13 Hourly hydrographs of simulated and observed discharges in Wadi Alkhoud during the event of (Jun. 6- 2007)

From these results of numerical simulation of rainfall-runoff modeling, there is a remarkable agreement between both of simulated and observed hydrographs of discharge in W. Al-Khoud which reflects an appropriate performance of the proposed approach to predict or forecast the future events in wadi system.

Furthermore, the characteristics of wadi runoff were evaluated in this research and they were concluded as follow:

- Both of hyetographs and hydrographs are not simultaneous, but there is a time lag in the hyetograph peaks with respect to hydrograph peaks.
- Hydrographs starting and cessation time is so short, it takes some hours.
- The model parameters of wadi system were identified based on these results where the average of runoff coefficients fluctuates between 0.608 and 0.653 for desert and 0.135 for forests. Roughness coefficient also fluctuates in the range from 0.02 to 0.07 for the different kinds of land use as listed in **Table (4.1)**.

The distribution maps of surface runoff in Wadi Al-Khoud reveal the characteristics of wadi flow during the different stages of the hydrographs. For

instance, at the early stage of flow or rising of the hydrograph limb toward the maximum peak, discontinuously surface flow appeared and with increasing the flow rate, these phenomena of discontinuously surface flow will be connected when it reaches to the maximum flow.

Then, in the stage of ascending of hydrograph, the discontinuous occurrence of surface flow will appear again until the flow will be zero flow. The discontinuous surface flow phenomena which appeared in the wadi system was declared in both space and time as shown in **Figure 4.14**.

Transmission losses were simultaneously evaluated with runoff simulation by using Walter's equation. The results of simulation reveal that transmission losses are affected by the volume of surface runoff as evidence that the rate of losses is linearly related to the volume of surface discharge which is similar to the conclusion of Walters (1990) and Jordan (1977). The distribution maps of transmission losses show the same behaviors as runoff due to the relationship between both of them which reflects the discontinuous occurrence as shown in **Figure 4.15**.

A sensitivity analysis of the model parameters have been done to get the optimal solution by trial-error calibration method. The optimal calibrated results show that RMSE= 14.580 and R2 =0.8897 which imply the reasonable model performance in terms of matching surface runoff volume, peak flow and time to peak for the selected period of simulation. These results declared that performance of the modified hydro-BEAM can be used in arid regions with respect of the identified parameters of the wadi system. Based on this sensitivity analysis, the model parameters have been listed in **Table (4.1)**

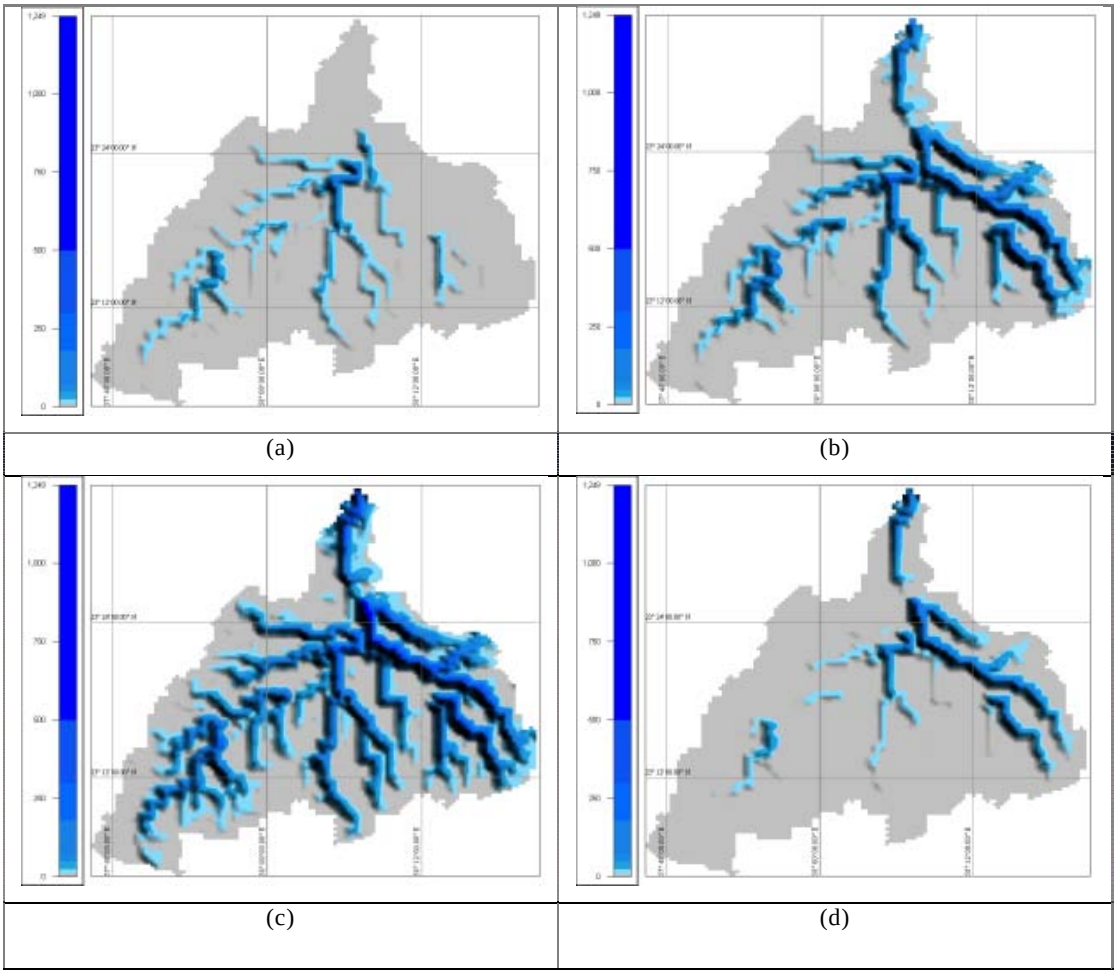

(a) (b)

(c) (d)

Figure 4.14 Distribution maps of surface runoff of event of (Mar. 18- 2007) in W. Al-Khoud; (A) Early stage of surface flow, ; (B) hydrograph is rising toward the maximum peak of discharge; (C) reaching to the maximum of distribution; (D) starting the recession of surface flow to zero flow.

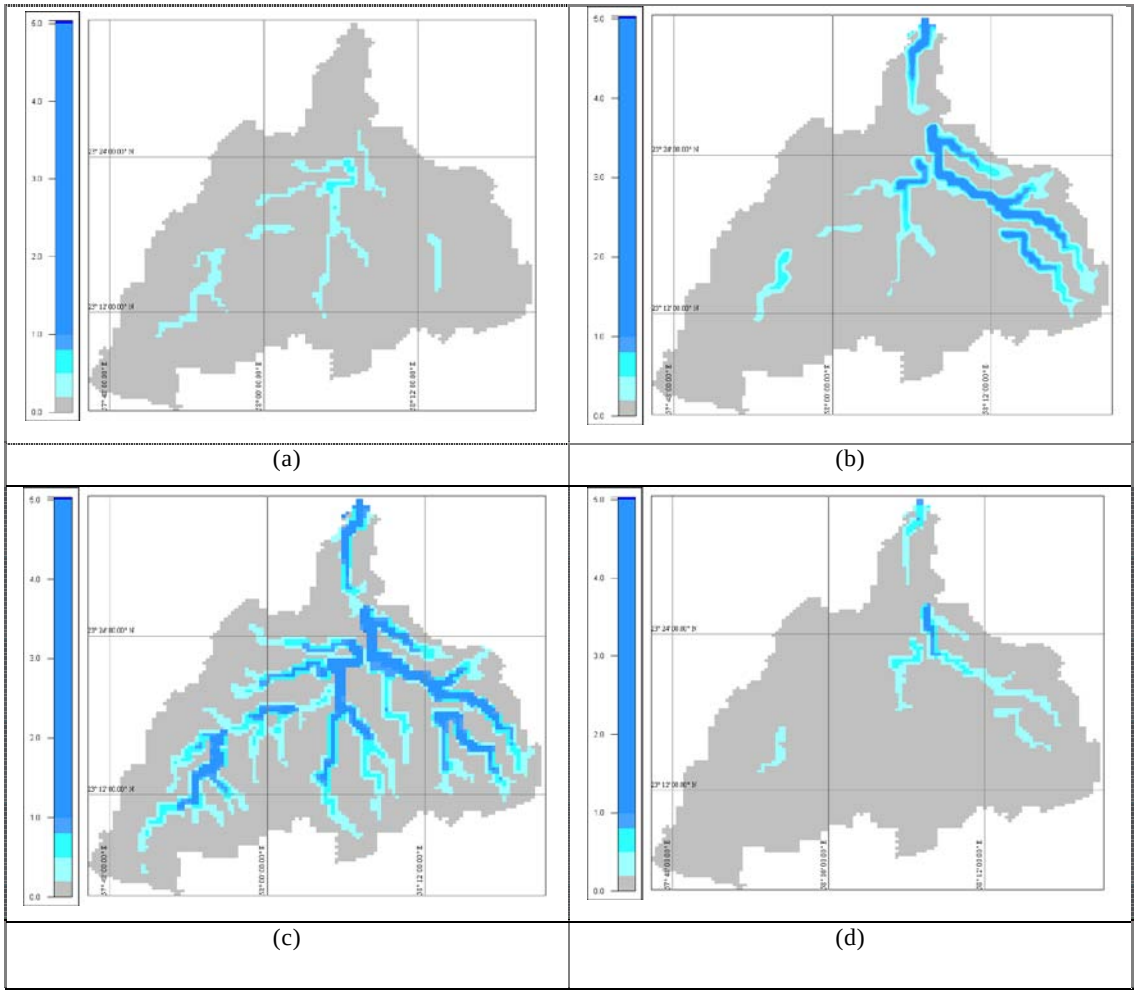

Figure 4.15 Distribution maps of transmission losses of event of (Mar. 18, 2007), (a) Early stage of transmission losses, (b) hydrograph is rising toward the maximum peak of transmission losses, (c) reaching to the maximum of distribution; (d) starting the recession of transmission losses to zero value.

Table 4.1 Calibrated parameters of HydroBEAM of arid regions

Parameters		Identification	units
Horizontal coefficient of permeability	B-Layer	0.58	d^{-1}
	C-Layer	0.004	d^{-1}
	D-Layer	0.03	d^{-1}
Vertical coefficient of permeability	B-Layer	0.4	d^{-1}
	C-Layer	0.001	d^{-1}
Layers Thickness	A-Layer	0.255	m
	B-Layer	2.500	m
	C-Layer	3.500	m
	D-Layer	10.000	m
Equivalent roughness coefficient	Desert	0.07	$m^{-1/3}s$
	River channel	0.026	$m^{-1/3}s$
Runoff coefficient	Desert	0.617	
Porosity	B-Layer	15.0	%
	C-Layer	15.0	%
	D-Layer	15.0	%
Finite difference interval	Spatial finite difference interval	500.000	m
	Time finite difference interval	200.000	Sec.

4.5. Wadi Ghat and Wadi Assiut Simulation

The proposed approach is also applied in terms of the comparative study between both of W. Ghat in Saudi Arabia, and in W. Assiut in Egypt as well as W. Al-Khoud, but the lack of observed data. W. Ghat and W. Assiut simulation results exhibit the same characteristics of runoff at W. Al-Khoud. Surface runoff hydrographs show steep rising and rapid ascending where the maximum peaks of discharge are $36m^3/s$ and $12.52m^3/s$ respectively. However, the time to peak of discharge and duration of flow are much longer in wadi Assiut than those of W. Al-Khoud and W. Ghat because the catchment area is larger and the catchment slope is gentler as shown in Figure 4.16 and Figure 4.17. From the available climatic data, the average of rainfall events in W. Al-Khoud is multiple occurring every year which are more frequent than those of W. Ghat and W. Assiut which is one event every two years and one event every five years.

Throughout the comparative studies between the three wadi basins, it is clear that they are exhibiting similar behaviors concerning surface runoff characteristics where surface runoff hydrographs show steep rising and rapid ascending. Moreover, they are depicting discontinuous surface flow at the early and lately stages of rising and ascending of hydrographs. The runoff behaviors are extremely affected by some factors such as the catchment area and slope which have a significant effect on the peak of discharge, the time to the peak, and the duration of flow. For instances, in W. Al-Khoud and W. Ghat, the area is smaller than W. Assiut but the discharge is higher at the downstream points of both of them because they are steeper than W. Assiut which have a significant effect on the travel time of water flow to reach the outlet point and consequently the peak discharge time to peak will be earlier than of wadi Assiut.

Also, the catchment area of W. Assiut is larger than the other two catchments which imply that the travel time of flow will be longer in W.Assiut than the others. Duration of flow is also variable as reported in **Table 4.2** where in W. Assiut, it is

longer than the other two wadis, but the flow is low comparing with the others due to the catchment characteristics as prescribed.

The distribution maps of surface runoff in wadi Assiut show the characteristics of wadi flow during the different stages of the hydrographs as similar as wadi al-Khoud and W.Ghat. They are depicting discontinuously surface flow at the early and late stages of rising and ascending of hydrographs (**Figure 4.18, Figure 4.19**).

Transmission losses in the studied wadis have been estimated simultaneously with runoff simulation by using Walter's equation. The results of simulation reveal that transmission losses are affected by the volume of surface runoff as the evidence that the rate of losses is linearly related to the volume of surface discharge. That means that they are very important as the main source of ground water recharge in the arid regions. Walters (1990) provided the evidence that the rate of loss is linearly related to the volume of surface discharge. These results ensure that there is linear relationship between both of surface flow volume and transmission losses in the wadi system.

The distribution maps of transmission losses depict the same behaviors as runoff which reflects the effect of surface flow on the transmission losses. You can see the discontinuous occurrence of transmission losses in Wadi Assiut as depicted in **Figure 4.20**.

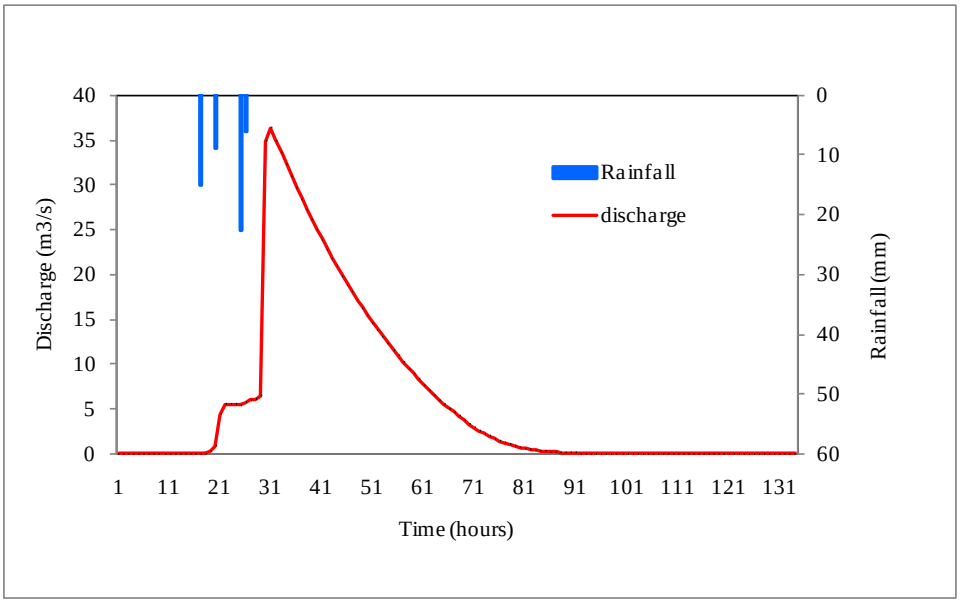

Figure 4.16 Hourly hydrograph of simulated discharge in W. Ghat during (May 11, 1982).

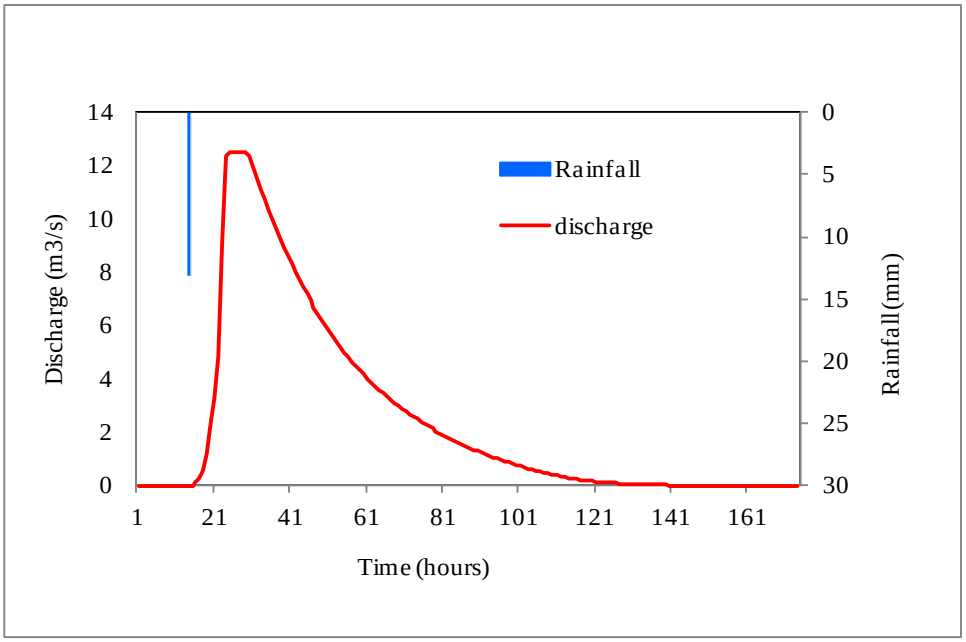

Figure 4.17 Hourly hydrograph of simulated discharge in W. Assiut during (Nov. 2-5, 1994).

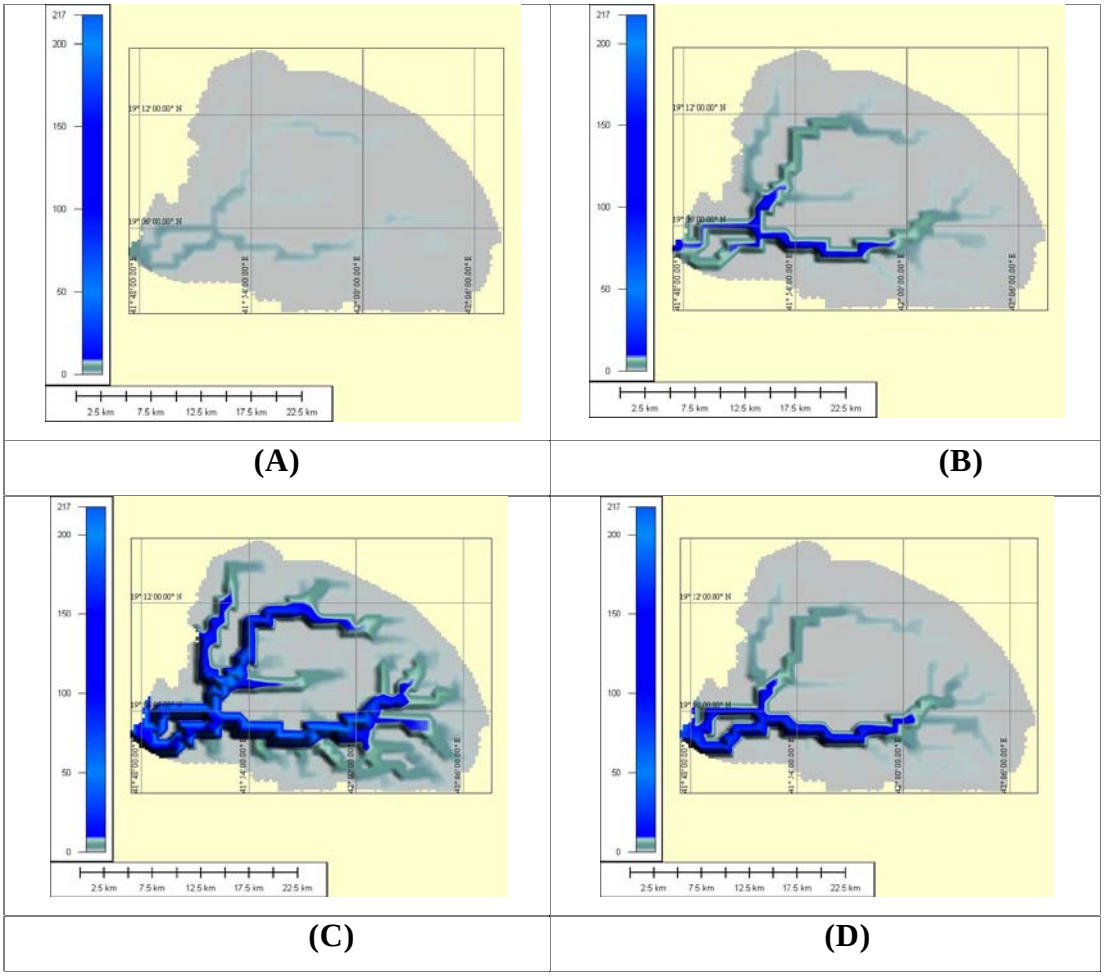

Figure 4.18 Distribution maps of surface runoff in W. Ghat; (A) Early stage of surface flow, ; (B) hydrograph is rising toward the maximum peak of discharge; (C) reaching to the maximum of distribution; (D) starting the recession of surface flow to zero flow.

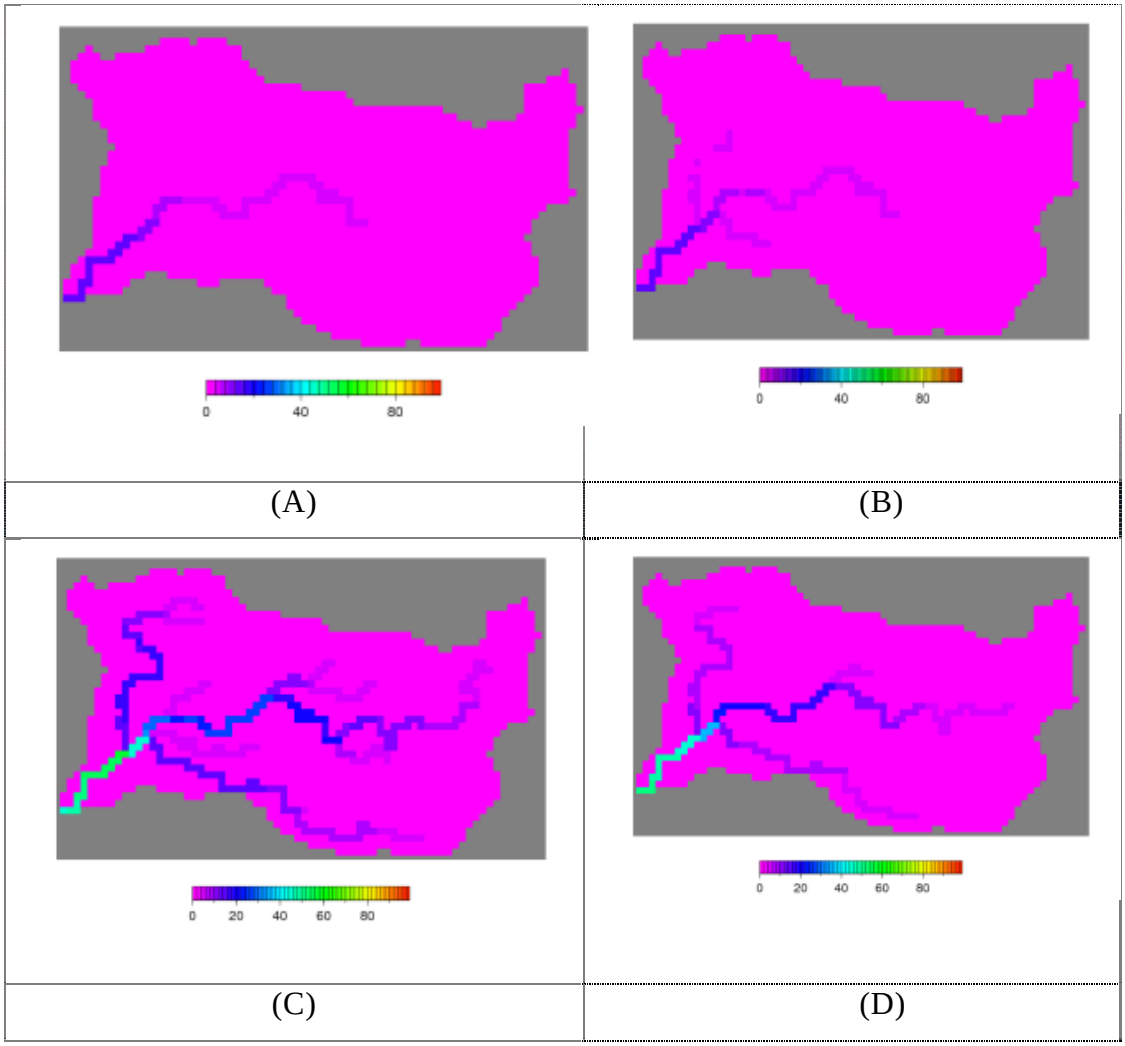

Figure 4.19 Distribution maps of surface runoff in W. Assiut; (A) Early stage of surface flow, ; (B) hydrograph is rising toward the maximum peak of discharge; (C) reaching to the maximum of distribution; (D) starting the recession of surface flow to zero flow.

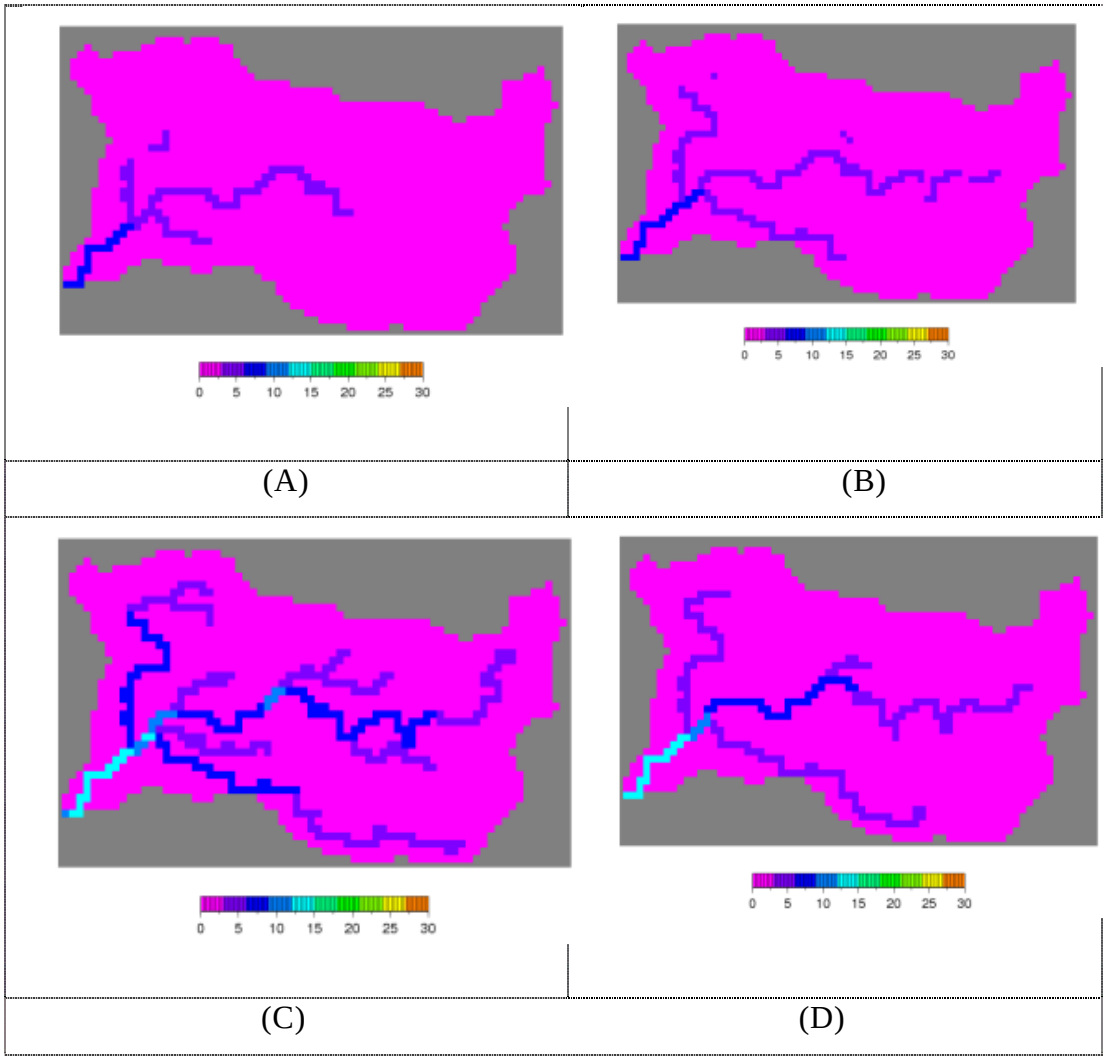

Figure 4.20 Distribution maps of transmission losses in W. Assiut; (A) Early stage of surface flow, ; (B) hydrograph is rising toward the maximum peak of discharge; (C) reaching to the maximum of distribution; (D) starting the recession of surface flow to zero flow.

In this research, a comparative study has been done between the target wadi basins to understand and declare the effect of some factors on runoff characteristics in Wadi system.

It is obvious from the aforementioned results of runoff and transmission losses in the targets basins that runoff behaviors are extremely affected by some factors. The catchment area has visible role to affect on the peak of discharge, time to reach to the peak, and the duration of flow as well as the maximum peak value, where in W. Al-Khoud and W. Ghat, the area is smaller than W. Assiut but the discharge is higher at the downstream points of both of them than W. Assiut. The reason is due to the travel time of water flow to reach the downstream point is shorter than in W. Assiut and consequently the peak discharge time to peak will be earlier than of wadi Assiut.

Slope and elevation have an important role on the runoff features where in W. Al-Khoud and W. Ghat the maximum elevation more than 2000 m which means that the slope will be steep, on the other hand in W. Assiut, the maximum elevation is approximately 900m and consequently the slope will be gentle. Which state that the surface runoff is higher in both of them than in W. Assiut as deduced from the numerical results of simulation as shown in **Table (4.2).**

That reveals the effect of slope on surface runoff where with increasing the maximum elevation and slope, the flow rate will be high and consequently the surface water will be increased. Moreover in the large area catchments, the availability of losses (evaporation, initial and transmission losses are high) as declared in the numerical results that initial and transmission losses are higher in Wadi Assiut than those of both wadi khoud and wadi Ghat due to the effect of catchment area of wadi Assiut is larger than the other two wadi catchment areas and hence affecting the flow rate.

As well known, the effect of rainfall rate and frequency are very observable as they are the main input resources of water in such regions. You can see the effect where in W. Al-khoud, the rainfall events are more frequent than those in W. Ghat

and W. Assiut during the simulated periods and thus the peak of discharge higher than in Ghat and Assiut wadis.

Table 4.2 Results of simulation of the three basins

	W. Khoud	W. Ghat	W. Assiut
Area (km2)	1874.84	649.55	7109
Slope	Steep	Steep	Gentle
Peak of discharge	838 m3/s	36 m3/s	12. 5m3/s
Time to peak	4-7 hrs	14 hrs	10 hrs
Flow duration	44 hrs	60 hrs	106 hrs
Runoff	88.98%	86.22%	92.47%
Initial & T. losses	11.02%	13.78%	7.53%

4.6. CONCLUSION

A Physically-based distributed hydrological model for the wadi system has been developed to simulate the surface runoff and transmission loss in the ephemeral streams throughout comparative studies between some Arabian wadi basins (W. Al-Khoud, W. Ghat and W. Assiut). It is concluded that the simulated runoff are completely coincide in their behaviors with the monitored one that prove an appropriate performance of the proposed model to predict the future flood events. From the distribution maps of surface runoff in the wadi system, the discontinuous surface flow is perfectly depicted as one of the most import characteristics of ephemeral streams. Transmission loss is affected by the volume

of surface runoff as the evidence that the rate of losses is linearly related to the volume of surface discharge.

A comparative study between some Arabian wadis has been done. Results of simulation declared that the runoff features are affected by the catchments area, slope, and rainfall events frequency and duration as listed in Table 1. Runoff features in the ephemeral streams are characterized by different behaviors from the runoff in the humid area based on the results as follow. i)-There is a time lag between hyetograph and hydrograph peaks. ii)-Flood event time including starting and cessation is short. iii)-Initial and transmission losses are considered the main source of subsurface water recharge. iv)-discontinuous surface flow in space and time occurrence.

It is concluded that the proposed approach is considered an applicable methodology in the arid areas and consequently a vital contribution to estimate distributed surface runoff and transmission losses in the other arid regions. Regional application for the proposed model in other arid regions for flash flood simulation was discussed.

Chapter Five

Flash Floods Simulation Using Satellite Remote Sensing Data

5.1. Introduction

The flash flood is characterized as flood leading to damage caused by heavy rainfall for short duration, steep slope and impervious layer as well as climate change which make it more sever and devastating. Infrequent surface water flow in the wadi system may cause natural flash flood hazards but it can be managed to be valuable water resources throughout an appropriate decision support based on effective methodologies.

The term ‘flash flood’ identifies a rapid hydrological response, with water levels reaching a peak within less than one hour to a few hours after the onset of the generating rain event (Creutin and Borga, 2003; Collier, 2007; Younis et al., 2008). In other words, flash flood is a typical natural phenomena which occurring in arid or semi-semi arid regions within short duration (several hours to a few days) and rapidly rising water flow level (reaching maximum peak flow in a few hours) due to the causative event of intense rainfall or dam failure resulting in a greater danger to human life and severe structural damages..

Flash flood is one of the most devastating hazards in terms of loss of human life and infrastructures. The main problem of flash floods is that warning times are very short, leaving typically only a few hours for civil protection services to act. Moreover, the most important challenge to calibrate and simulate flash floods in arid regions is that good observational networks of both rainfall and discharge are rare.

Flood occurrences are complex since they depend on interactions between many geological and morphological characteristics of the basins, including rock types, elevation, slope, sediments transport, and flood plain area. Moreover, hydrological phenomena, such as rainfall, runoff, evaporation, and surface and groundwater storage (Farquharson et al. 1992; Flerchinger and Cooly 2000; Şen 2004; Nouh 2006) can affect floods.

According to Few et al. (2004), each flood acquires some particular and inherent characteristics of the occurrence locality such as flow velocity and height, duration, and rate of water-level rise.

Responsible factors for the short duration of the flash flood include intense rains that persist on an area for a few hours, steep slope, impermeable surfaces, and sudden release of impounded water (Georgakakos, 1986). Hence, particular hydrological characteristics such as small basins, steep slopes and low infiltration capacity combined with a meteorological event contribute to the flash flood formation.

Long-term rainfall data and their analysis are limited in most of arid regions. This may partially be due to (1) large inaccessible and uninhabitable areas, (2) lack of adequate network of monitoring stations (rain gauges), (3) non-suitability of large areas for agriculture, (4) poor data quality and (5) lack of the personnel for effective database management and analysis.

Vulnerability to flash floods will probably increase in the coming decades due to evolving land use and the modification of the pluviometric regime associated with the evolution of the climate (Parry et al., 2007; Palmer and Raisanen, 2002; Rosso and Rulli, 2002). As pointed out by many authors, the quality of flood prediction that is based upon hydrological simulations depends to a high degree upon the quality of the measurements and forecasts of precipitation. Also, it must be emphasized that the early warning system is indispensable for the reduction in damages associated with flash floods.

In deserts, flash floods can be particularly deadly for several reasons. First,

storms in arid regions are infrequent, but they can deliver an enormous amount of rain in a very short time. Second, these rains often fall on poorly-absorbent and often clay-like soil, which greatly increase the amount of runoff that rivers and other water channels have to handle. In addition, these regions may not have the infrastructure that wetter regions have to divert water from structures and roads, such as storm drains and retention basins, either because of sparse population, poverty or because residents believe that the risk of flash floods is not high enough to justify the expense. In fact, in some areas, desert roads frequently cross dry rivers and creek beds without bridges. From the driver's perspective, there may be clear weather, when unexpectedly a river forms ahead of or around the vehicle in a matter of seconds (Thomas (2004)). Finally, the lack of regular rain to clear water channels may cause flash floods in deserts to be headed by large amounts of debris, such as rocks, branches and logs.

The influence of rainfall representation on the modeling of the hydrologic response is expected to depend on complex interactions between the rainfall space-time variability, the variability of the catchment soil and landscape properties, and the spatial scale (i.e. catchment area) of the problem (Obled et al., 1994; Woods and Sivapalan, 1999; Bell and Moore, 2000; Smith et al., 2004). River hydrograph forecasts are very dependent upon the input rainfall data used.

Flash floods are characterized by infrequent occurring in arid regions, it so difficult to know when it will come. It is important to show some of the past flash flood events which hit Egypt and their damage or impact on the human life. Fron the history of flash flood events in Egypt, it is found that Egypt have been affected by it in the following years, Oct. 1987, Dec. 1991, Feb. 1992, Nov. 1994, Nov. 1996, Mar. 1997 as described in **Table 5.1** .

Table 5.1 Flash flood history in Egypt

Detailed Locations	Began (mm/dd/yy)	Ended (mm/dd/yy)	Dead	Main Cause	Region (sq km)	More details
Lebanon - Eastern Bekaa Valley, Egypt - Sinai Penninsula,	10/17/87	10/19/87	10	Brief torrential rain	12,690	
Sidi Abdel-Qadar	5-Dec-91	6-Dec-91		Dam/Levy, break or release	3,170	1991_flood: Irrigation Dam cracked, flooding the village.
Turkey, Egypt	20-Feb-92	26-Feb-92	200	Rain and snowmelt	81,540	1992_flood: Extremely harsh winter in the middle east - heavy rain and snow.
Provinces: Asyut - Dronka (Durunka), Sohag, Qena	2-Nov-94	8-Nov-94	593	Heavy rain	44,070	1994 : Flood waters carrying burning oil from a fuel depot swept through Dronka. 507 killed in Dronka, 86 killed by flooding in other provinces. Sohag: 750,000 oxen, goats, sheep, and poultry killed. 2,513 homes collapsed and 4,200 hectares (10,400 acres) of land flooded.
Provinces: Aswan, Sohag, Asyut, Minya, Qena	13-Nov-96	25-Nov-96	23	Heavy Rain	37,940	1996: Thousands of acres of land flooded. 260 houses destroyed.
North: Cairo region	2-Mar-97	4-Mar-97		Heavy rain	68,460	

The lack of observations in most flash flood prone basins, therefore, necessitates the development of a methodology to simulate and forecast flash flood is so urgently needed in the severe current situation. The need for water in these areas increases day by day due to population growth, economic developments, urbanization, and consequently, water management using all the available resources is becoming increasing crucial. Furthermore, the danger also comes from the rarity of the phenomenon, which demands a new observation strategy, as well as new forecasting methodology.

Flash floods are sporadic torrential floods which are caused by the extreme rainfall events resulting in great havoc and excessive loss of life and property in the urban areas and infrastructure of people. Effective water management and utilization of wadi surface flow of flash floods based on using Remote Sensing data are desperately needed. In this study, a trial is made to simulate the flash flood events and to evaluate the water resources in the Nile River at the Egyptian

part especially to study the effect of the wadi basins as the main sub basins of Nile River from the point of view of flash flood simulation using the remote sensing data due to the scarcity of observed data. Also, flash flood simulation has been applied for wadi El-Arish, Sinai Peninsula, Egypt. By this reach, a commendable contribution of the wadi basins as water resources can be assessed and managed as well as its effect of the Nile Delta.

So, the main objectives of this chapter are summarized as follow:

1- Using the remote sensing data for flash flood simulation in the wadi basins in the Nile River and wadi El-Arish, Sinai Peninsula, Egypt to overcome the challenge of data paucity in arid regions.
2- Assessment and evaluating of the wadi basins contribution into the Nile River and wadi El-Arish during the flash flood events to utilize flash flood water as a significant water resource in arid areas.
3- The threat of Flash floods, how to control and how to reduce their devastating and dangerous.

5.2. The Target Wadi Basins

5.2.1. The Nile River Basin, Egypt

The Nile River is the longest international river system in the world. It flows about 6,700 km through ten countries before reaching the Mediterranean Sea. Its headwaters are in Lake Victoria at about 4º S latitude. It has a drainage area of about 3.35 million km^2, which covers 10% of the African continent, roughly equivalent to half the area of the continental United States. Egypt and the Sudan are the two major users of this river, while Ethiopia is the primary contributor to the bulk of runoff.

The major lakes in the basin (Lakes Victoria, Nasser and Tana) account for

81,500 km^2 and the area covered by swamps is an additional 69,700 km^2 (Biswas, 1994). Precipitation is to a wide extent governed by the movement of the Inter-Tropical Convergence Zone (ITCZ) and its interaction with topography. In general, precipitation increases from north to south, and with elevation. Precipitation is virtually zero in the Sahara desert, and increases southward to about 1200–1600 mm/yr on the Ethiopian and Equatorial Lakes Plateaus (Mohamed et al., 2005). The Nile is formed by three tributaries, the Blue Nile, the White Nile, and the Atbara. The flow of the Blue Nile is strongly seasonal because its runoff is primarily driven by monsoon precipitation. The Blue Nile contributes about sixty percent of the total flow of the Nile, whereas the Baro-Akobo (Sobat), and Tekezze (Atbara) contribute slightly less than fifteen percent each.

The headwaters of all the tributaries of the Blue Nile are in the highlands of Ethiopia, and the bulk of their runoff (70% on average) occurs between July and September. Among the tributaries of the Blue Nile, the Upper Blue Nile (with drainage area 175,000 km2), which contributes about 50% of the Nile's flow at High Aswan Dam (HAD) in Egypt, is the most important. The White Nile and the Blue Nile join north of Khartoum, where they are joined by the Atbara. The river then flows north through the Lake Nasser in Egypt, the second largest man-made lake in the world, before splitting into two major distributaries just north of Cairo, the Rosetta branch to the west and the Darneita to the east.

In 1996, the UNEP Executive Director stated that in the future, it was most likely that the complaints and problems caused by the shortage of water supplies would be caused through transboundary conflicts. Furthermore, the world is heading towards a water crisis in several regions, notably in the Middle East and North Africa, where the available water per capita is 1,247m3/year.

In this study, the Nile River Basin in Egypt (**Figure 5.1**) is selected due to its significant as the main water resource for domestic and agricultural and industrial purposes. The majority of population and agriculture fields are spreading along the Nile River and at the Nile Delta. The whole selected basin is starting after Aswan

High Dam to the entrance of Nile Delta. It is located between Lon. 35°00′ E & 28°00′ W and lat. 32°00′ N & 22°00′ S. The total catchment area is 184,000 km^2 and it has many sub-catchments of wadi basins which flow toward the main channel of Nile River from both Eastern and Western deserts.

Egypt occupies a portion of the arid to semi-arid belt of Africa. The climate is characterized by a long dry summer and a short temperate winter with a rainfall period from October to March (Saleh, 1980).

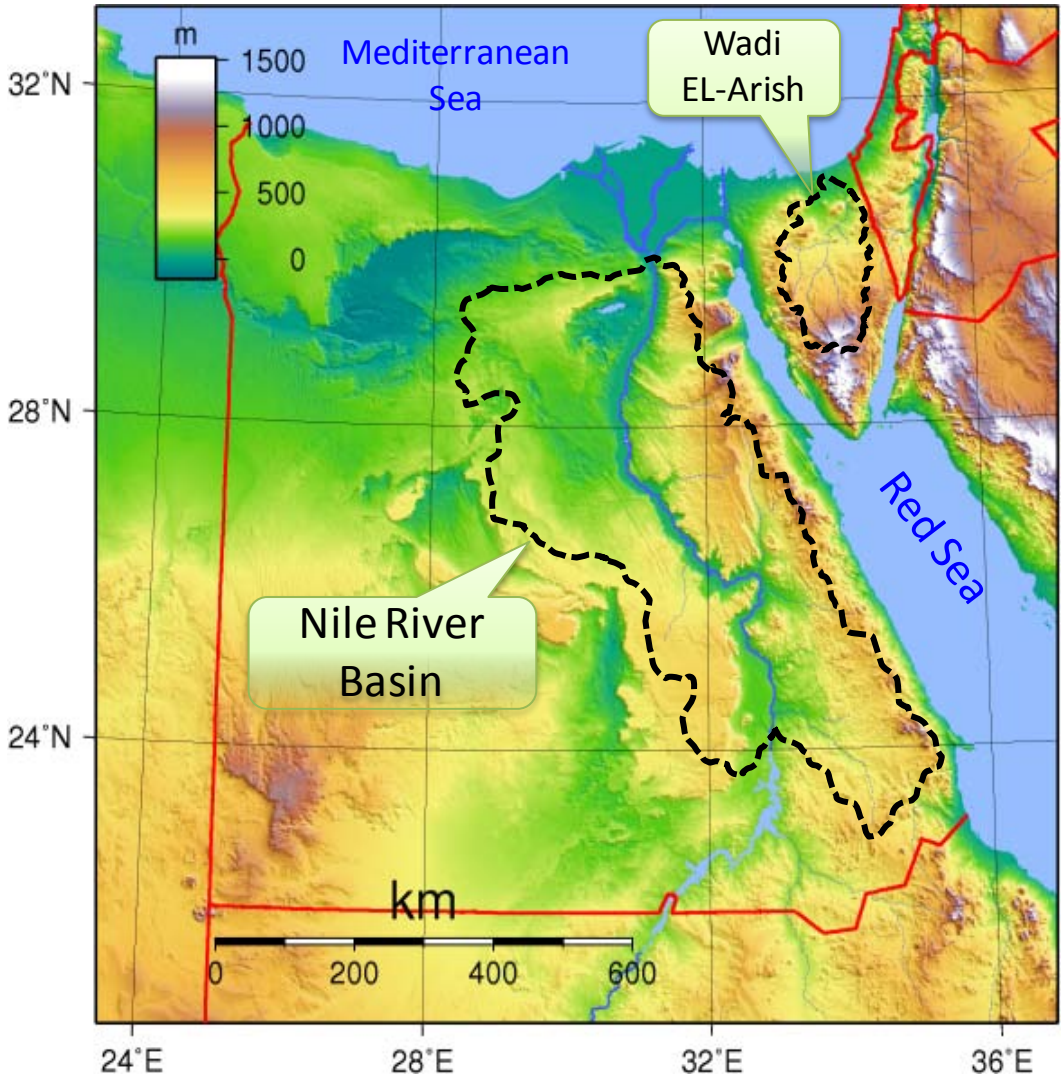

Figure 5.1 Location Map of Nile River Basin and Wadi El-Arish, Sinai Peninsula in Egypt

5.2.2. Wadi El-Arish, Sinai Peninsula, Egypt

El-Arish is the capital and largest city (with 114,900 inhabitants as of 2002 of the Egyptian governorate of North Sinai, lying on the Mediterranean coast of the Sinai Peninsula, 344 kilometers (214 miles) northeast of Cairo. Wadi El-Arish is flow toward the Mediterranean Sea and its downstream part is El-Arish City as shown in Figure 5.1. This big wadi infrequently receives flash flood water from much of north and central Sinai which make a great threat for the human life and their properties of El-Arish City residents.

Wadi El Arish is the largest ephemeral stream system of the Sinai Peninsula. Its catchment area is calculated about 20,700 km^2 through GIS processing of DEM, which is about one-third of the Sinai Peninsula area.

There are several areas in Sinai Peninsula have subjected to flash flood events especially during the fall and winter seasons. These floods cause severe damage and loss of life and hinder the development in these areas. On the contrary, the floodwaters are important source for the sustainable settlement of the Bedouins. Simulation of flash floods at this active and important region is also needed especially after the last damage of flash flood of Jan, 2010. Furthermore, developing the powerful hydrological model which can simulate and predict the flash flood is desperately demanded for application to predict the risk of the expected flash flood and hence to avoid or minimize the level of disasters. Therefore, one of the main important targets in this study is to simulate the flash flood of Jan 18-20, 2010 which hit Sinai region causing many damages for human life and infrastructures.

The climate of the basin is similar to that characteristic of other desert areas. The region has an extremely arid, long, hot, and rainless summer period and a mild winter in which storms occur infrequently. Rainfall occurs mainly during the

winter season, which runs from November to March, and sometimes during spring or fall. It rarely rains between April and October and this precipitation almost immediately evaporates upon contact with the ground. During winter, some localized areas experience short periods of rain, but heavy rainfall that occasionally cause the wadis to overflow and result in flooding. Average annual precipitation in the interior of the basin is less than 30 mm as compared with the average annual rainfall along the eastern Egyptian Mediterranean coast of about 90 mm (Smith et al., 1997).

The growing population and increasing industrial and agricultural activities create a large demand for water resources for people need as well as flash flood protection warning system. El-Arish area has the highest annual precipitation all over Egypt, where it receives about 300 mm/year. Therefore, the city depends on its fresh shallow groundwater that is produced from Quaternary aquifers of delta Wadi El-Arish (Dames and Moor, 1985). Sinai peninsula is located and bounded from the South by Mediterranean Sea and from the East Gulf of Aqaba and from the West by the Gulf of Suez and also it is considered the border between Egypt and Palestine country from the Northeastern side as shown in Figure 5.1. The intensity of rain fall at the eastern portion of the El-Arish is greater than that measured at the western side.

5.3. Climate conditions

The climate of Africa is both varied and varying. Varied, because climate ranges from humid equatorial to seasonally arid and sub-tropical Mediterranean and varying because all these climates exhibit differing degrees of temporal and spatial variability. Flooding and droughts will be increasingly difficult to cope with in the face of increasing pressures on water supplies due to rapid population growth and dwindling resources. Future changes and uncertainties in the allocation of Nile water resources may have significant effects on local and regional economies,

agricultural production, energy availability, and environmental quality (NBI, 2001, Hulme et al., 2005, Conway et al., 1993, Yates et al., 1998). Water resource planning based on the concept of a stationary climate is increasingly considered inadequate for sustainable water resources management (Mohamed et al., 2005). In addition to natural variability, which is incorporated in existing water planning methods, new water projects will have to deal with uncertainty associated with population growth and trends in climate change. Therefore, understanding the uncertainty in projected climate change over the next century, which is attributable both to uncertainty in the future emissions pathway (related to policy decisions and public response) and uncertainties in model projections (due to differing sensitivities of the GCMs to perturbations in atmospheric composition), is essential to understanding how the economy of the Nile basin will evolve, including social and environmental impacts.

5.4. Data Availability and Analysis

The most important factor affecting the hydraulic behavior of the wadi basins is rainfall. Its duration, intensity, distribution, and return periods are major influences. This climate pattern can be described by considering various air masses that affect rainfall distribution. The study area possesses different physiographic and topographic features. As well known, the hydrological modeling for flash flood forecasting in arid regions has no enough data for the current research however it's urgently needed. So, we are trying in this research to discuss GSMaP data for its feasibility for use to flash flooding simulation in such areas.

The Global Satellite Mapping of Precipitation (GSMaP) has been used in this simulation due to the paucity of data in arid regions (http://sharaku.eorc.jaxa.jp/GSMaP_crest/). The GSMaP project was promoted for a study "Production of a high-precision, high-resolution global precipitation map using satellite data," sponsored by Core Research for Evolutional Science and

Technology (CREST) of the Japan Science and Technology Agency (JST) during 2002-2007. Since 2007, GSMaP project activities are promoted by the JAXA Precipitation Measuring Mission (PMM) Science Team. There are two kinds of horizontal resolution of GSMaP product are 0.1 x 0.1 lat/lon degree grid and 0.25 x 0.25 lat/lon degree grid.

There are two kinds of horizontal resolution as:

- **0.1 x 0.1 lat/lon degree grid:**

Products: **GSMaP_MVK+, GSMaP_MVK**

Grid of those files consists of 3600 x 1200 pixels, which are longitude-latitude elements corresponding to a 0.1 x 0.1 degree grid that covers the global region from 60N to 60S. The center longitude and latitude of the first pixel [1,1] (left top corner) is [0.05E, 59.95N] (**Figure 5.2**).

- **0.25 x 0.25 lat/lon degree grid**

Products: GSMaP_MWR

Grid of those files consists of 1440 x 480 pixels, which are longitude-latitude elements corresponding to a 0.25 x 0.25 degree grid that covers the global region from 60N to 60S. The center longitude and latitude of the first pixel [1,1] (left top corner) is [0.125E, 58.75N].

For the purpose of validation of GSMaP product, a comparative study between GSMaP and The Global Precipitation Climatology Center (GPCC; http://gpcc.dwd.de) has been carried out in the arid and semi-arid all over the world to show the bias of GSMaP product with the monitored data of GPCC product. GPCC products, gauge-based gridded monthly precipitation data sets for the global land surface, are available in spatial resolutions of 1.0° x 1.0° and 2.5° x 2.5° geographical latitude by longitude, non real-time products based on the complete GPCC monthly rainfall station data-base (the largest monthly precipitation station database of the world with data from more than 70,000 different stations) are also available in 0.5° x 0.5° resolution.

GPCC gridded monthly precipitation data from 2003 to 2006 with 1.0° x 1.0° spatial resolutions were used in this research for comparison with GSMAP. About 50721 global distribution numbers of monthly precipitation stations are available on GPCC in June as can be seen in **Figure 5.3**.

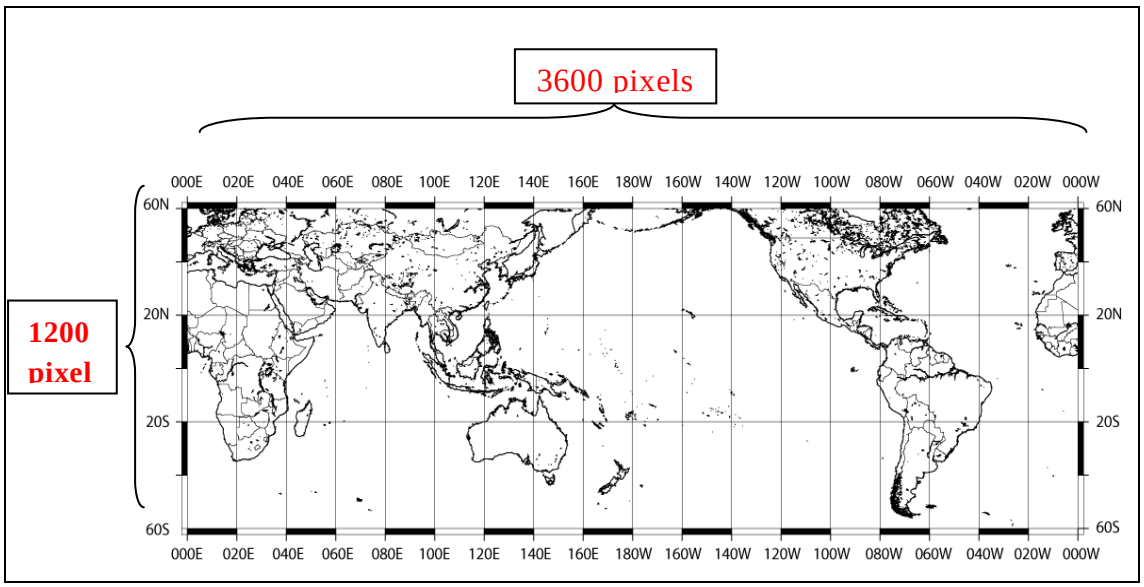

Figure 5.2 Data Coverage Map for 0.1 x 0.1 deg. lat/lon

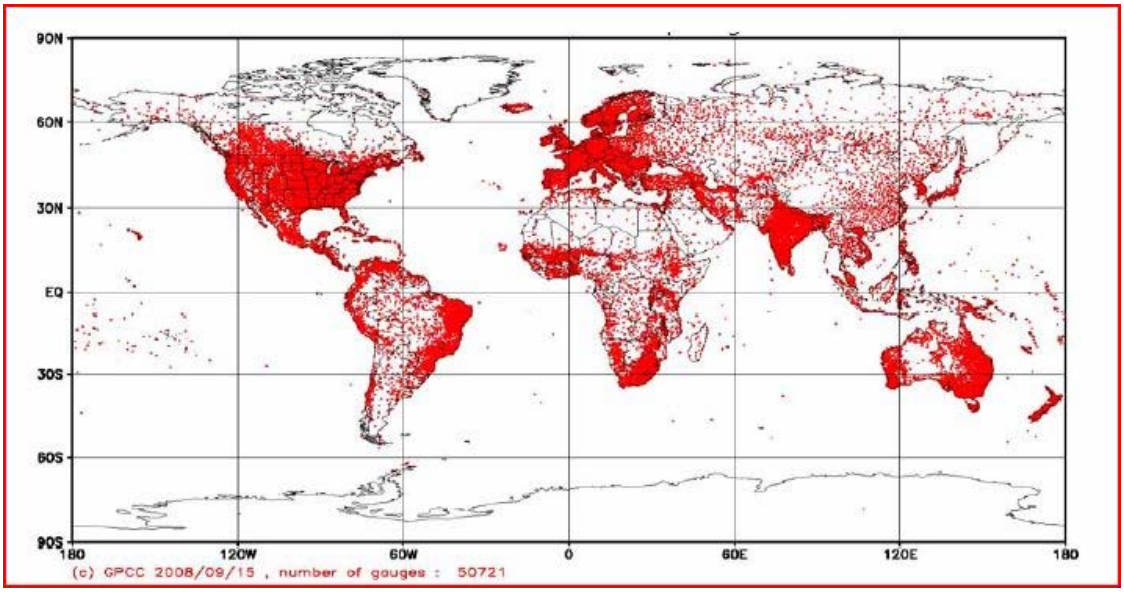

Figure 5.3 Global distribution number of monthly precipitation stations in June 50721 are available on GPCC Database (Schneider et al., 2008).

In the downloaded data, 64800 grid cells involving horizontal 360 numbers with vertical 180 numbers in 1.0° x 1.0° spatial resolutions were gridded.

For the purpose of calibrate GSMaP product, eleven arid zone sectors are selected to assess the bias of GSMAP data to know how it can be used effectively, the selected sectors are defined in the world map as illustrated in **Figure 5.4.**

In this study, statistical analysis has been performed for the GSMaP data as comparison with GPCC data, both of them are monthly data and 0.1 x 0.1 degree spatial resolution, also, the analysis has been done for the data from 2003 to 2006 considering threshold greater than 3 mm/month. In this statistical analysis the bias value is the result of dividing average of GSMaP by the average of GPCC monthly data which means as long as the bias is more closed to 1.0 value that means the correlation is good or perfect agreement.

The results in most of the arid regions all over the world based on the eleven selected sectors show us a systematic seasonal bias as overestimated or underestimated based on the sectors. The selected data are chosen from 2003 to 2006 and the bias is averaged based on the seasons where in some seasons GSMaP is overestimated in the summer and in the winter, it means all the year but with different value of bias as shown in sector number 1 (North-West of Africa) as listed in **table 5.2 and Figure 5.5**, for instance from June–Oct, the bias is 2.04 which means GSMaP is overestimated about 50 percent and during the period from Nov. to May, the averaged bias is 1.41 as listed in **Table (5.2)**.

In other regions, the averaged bias of GSMaP is underestimated all of the year with variable values, for example in sector number 11 (China), the averaged bias is 0.964 (very small value) during the period from March to June and the bias is 0.722 from July to Feb., it means that GSMaP has a bias as underestimated all the year.

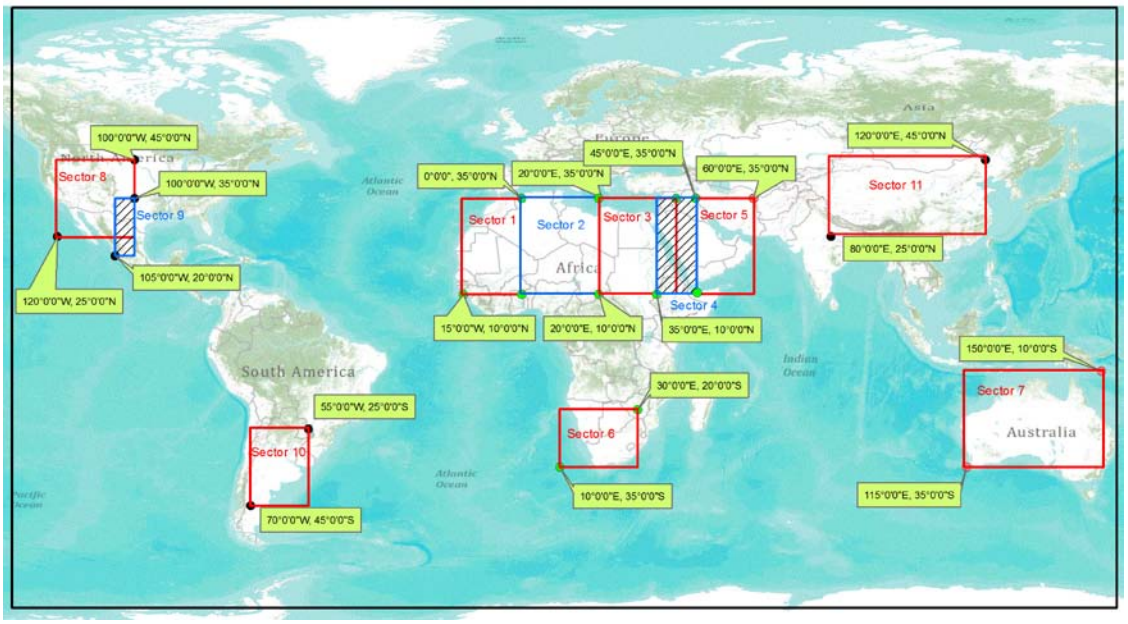

Figure 5.4 Global map showing the selected sectors of arid zones

In some areas, there are bias values as overestimated in the period from April to Oct and underestimated in the period from Nov. to Mach. Such as sectors 3 and 4. In South Africa; sector number 6, GSMAP is averagely underestimated during the period from (Mar. to Aug.) and the bias is about 0.783 but it is overestimated during the period from Sept. to Feb. and the bias is about 1.4 as shown in **Figure 5.5**.

From these results as shown in details in **Table 5.2 and Figure 5.5**, it can be summarized that GSMaP product can be used after bias correction at any arid regions with referring to the calculated results of this study and hence the corrected data have used of Egypt after the bias correction. Bias correction for the data is become easy because all the results show a systematic seasonal bias.

Table 5.2 Statistical analysis results of bias correction of GSMaP

Sector	Months (2003-2006)												R2
	J	F	M	A	M	J	J	A	S	O	N	D	
1	1.41					2.04					1.41		0.86
2	1.83					1.58					1.83		0.91
3	0.54					1.65					0.54		0.832
4	0.70					1.25					0.70		0.124
5	0.70					1.26					0.70		0.74
6	1.40					0.78					1.40		0.837
7						0.65					1.18		0.91
8	1.87					1.14					0.70		0.55
9	1.84					0.97							0.66
10	0.89					1.88					0.89		0.344
11	0.72					0.96					0.72		0.94

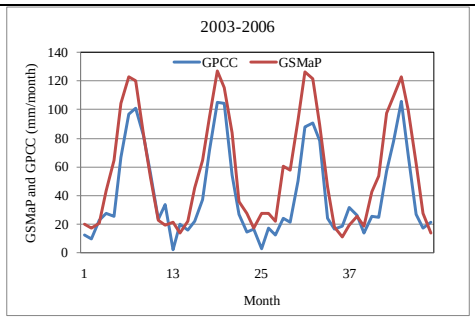

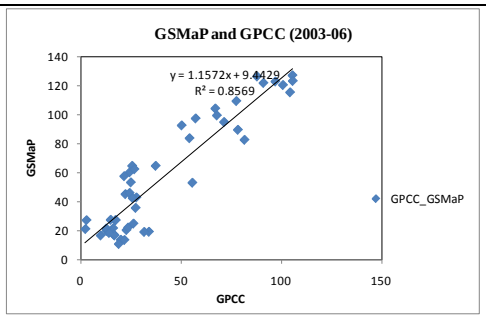

Sector 1

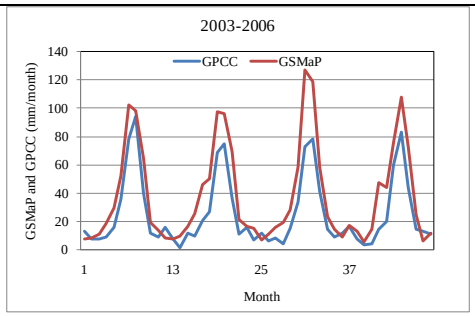

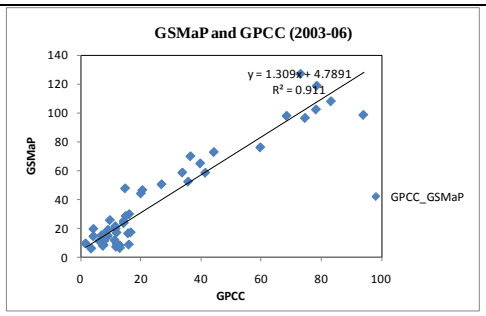

Sector 2

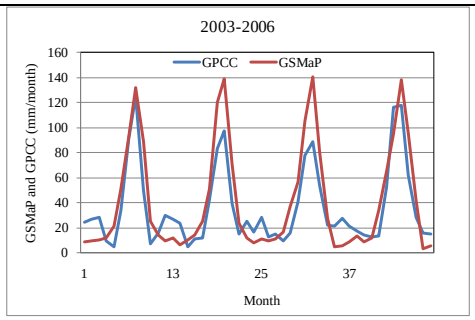

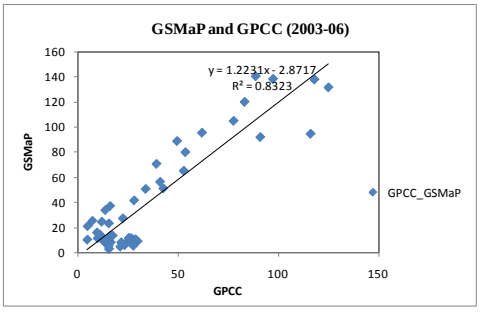

Sector 3

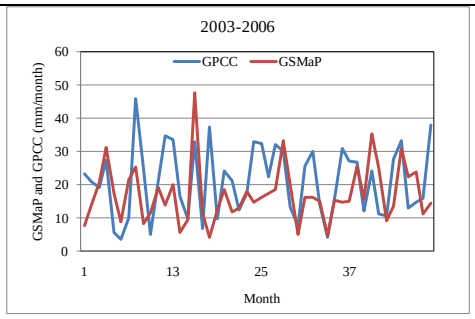

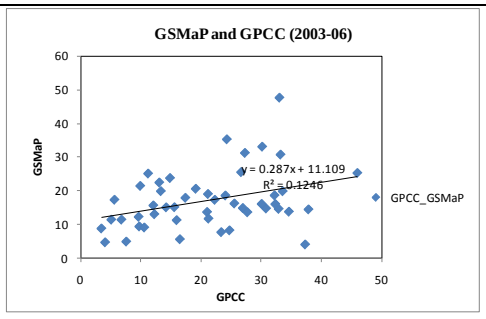

Sector 4

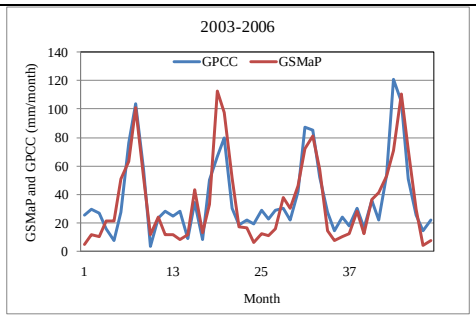

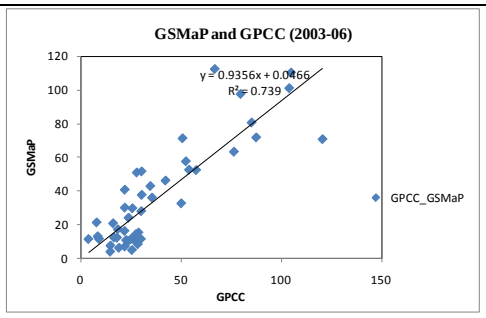

Sector 5

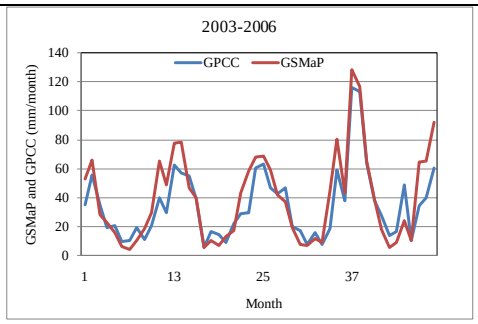

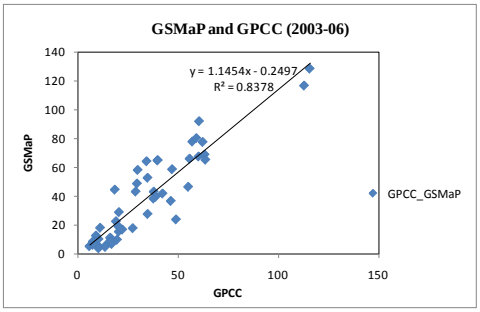

Sector 6

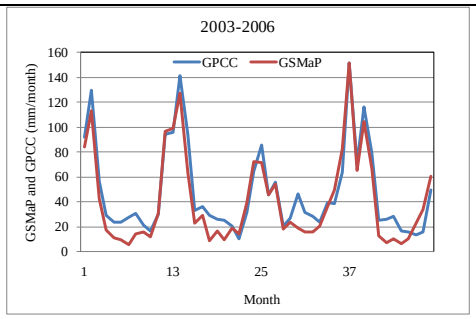

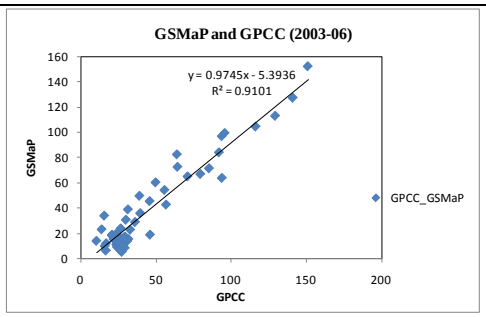

Sector 7

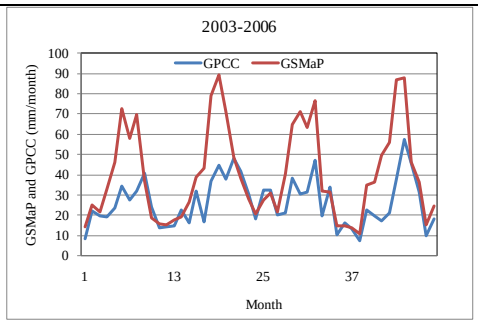

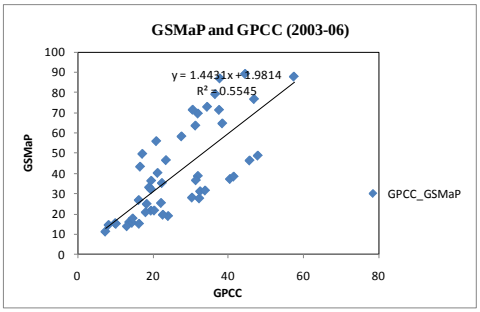

Sector 8

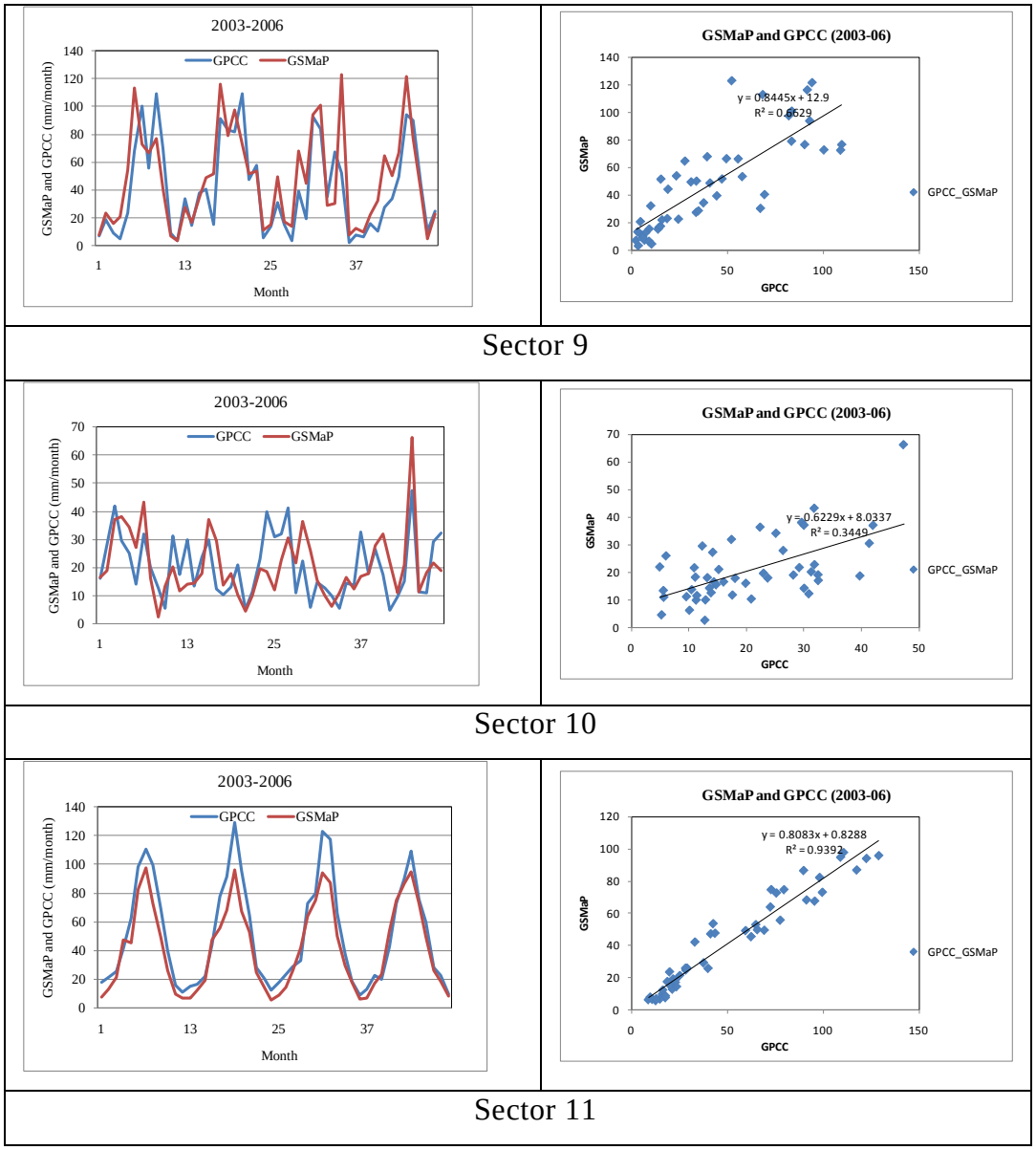

Figure 5.5 Hydrographs and scatter plots for the comparative between GSMaP and GPCC Data at the selected eleven sectors

5.5. Methodology

A physical-based distributed hydrological model; Hydro-BEAM (Hydrological River Basin Environmental Assessment Model) which has been described in the aforementioned chapters is used to simulate flash floods at wadi basins of the Nile River and Wadi El-Arish, Sinai Peninsula, Egypt, relying on its calibration at wadi

Al-Khoud in Oman. The simulation of flash flood has been done with 10 km by 10 km spatial resolution because GSMaP Product is available in this spatial resolution only. In case of finer resolution as 1km by 1 km, it is needed to use downscaling techniques to use these data. The calculation processes are summarized as follow: (1) picking up of GSMaP data of the target basins, (2) determination and delineation of the catchments and setting of modeled mesh spatial resolution, (3) Statistical analysis for bias correction of GSMaP product using GPCC product, and (4) using Hydro-BEAM for simulation, as depicted in the Flow chart of calculation process **Figure 5.6a**.

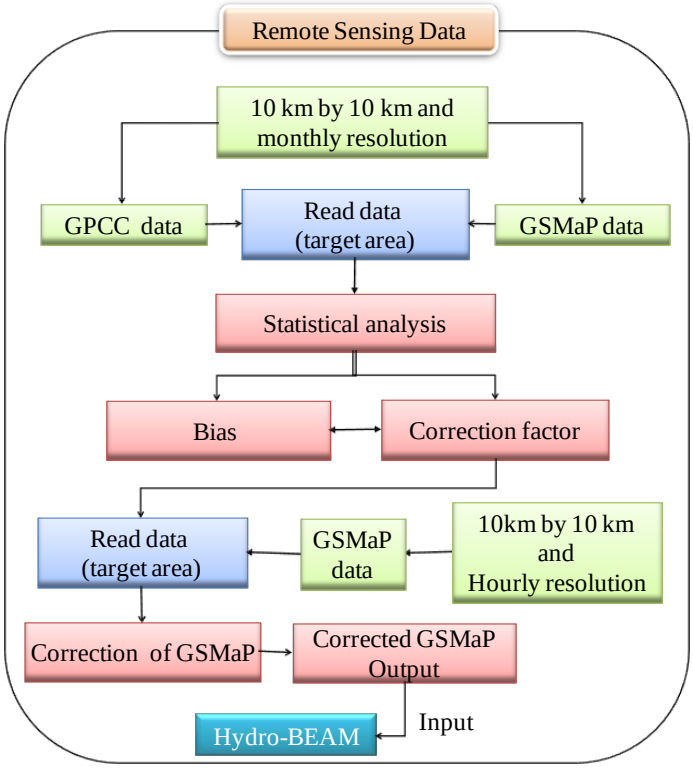

Figure 5.6a Flow chart for linking GSMaP with Hydro-BEAM.

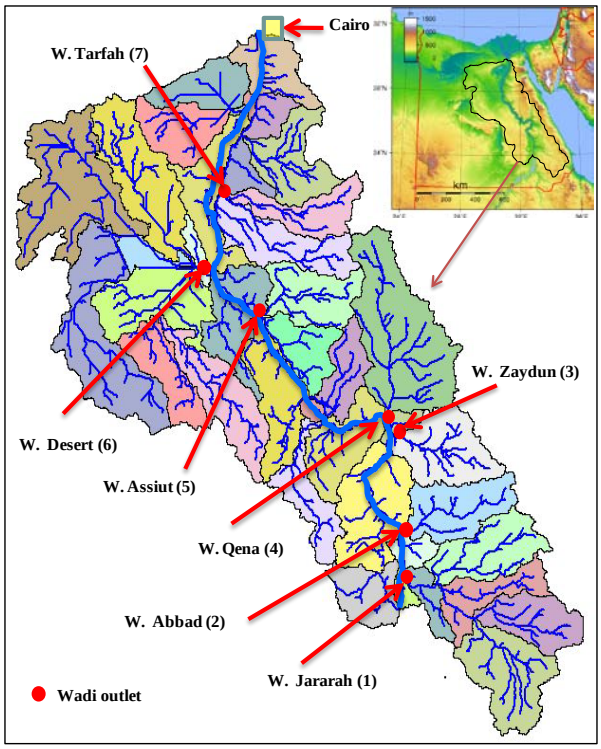

Figure 5.6b Wadi catchments of Nile River Basin in Egypt showing the target wadi outlets for flash flood simulation

The data of digital elevation model (Figure 5.7a) was processed using Arcview GIS to determine the watersheds and to delineate stream networks of the target wadi basins. The studied wadi basins are determined and processed using GIS as shown in wadi catchments map **Figure 5.6**. The whole selected basin is starting form after Aswan High Dam to the entrance of Nile Delta. It is located between Lon. 35°00′ E & 28°00 W ′ and lat. 32°00′ N & 22°00 S ′.

The land use data of the world, GLCC (Global Land Cover Characterization) and ECOCLIMAP Data (a global database of land and surface parameters) were used to identify the land use types. The global data are reclassified from 24 types into 5 types as follow; Forests, field, desert, city, water. In the target basin, most of land use is desert and the others such as field, urban, water are rarely distributed in the catchment except along the Nile River as shown in **Figure 5.7b**.

The Global Satellite Mapping of Precipitation (GSMaP) has been used in this

simulation due to the paucity of data in arid regions after the bias correction depending on its comparison with the monitored data of GPCC.

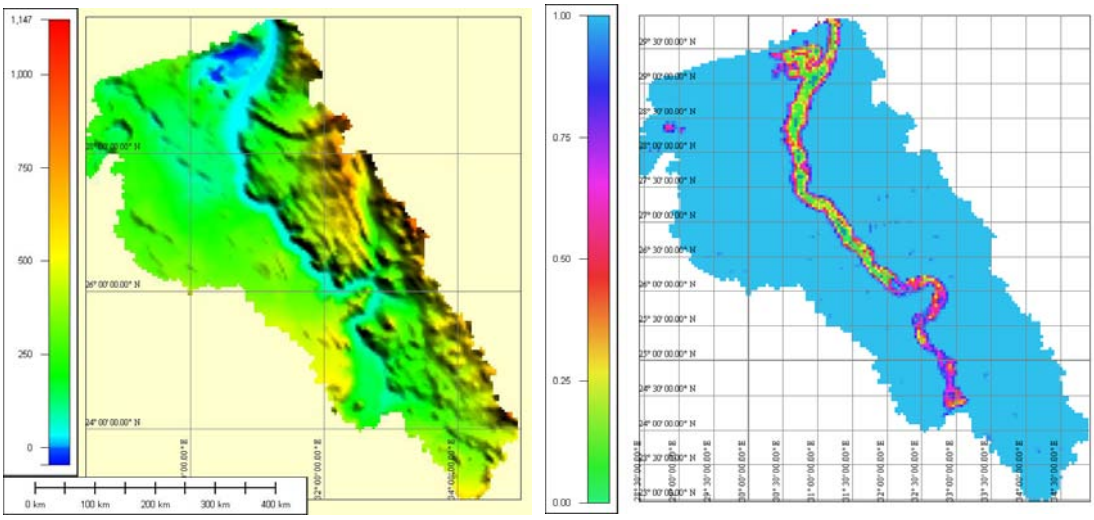

(a) (b)

Figure 5.7 a) Digital Elevation model of the target basin, b) Land use distribution map of desert in Nile River basin

5.6. FLASH FLOODING SIMULATION at NILE RIVER BASIN

The simulation has been done using GSMaP data as the main input of rainfall into Hydro-BEAM in the target wadi basins. For this simulation, only the strong events have been chosen. The simulated results of flash flood event in the studied wadi basins exhibit that the flow characteristics of flash flood where it takes a few hours to reach to the maximum peak and then gradually reducing until cessation of the event. In other words, it is showing extremely steep and rapid rising to maximum flow throughout a few hours.

The simulation of flash flood events of January 18-20 of 2010 and is discussed due to its importance as new event in Egypt. Additionally, the simulation has been carried out to different flash flood events such as; the event of Feb.11-14, 2003; Dec.18-22, 2004; Apr.22-26, 2005; and Jan. 18-20, 2010 for more understanding

of flash flood behaviors.

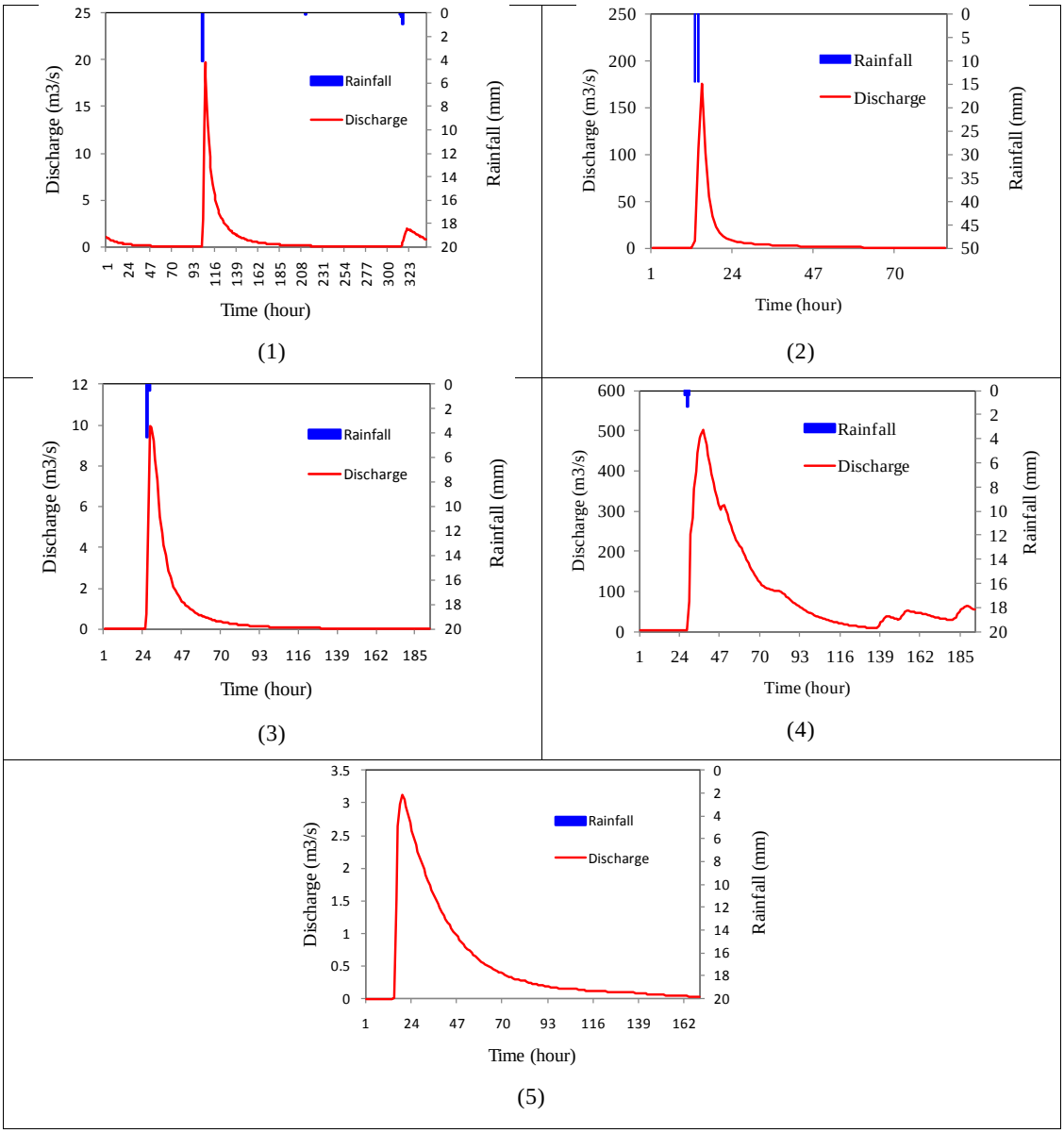

Figure 5.8 Simulated flash flood of event (2010/Jan.18-20) at several wadi outlets; 1) w. Jararah; 2) w. Abbad; 3) w. Zaydun; 4)w. Qena; and 5)w. Assiut.

The events have been chosen based on two factors, the first is the availability of GSMaP product and the second one is the biggest events only are selected. The flood event which hit Egypt on Jan. 18-20, 2010; it was devastating where some people died with a big demolition of their infrastructure. The simulated results

present remarkable characteristics of flash flood hydrograph as reaching to maximum peak flow (which is variable relying on the outlet of wadis) throughout short time.

The results of simulation of the event of Jan. 18-20, 2010 show that flash flood characteristics are highly variable (**Figure 5.8**) from one location to the others in terms of flow rate and time to reach the maximum peak, for instance, at the outlet of wadi Qena the flow is very severe flow about 502.7m3/s and it takes about 11 hours to reach it, but at wadi Assiut outlet the flow is about 2.9m3/s and the time to peak is 5 hours. On the other hand, there are some others wadis which have no flow at the same event such as W. Tarfah and wadi Desert. In terms of evaluation of wadi basins as water contribution into Nile River, the flow volume of water which can reach to the downstream point of each wadi during the flash flood event has been calculated and listed in **table 5.3**. Moreover, because the significant of time to peak and flow duration in flash flood analysis, they have been listed too in table 5.3.

Table 5.3 Simulation results of event (2010/Jan.18-20)

Wadi Name	Location	Time to peak (hours)	Peak disch. (m^3/s)	Flow Volume (m3)
Jararah (1)	32.9E, 24.5N	4	19.7	8.01921E+05
Abbad (2)	32.9E, 24.9N	3	174	2.27200E+06
Zaydun (3)	32.8E, 25.9N	3	9.97	4.24185E+05
Qena (4)	32.7E, 27.3N	11	502.7	6.85286E+07
Assiut (5)	31.3E, 27.2N	5	2.9	3.02180E+05
W. Desert(6)	32.0E, 26.1N			
At-Tarfah (7)	30.7E, 28.4N			
Total				7.23289E+07

The simulation results of the event of Feb.11-14, 2003 exhibit that the occurrence of variability of flow rate in space and time in the target wadi basins of Nile River as well as the time to reach the maximum peak of discharge is also changeable from one position to another. In this event, wadi Assiut is show discharge about 103.4m3/s and time to peak is 15 hours but in wadi Qena it is about 69.5m3/s which means that it is smaller than Assiut however the same time to peak as declared in details in **Figure 5.9**. Contribution of wadi basins water into Nile River, the flow volume of water which can reach to the downstream point of each wadi has been calculated and listed in **Table 5.4**. Furthermore, because the significant of time to peak and flow duration in flash flood analysis, they have been listed too in **Table 5.4**.

Additionally, the simulation of the flash flood event of Dec.18-22, 2004 is also carried out (Figure 5.10) and it show that wadis of Jararah, Abbad and Zydun have no flow in this event but they have flow in the other events of 2003, and 2010, and 2005. This is an implication for the effect of spatiotemporal variation of rainfall in arid regions. The time to reach the maximum discharge peaks is changeable in the range of 11 in Assiut to 15 hours in Qena. Time to peak and flow duration and contribution of wadi basins water into Nile River have been calculated and listed in **table 5.5**.

The flash flood event of Apr.22-26, 2005 is also simulated (**Figure 5.11**) for more discussion of flash flood events in the target basin. The time to reach the maximum discharge peaks is changeable in the range of 9 at W. Zaydun to 15 hours in Qena. Time to peak and flow duration and contribution of wadi basins water into Nile River have been calculated and listed in table 5.6. From the results of simulation, most of the wadis have flow due to the overall distribution of rainfall effect in this event.

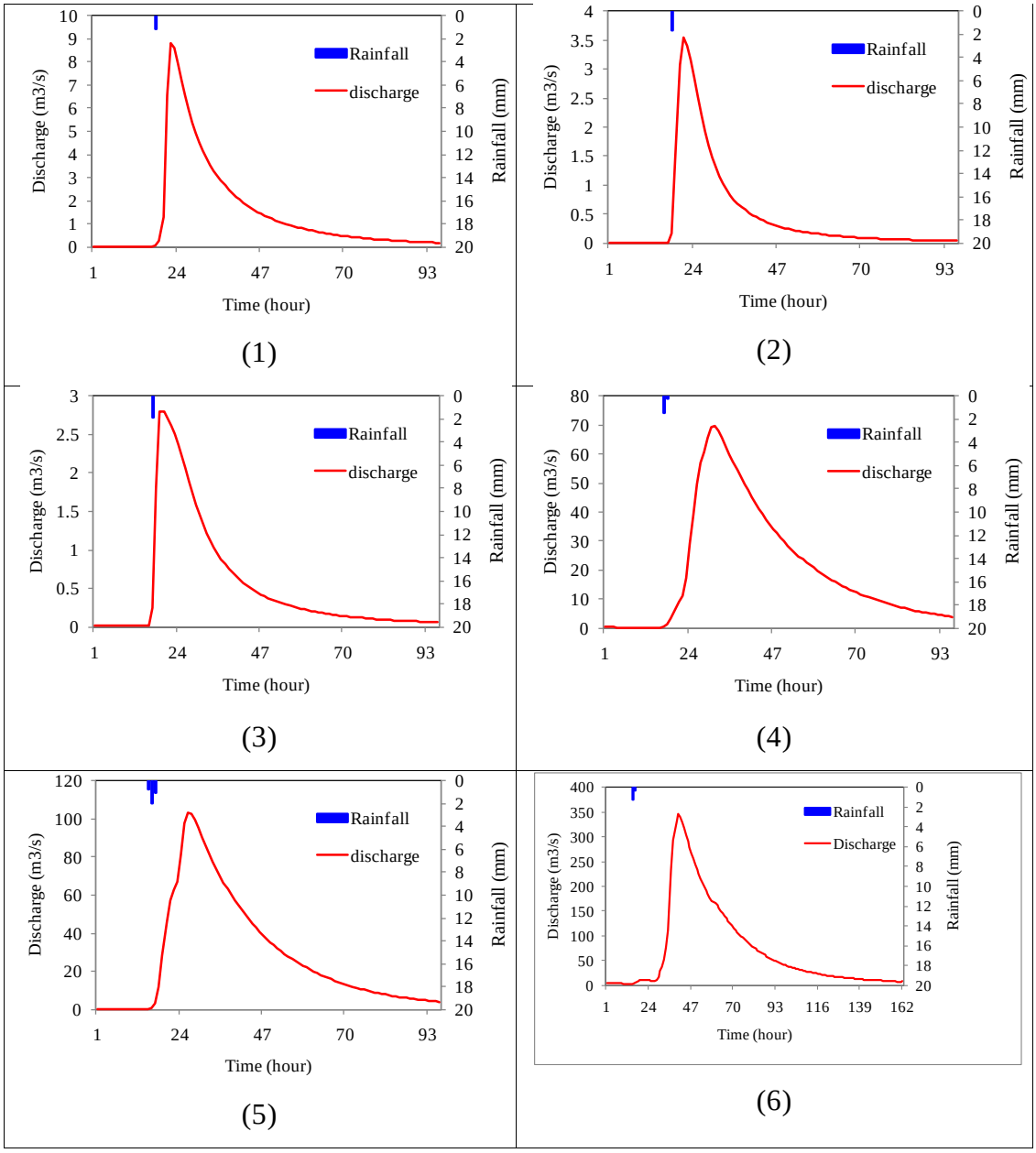

Figure 5.9 Simulated flash flood of event (Feb.11-14, 2003) at several wadi outlets; 1) w. Jararah; 2) w. Abbad; 3) w. Zaydun; 4)w. Qena; 5)w. Assiut; 6)W. Western Desert.

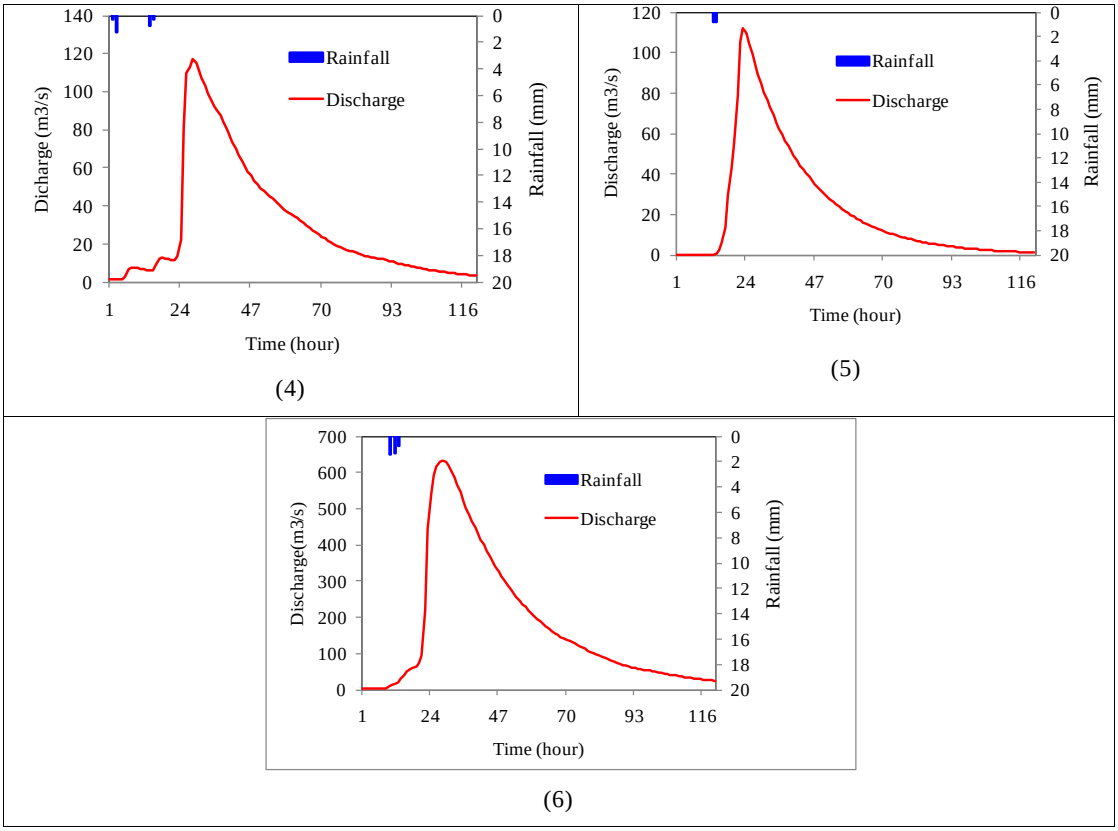

Figure 5.10 Simulated flash flood of event (Dec.18-22, 2004) at several wadi outlets; 4) W. Qena; 5) W. Assiut; 6) W. Western Desert.

The distribution maps of GSMaP precipitation(**Figures. 5.11, 5.12, 5.14, 5.14**) of the events of (Feb., 2003; Dec., 2004; and Apr., 2005, Jan., 2010;) in the whole catchment of Nile River in Egypt part show that there are highly variation of rainfall distribution in space and time. The rainfall events of Feb., 2003 and Dec., 2004 are mainly concentrated on the downstream part of the whole catchment but the event of Apr., 2005 is more spreading on the middle and downstream of it. The last event of Jan., 201 affects the upstream area near to Aswan Dam.

Table 5.4 Simulation results of event (Feb.11-14, 2003)

Wadi Name	Location	Time to peak (hours)	Peak discharge (m^3/s)	Flow Volume (m3)
Jararah (1)	32.9E, 24.5N	5	8.8	4.889609E+05
Abbad (2)	32.9E, 24.9N	5	3.5	1.581304E+05
Zaydun (3)	32.8E, 25.9N	3	2.79	1.819197E+05
Qena (4)	32.7E, 27.3N	15	69.5	7.137293E+06
Assiut (5)	31.3E, 27.2N	12	103.4	9.437274E+06
W. Desert (6)	32.0E, 26.1N	23	333.4	4.016920E+07
At-Tarfah (7)	30.7E, 28.4N			
Total				5.75728E+07

Table 5.5 Simulation results of event (Dec.18-22, 2004)

Wadi Name	Location	Time to peak (hours)	Peak discharge (m^3/s)	Flow Volume (m3)
Jararah (1)	32.9E, 24.5N			
Abbad (2)	32.9E, 24.9N			
Zaydun (3)	32.8E, 25.9N			
Qena (4)	32.7E, 27.3N	17	114.9	1.278597E+07
Assiut (5)	31.3E, 27.2N	11	112.1	9.288250E+06
W. Desert(6)	32.0E, 26.1N	18	632.9	7.436089E+07
At-Tarfah (7)	30.7E, 28.4N			
Total				9.64351E+07

Table 5.6 Simulation results of event (Apr.22-26, 2005)

Wadi Name	Location	Time to peak (hours)	Peak disch. (m^3/s)	Flow Volume (m3)
Jararah (1)	32.9E, 24.5N	12	93.0	3.432220E+06
Abbad (2)	32.9E, 24.9N	12	95.6	2.215871E+06
Zaydun (3)	32.8E, 25.9N	9	36. 9	1.457313E+06
Qena (4)	32.7E, 27.3N	15	385.8	3.781495E+07
Assiut (5)	31.3E, 27.2N	14	71.0	6.675108E+06
W. Desert(6)	32.0E, 26.1N			
At-Tarfah (7)	30.7E, 28.4N			
Total				1.95474E+08

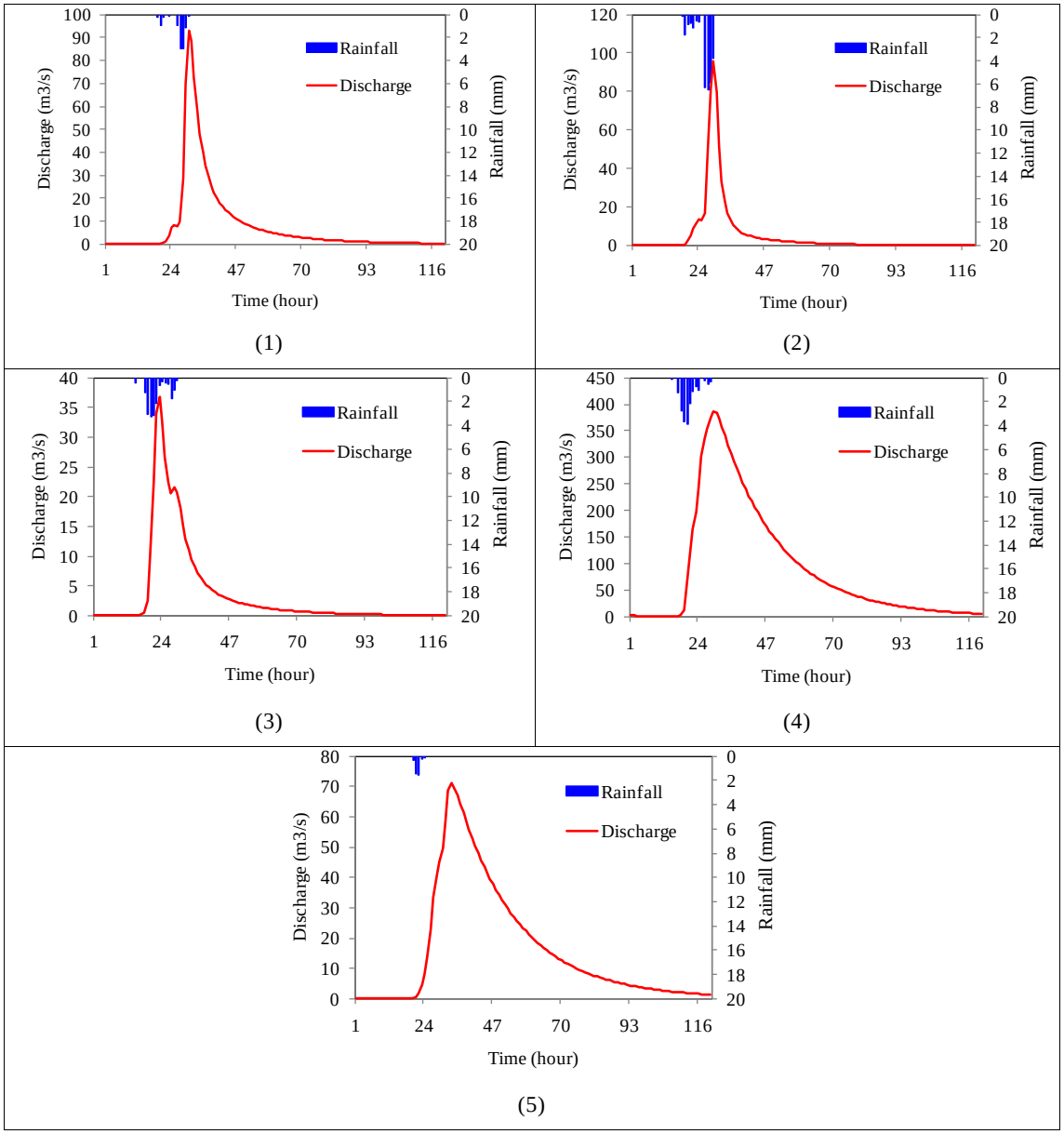

Figure 5.11 Simulated flash flood of event (Apr.22-26, 2005) at several wadi outlets; 1) w. Jararah; 2) w. Abbad; 3) w. Zaydun; 4)w. Qena; 5)w. Assiut.

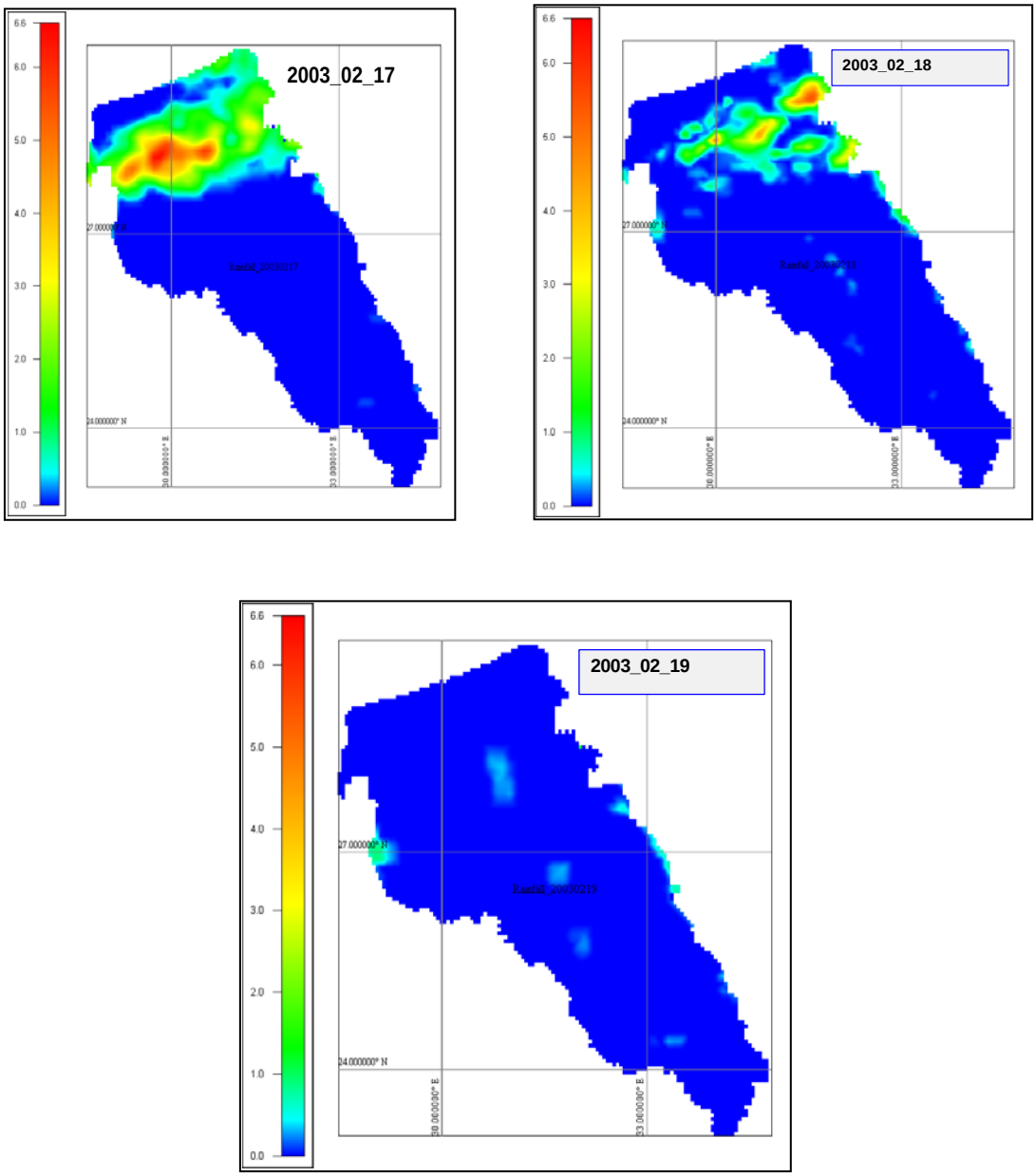

Figure 5.12 Distribution maps of rainfall (mm/h) of GSMaP product at the Nile River basin in Egypt during the two event of Feb (11-12) and (17-18) of 2003.

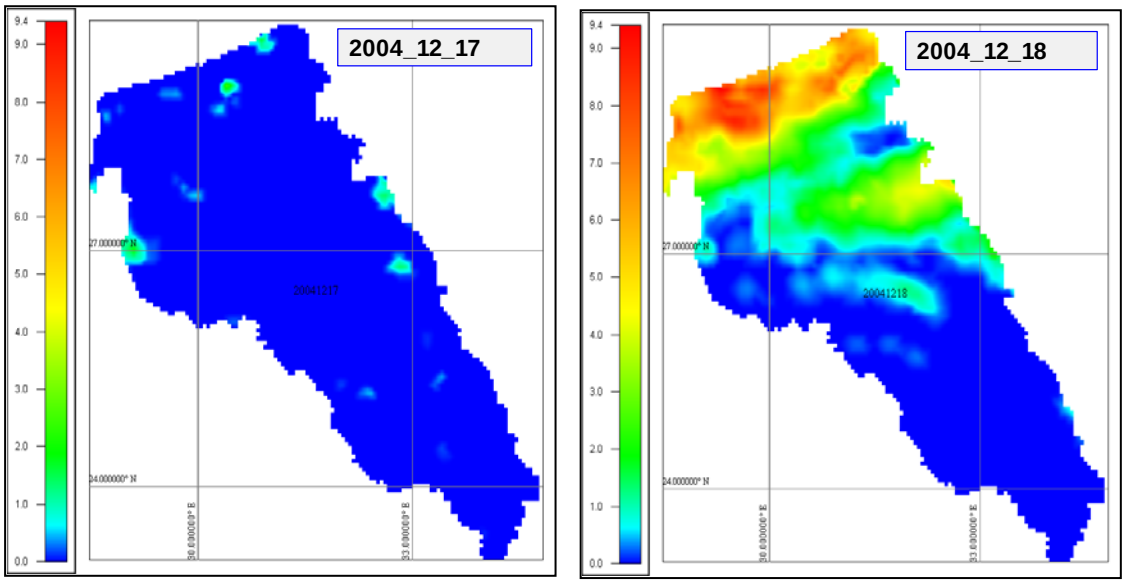

Figure 5.13 Distribution maps of rainfall (mm/h) of GSMaP product at the Nile River basin in Egypt during the event of Dec (17-22) of 2004.

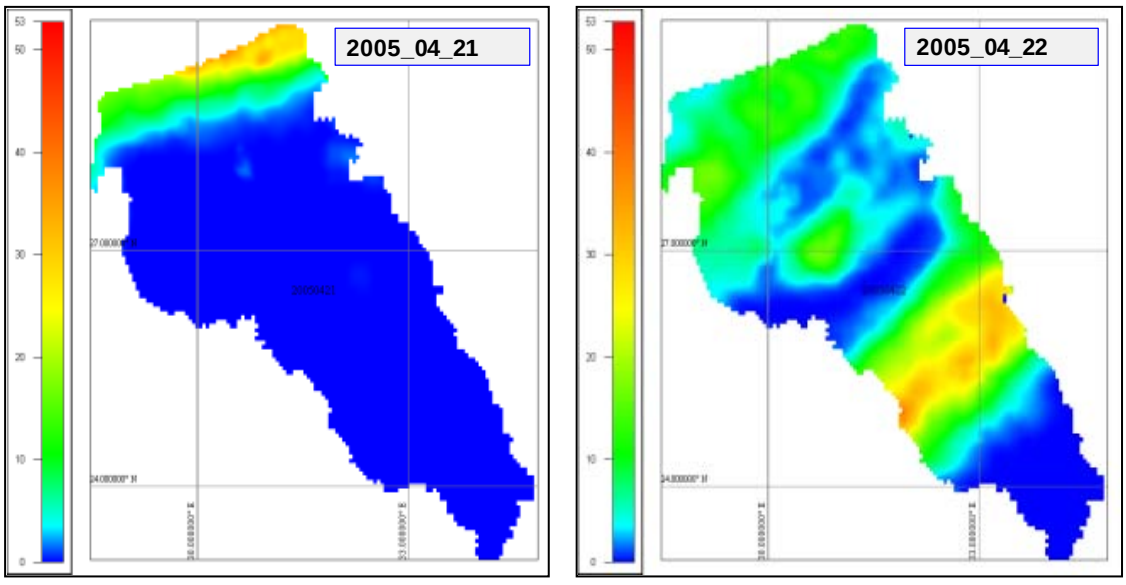

Figure 5.14 Distribution maps of rainfall (mm/h) of GSMaP product at the Nile River basin in Egypt during the event of Apr. (20-23) of 2005.

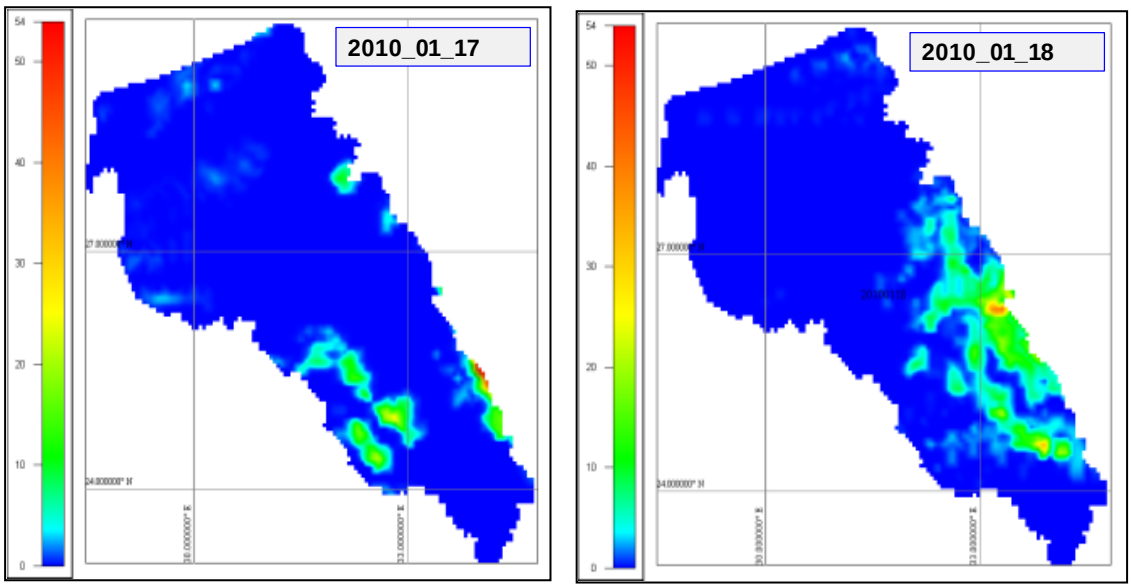

Figure 5.15 Distribution maps of rainfall (mm/h) of GSMaP product at the Nile River basin in Egypt during the event of Jan. (17-18) of 2010.

As consequence of rainfall, distribution the flash flood distribution in the target basin is mainly affected by the wadi catchments and the rainfall distribution, where this event of Jan 18-20 is concentrating in the upstream part of the whole catchments near to Aswan and Qena cities. It reveals the high variability of discharge distribution due to the spatiotemporal variability of rainfall during the four events as depicted in **Figures 5.16, 5.17, 5.18, and 5.19** are illustrating the hourly distribution of flash flood of the four events (Feb., 2003; Dec., 2004; and Apr., 2005, Jan., 2010;).

Moreover, the flow distribution in the target basin is affected by catchments areas and geomorphologic conditions of wadi catchments. Also, it can show discontinues surface flow in the whole catchment, especially during the beginning and ending of the flash flood event. It is obvious from these distribution maps of rainfall and corresponding discharge in the whole catchment that they are scattering with highly variation in space and time. For instance both of the events (2003 and 2004) are spreading in the northern and middle of the catchment as shown in **Figures 5.12, 5.13** for rainfall and **Figures 5.16, 5.17** for discharge. The

event of 2005 is scattering in the whole basin as illustrated in **Figures 5.14** and **Figure 5.18** representing of rainfall and discharge. On the other hand, the event of 2010, it concentrating in the southern part near to Aswan and Qena cities as shown in **Figure 5.15** for rainfall and **Figure 5.9** for discharge.

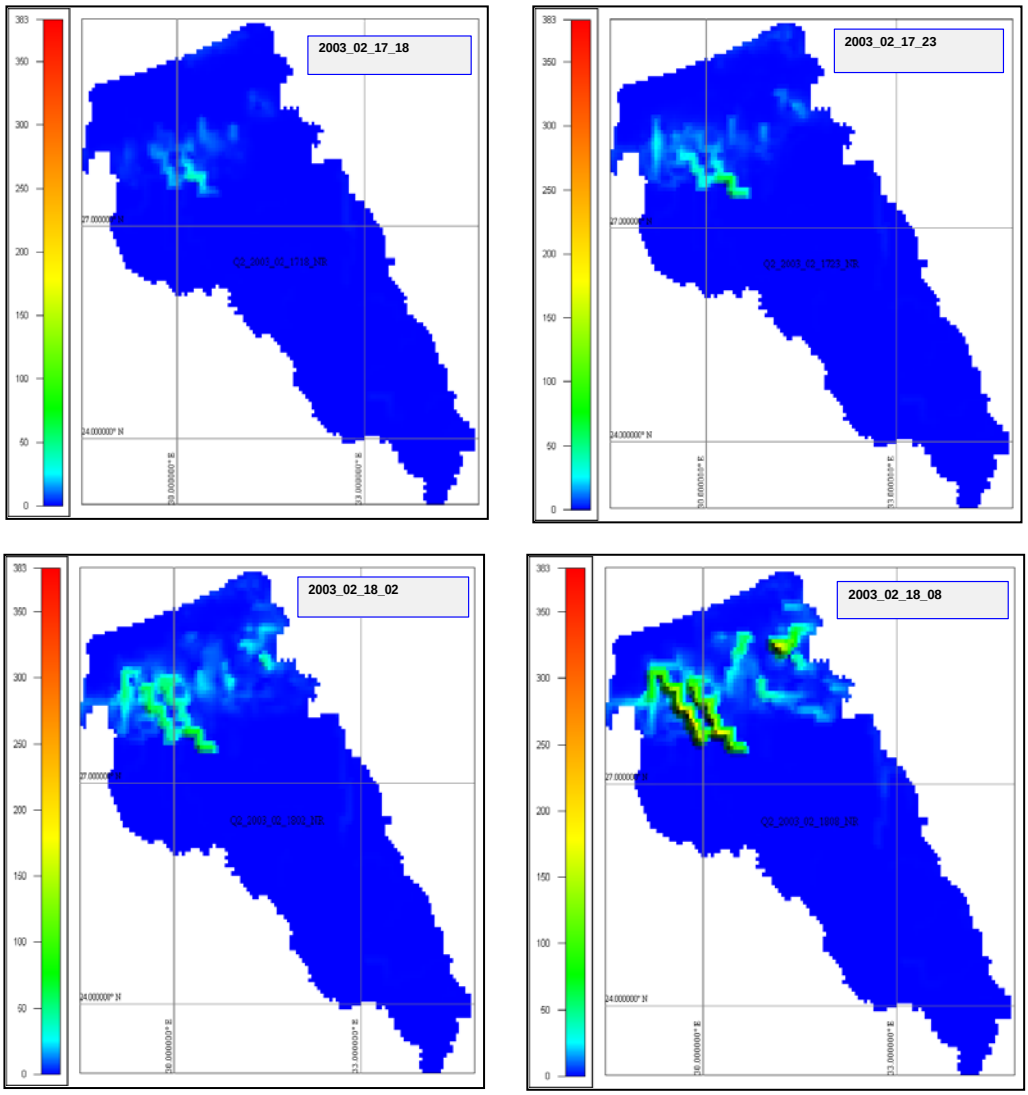

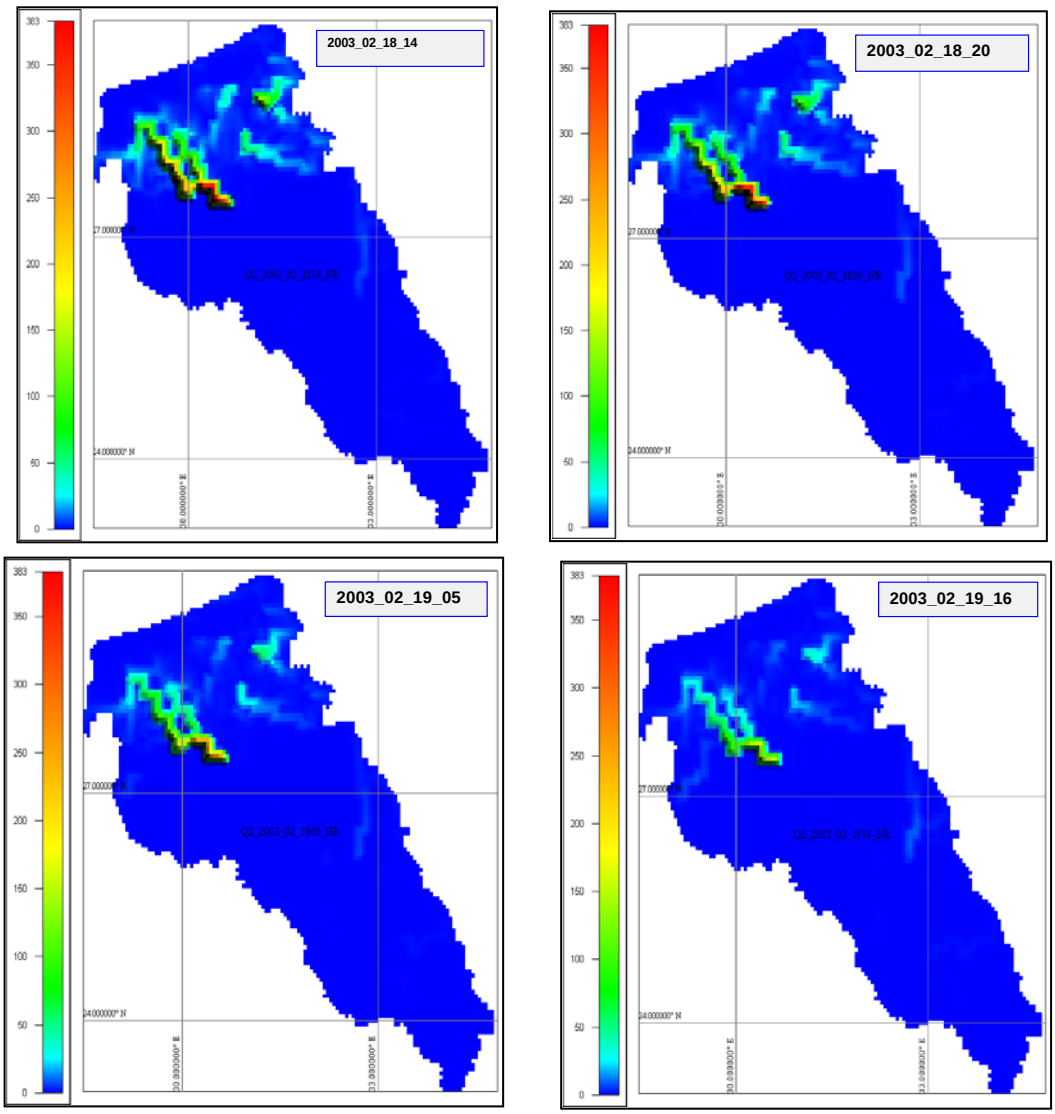

Figure 5.16 Distribution maps for discharge (m^3/s) at the Nile River basin in Egypt during the event of Jan 17-19 of 2003 showing the high variability of surface runoff in space and time.

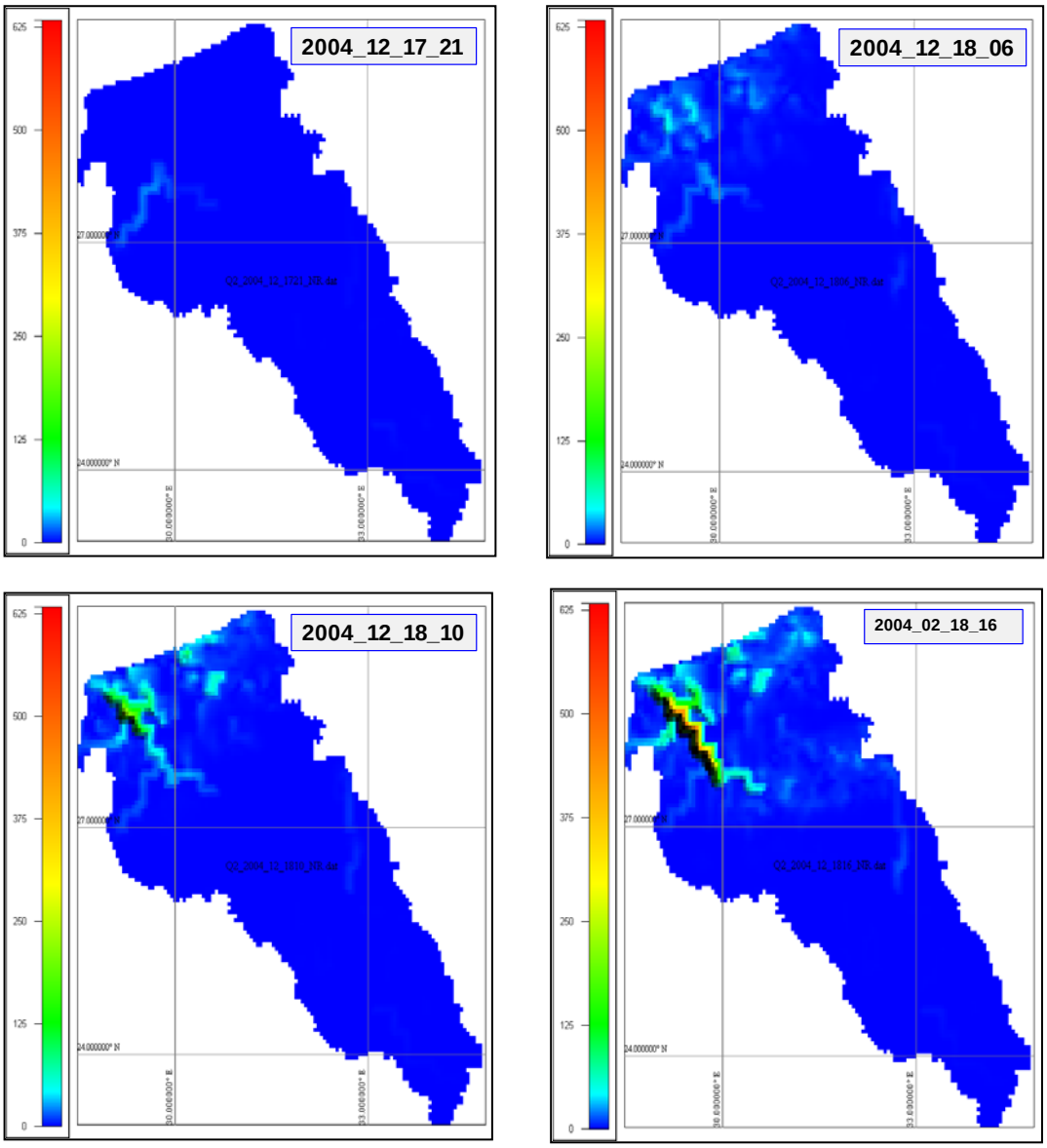
2004_12_17_21
2004_12_18_06
2004_12_18_10
2004_02_18_16

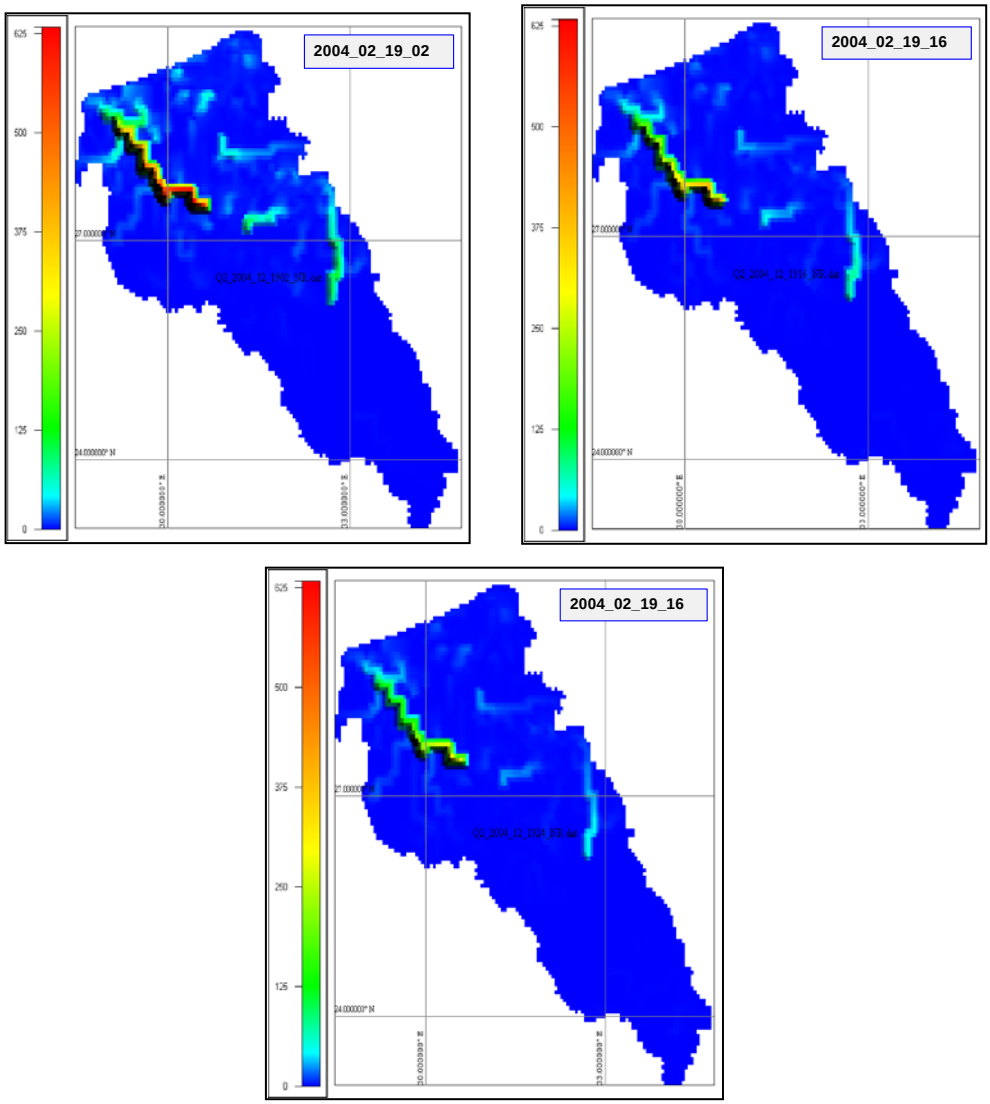

Figure 5.17 Distribution maps for discharge (m^3/s) at the Nile River in Egypt during the event of Jan 17-19 of 2004 showing the high variability of surface runoff in space and time.

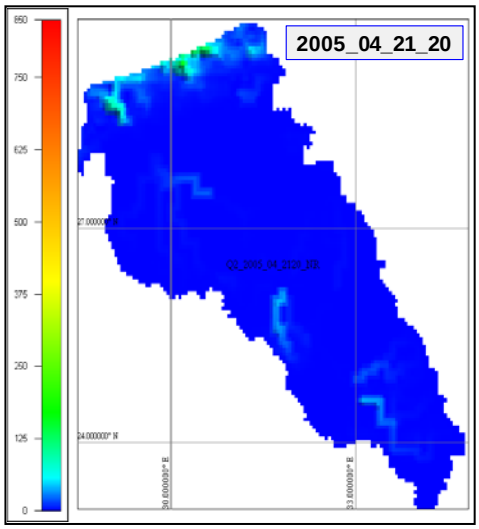
2005_04_21_20

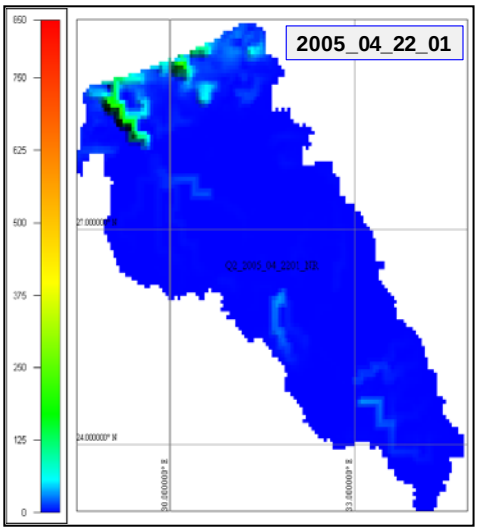
2005_04_22_01

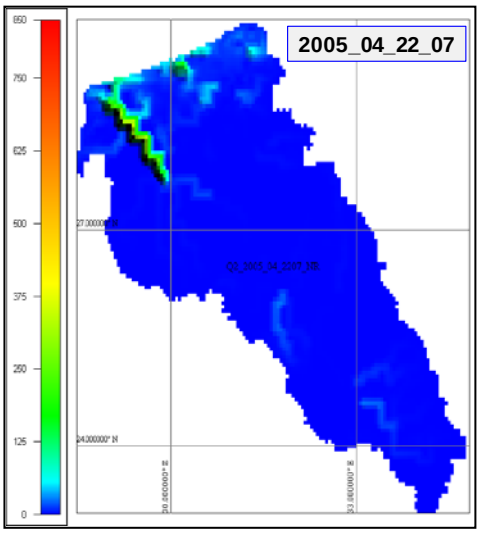
2005_04_22_07

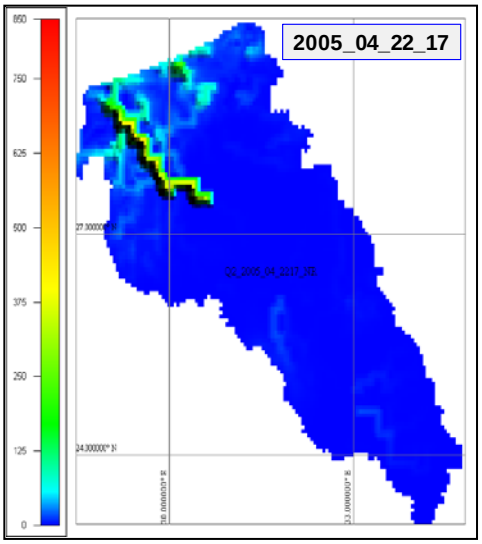
2005_04_22_17

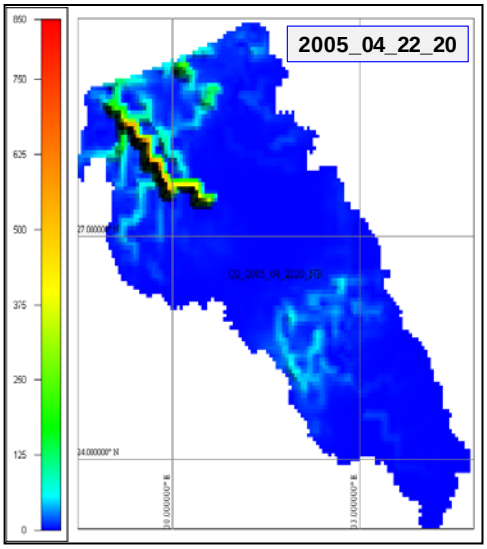
2005_04_22_20

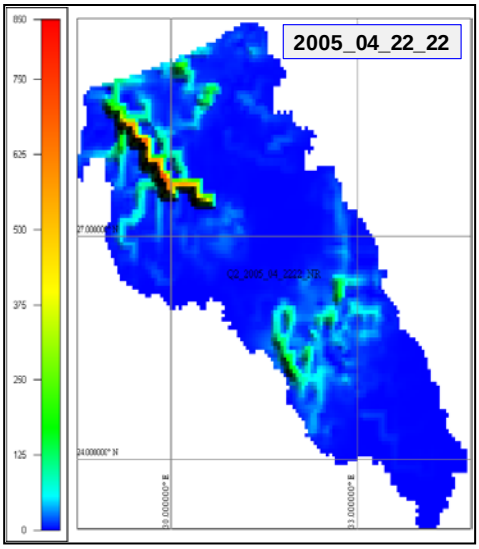
2005_04_22_22

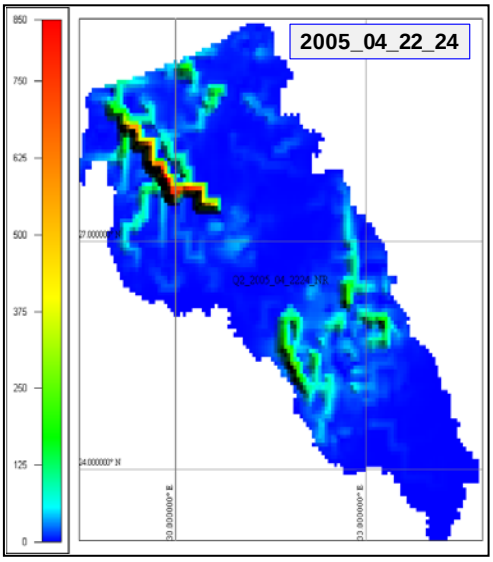

Figure 5.18 Distribution maps of discharge (m^3/s) at the Nile River basin in Egypt during the event of Jan 20-22 of 2005.

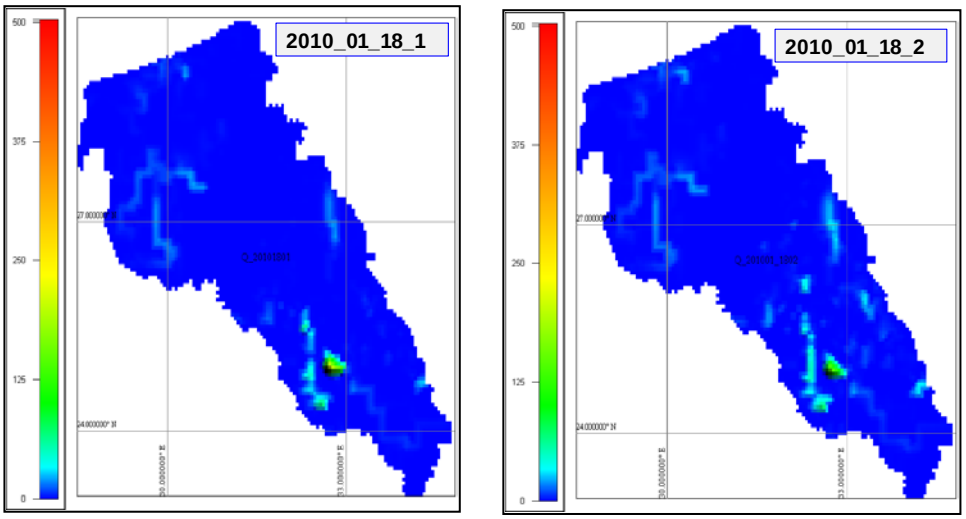

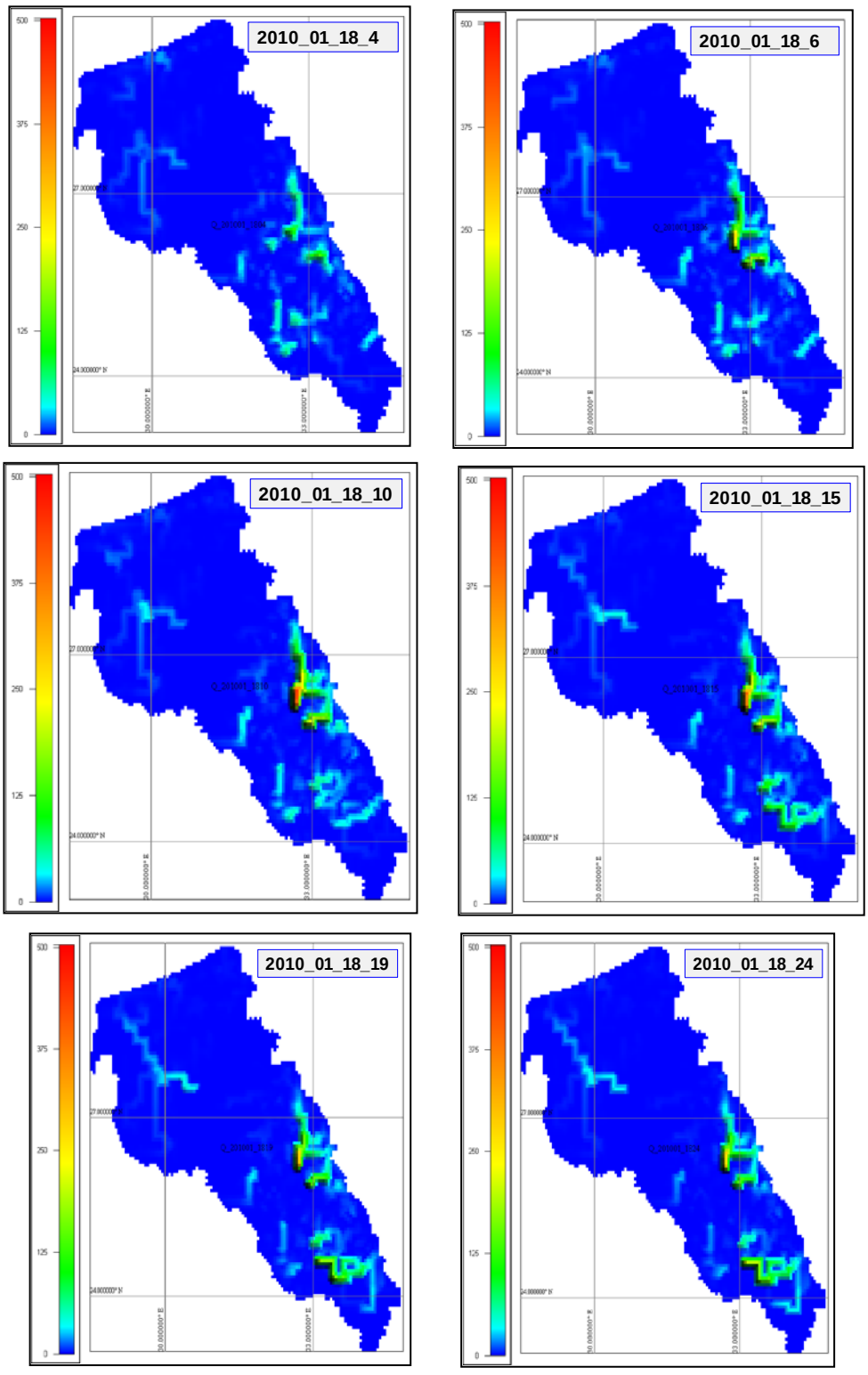
2010_01_18_4
2010_01_18_6
2010_01_18_10
2010_01_18_15
2010_01_18_19
2010_01_18_24

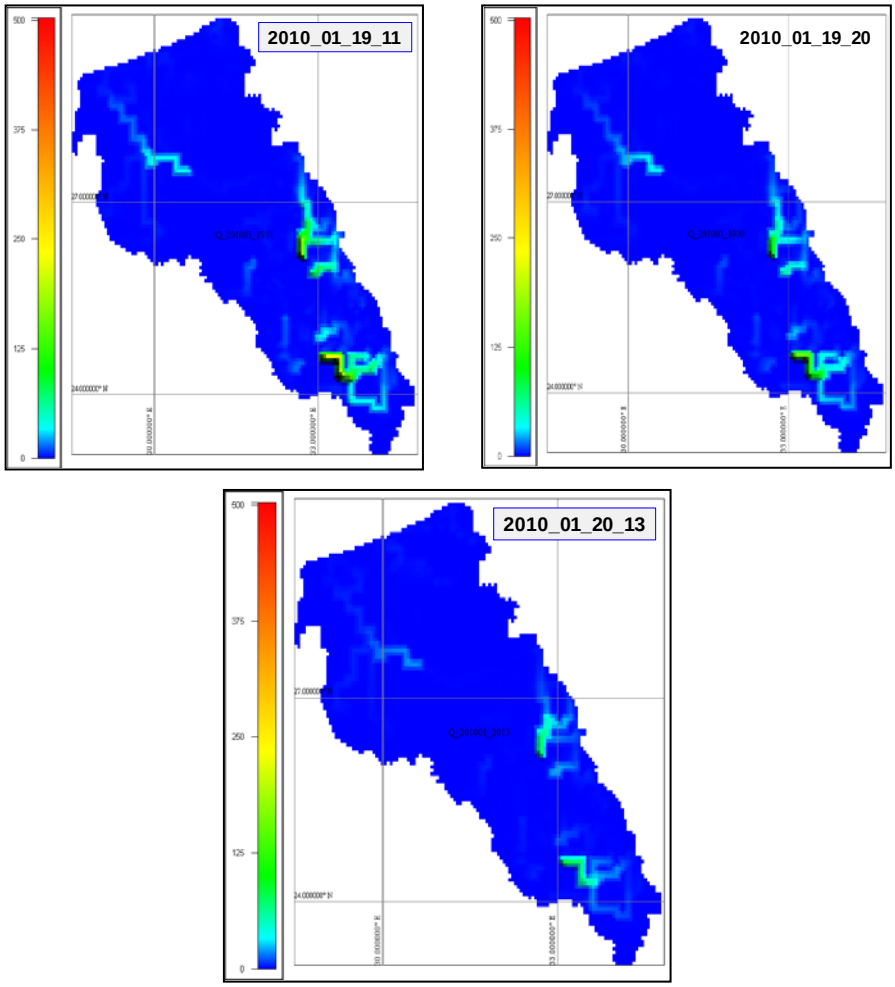

Figure 5.19 Distribution maps for discharge (m^3/s) at the Nile River basin in Egypt during the event of Jan 18-20 of 2010.

5.7. FLASH FLOOD SIMULATION at WADI EL-ARISH, SINAI

GSMaP data as the main input of rainfall is used for flash flood simulation at wadi El-Arish, Sinai Peninsula. The simulation of flash flood event of January 18-20 of 2010 and is discussed in this part due to its importance as new event in Egypt and the effect on wadi El-Arish residents and their infrastructure.

The flood event which hit Egypt on Jan. 18-20, 2010; it was devastating where some people died with a big demolition of their infrastructure. The simulated

results present remarkable characteristics of flash flood hydrograph as reaching to maximum peak flow (about 1-2 thousands of cubic meter per second).

Six outlet points have been selected based on the sub-catchments for this simulation as shown in **Figure 5. 19**. The results of simulation of the event of Jan. 18-20, 2010 show that flash flood characteristics are highly variable from from one outlet to the others in terms of flow rate and time to reach the maximum peak within the whole watershed. For instance, at the downstream outlet at the Mediterranean Sea of wadi El-Arish the flow is very severe flow about 2864.84m^3/s.

In terms of evaluation of sub-catchments water contribution towards the main outlet of wadi El-Arish, the flow volume of water which can reach to the downstream point of each sub-basin has been calculated and listed in **Table 5.7**. Moreover, because the significant of the time to peak and the flow duration in flash flood analysis, they have been listed too in **Table 5.7**.

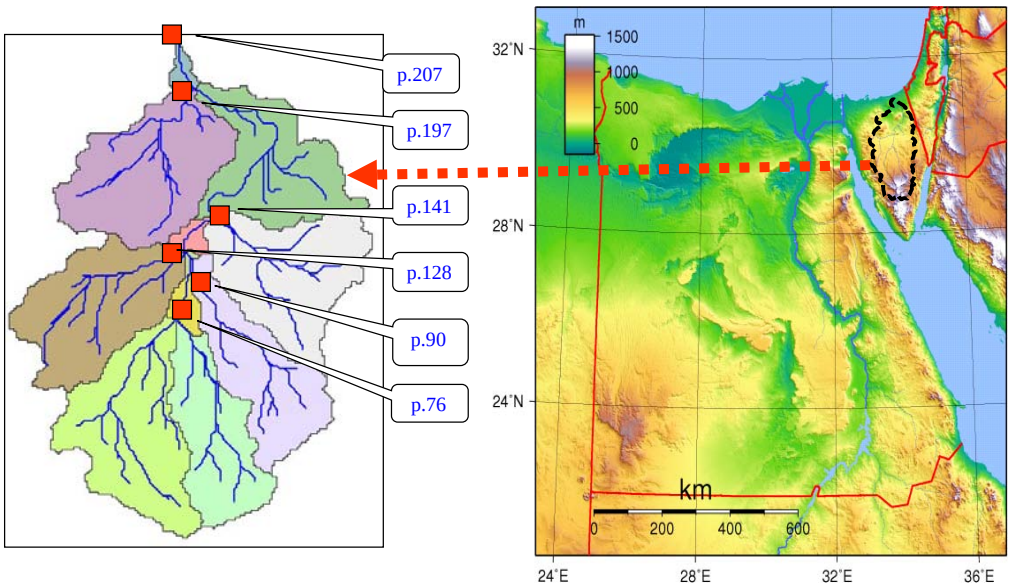

Figure 5.20 Sub-catchments of wadi El-Arish, Sinai Peninsula in Egypt showing the target outlets for flash flood simulation.

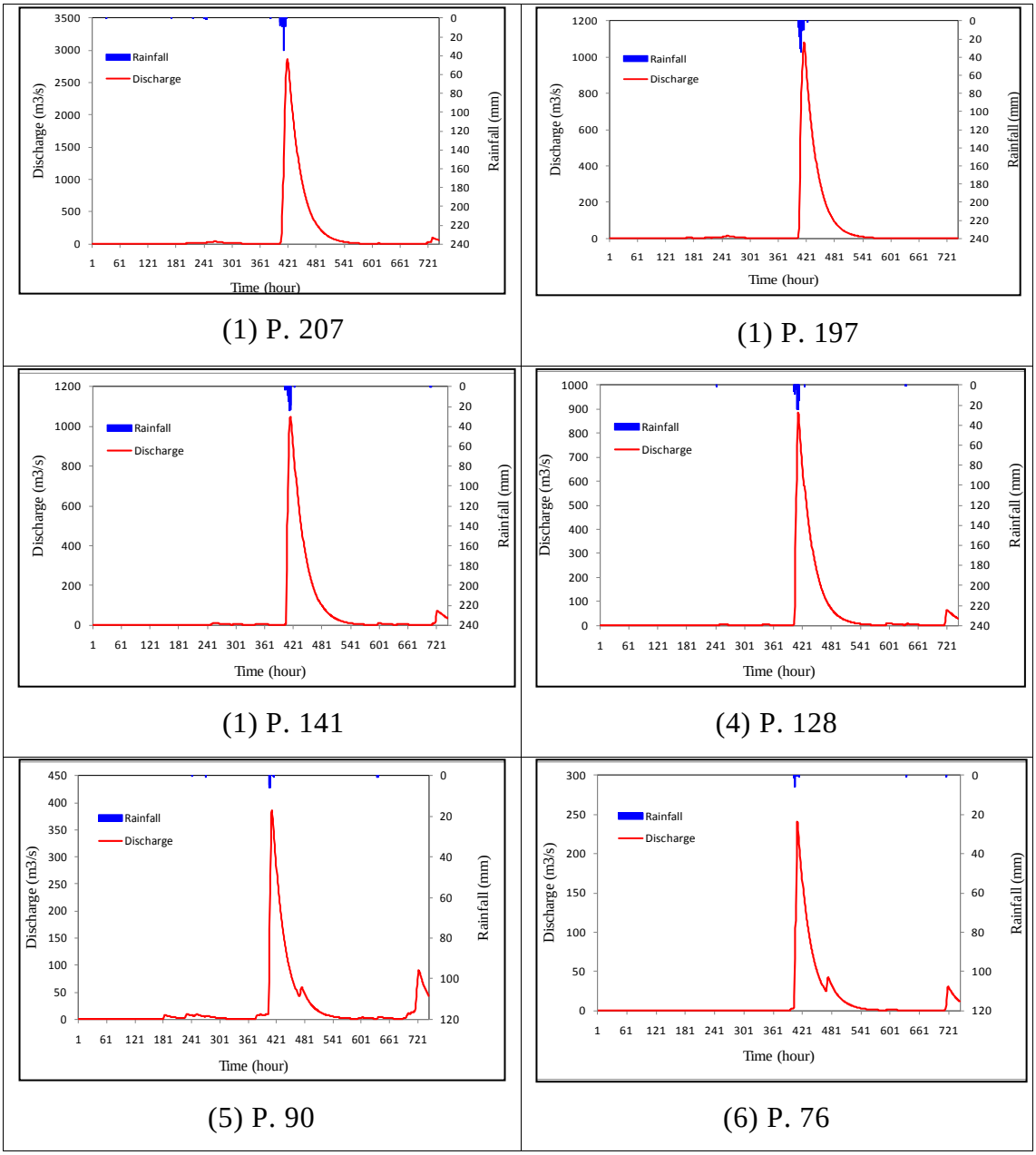

Figure 5.20 Simulated flash flood of event (Apr.18-22, 2010) at several sub-catchment outlets of wadi El-Arish; 1) P. 207; 2) p.197; 3) p. 141; 4) p. 128; 5) p. 90; and 6) p. 76.

Table 5.7 Simulation results of event (Dec.18-22, 2010) at wadi El-Arish

Sub-catchments of Wadi El-Arish Outlets	Location	Time to peak (hours)	Peak discharge (m3/s)	Flow Volume (m3)
W. El-Arish (p.207)	33.8E, 30.7N	17	2864.84	3.54E+08
W. El-Arish (p.197)	33.8E, 30.4N	14	1080.38	1.26E+08
W. Griha (p.141)	33.9E, 29.9N	13	1050.41	1.26E+08
W. Elbarok (p.128)	33.7E, 29.8N	10	885.38	9.9E+07
W. Eqabah (p.90)	33.8E, 29.5N	7	386.66	4.5E+07
W. Abu-Tarifieh (p.76)	33.7E, 29.4N	8	240.52	2.7E+07

5.8. Hourly Rainfall Distribution of Egypt

GSMaP Rainfall product has been extracted and drawn on the distribution map of Egypt as follow to show the effective regions from the last event of January 17-20, 2010. It is clear that from the maps the most affected areas are Sinai Peninsula and the coastal part of Red Sea including some parts around Aswan city as shown in **Figures (5.22, 5.23, and 5.24).**

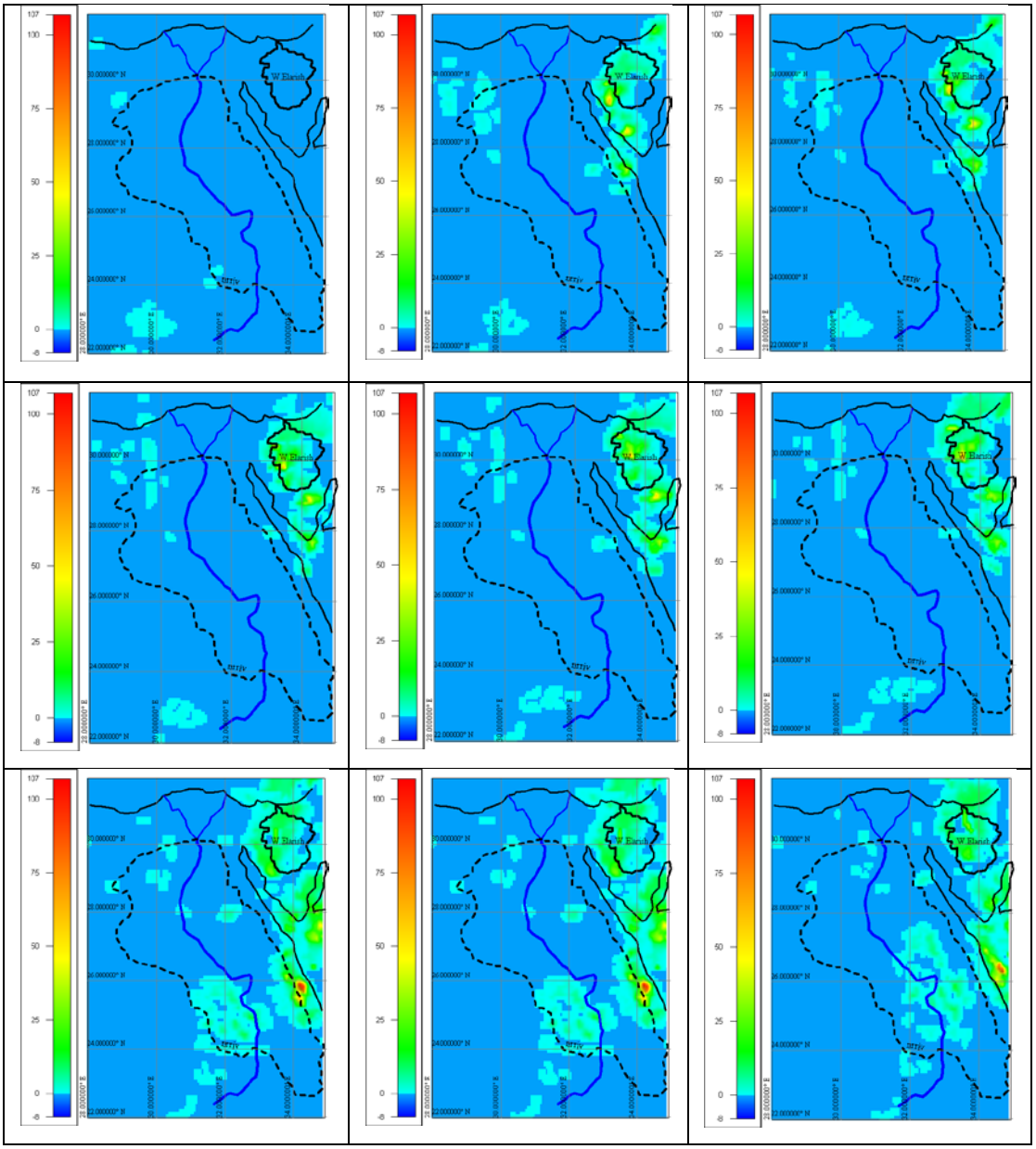

Figure 5.22 Distribution maps for rainfall (mm/h, 10 km ×10 km resolution) at the Nile River basin and wadi El-Arish, Sinai, Egypt during the event of Jan 17-19 of 2010 (17day/17hr-18day/01hr).

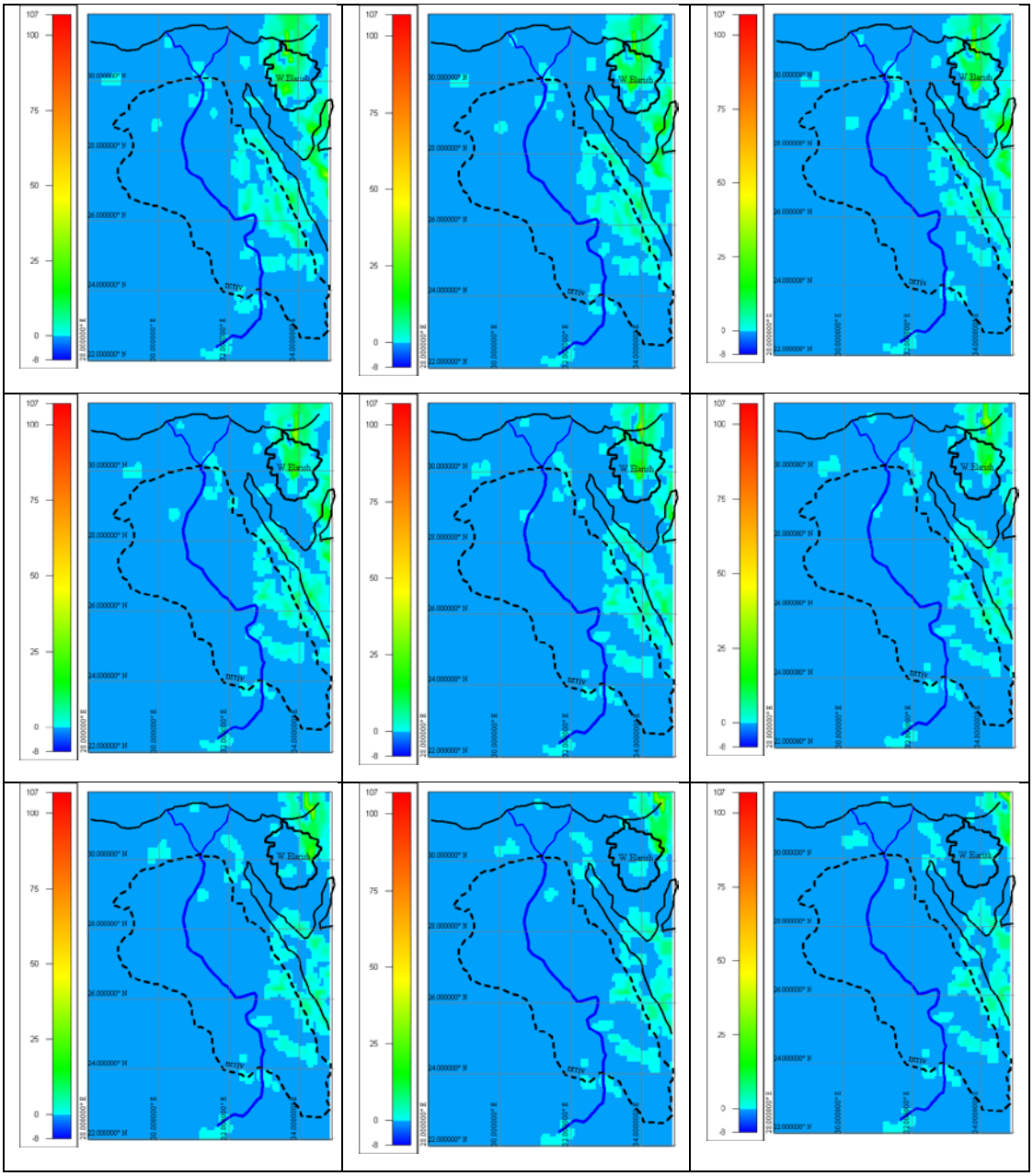

Figure 5.23 Distribution maps for rainfall (mm/h, 10 km ×10 km resolution) at the Nile River basin and wadi El-Arish, Sinai, Egypt during the event of Jan 17-19 of 2010 (18day/02hr -18day/10hr).

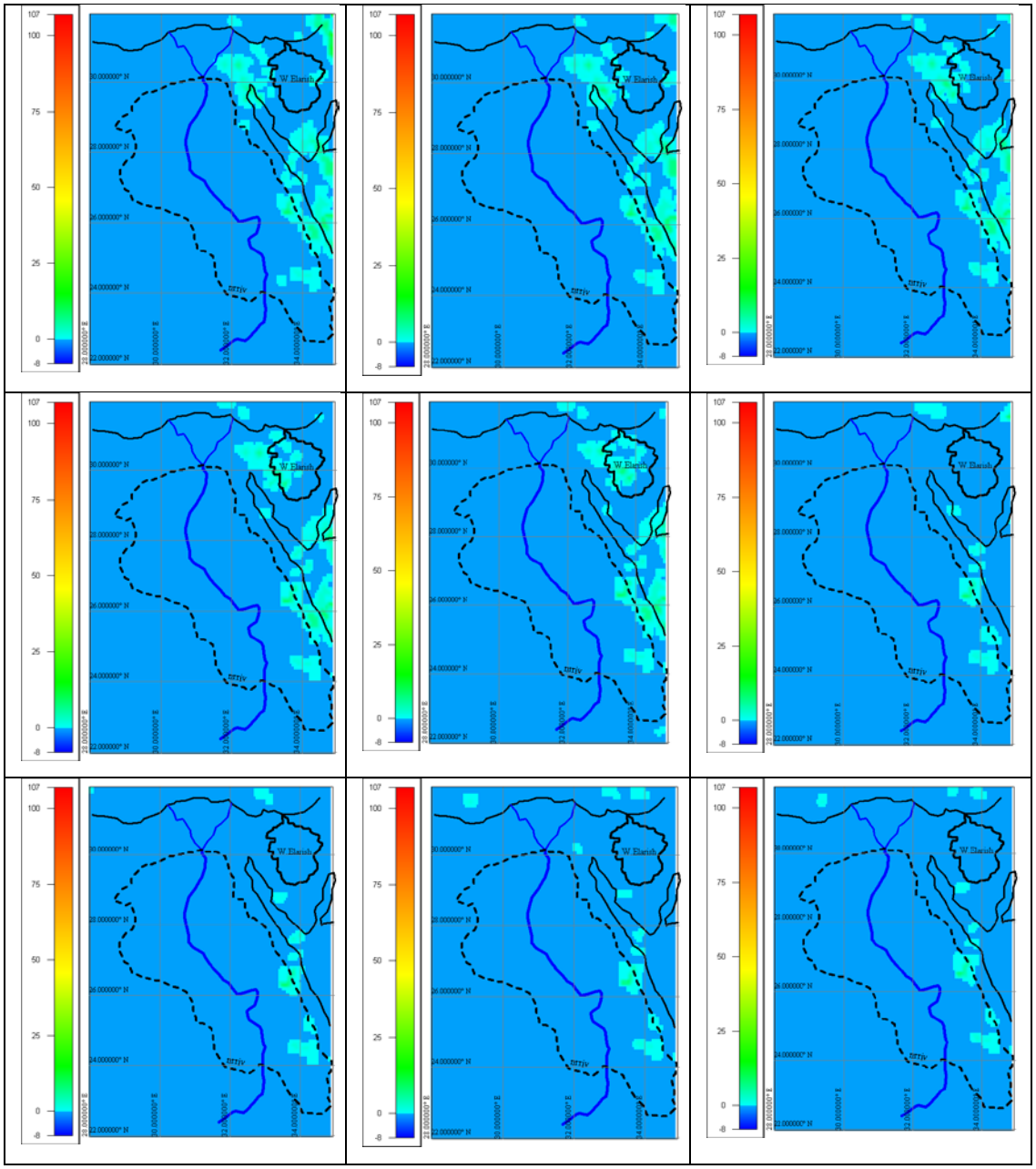

Figure 5.24 Distribution maps for rainfall (mm/h, 10 km ×10 km resolution) at the Nile River basin and wadi El-Arish, Sinai, Egypt during the event of Jan 17-19 of 2010 (18day/11hr -18day/19hr).

5.9. Flash flood as new water resources

Egypt is one of several arid and semi-arid countries that suffer from the flash flood and water scarcity hazards. It is beginning to outstrip available water supply due to its increasing population, coupled with limited water resources and attendant increases in need for water. There is an urgent need to secure and utilize new supplies of water in order to sustain the minimum water base.

However, Flash floods are devastating and represent as a big threat for human kind and arid environment, flash flood water can be utilized and management in a proper way to be useful as water resources in arid regions with proposing the powerful management system or scenarios. The main water resource in Egypt is the Nile River. Water resources management are so crucial and important in arid regions due to the shortage of rainfall and high evaporation an transmission losses, that is pushing us to think about a practical way to solve this problem as well as protecting people form flash flood and proposing good management system for water resources evaluation and the best way for utilization it. In this study, one of our significant targets is to evaluate the flash flood water as water resources by assessment how much wadi basins can contribute to the Nile River. The contribution of some wadi basins into the main channel of Nile River is numerically estimated during the event from (Jan., 2010; Feb., 2003; Dec., 2004; and Apr., 2005) are listed in **Tables 5.3, 5.4, 5.5, and 5.6** with identification of the outlet points and wadi names. From these results, it is clear that how much of flash flood of wadi can contribute into the Nile River as additional water resources however its difficulty to control and management it to avoid or avert the devastating effect of it on the downstream areas along the Nile River. The contributed water flow volume in the downstream point of wadis is varying from one wadi to the others as listed in **Tables 5.3, 5.4, 5.5, 5.6, and 5.7**.

5.10. Flash flood threat evaluation

Simulation results of flash flooding in both Nile River basin and wadi El-Arish in Sinai Peninsula show how much the big threat of flash flood in wadi basins. It investigated that form the distribution maps of flash flood is highly variable from one wadi to another, in other words from one position to the other positions relying of the rainfall events spatial and temporal distribution and geomorphologic and topographic conditions in wadi catchments. It seems the most affected region in every wadi basin is the downstream area while the flash flood water is accumulated in that regions and the flow volume is so big.

The remarks of the spatial variability of flash flood occurrence is illustrated in the flash flood event of Jan, 2010 where only wadi Qena, wadi Zaydun, wadi Abbad, and wadi Jaraah as shown in **Figure 5.25**.

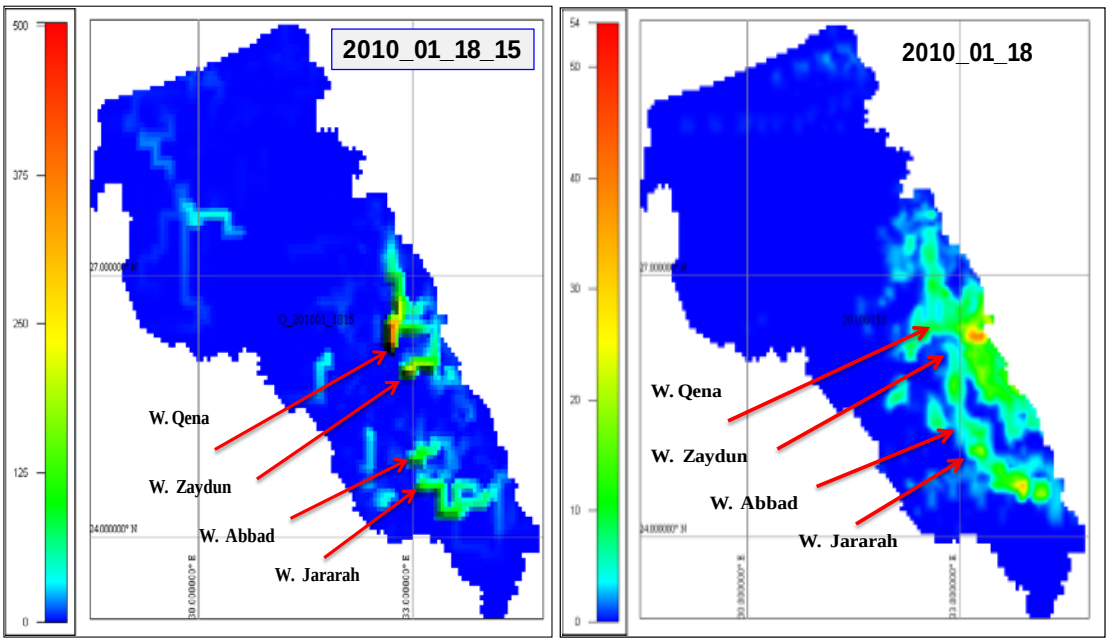

(a) (b)

Figure 5.25 Distribution maps of flow discharge (m^3/s) (a) and rainfall (mm/h) of the event of Jan, 2010 at the Nile River Basin showing the affected regions.

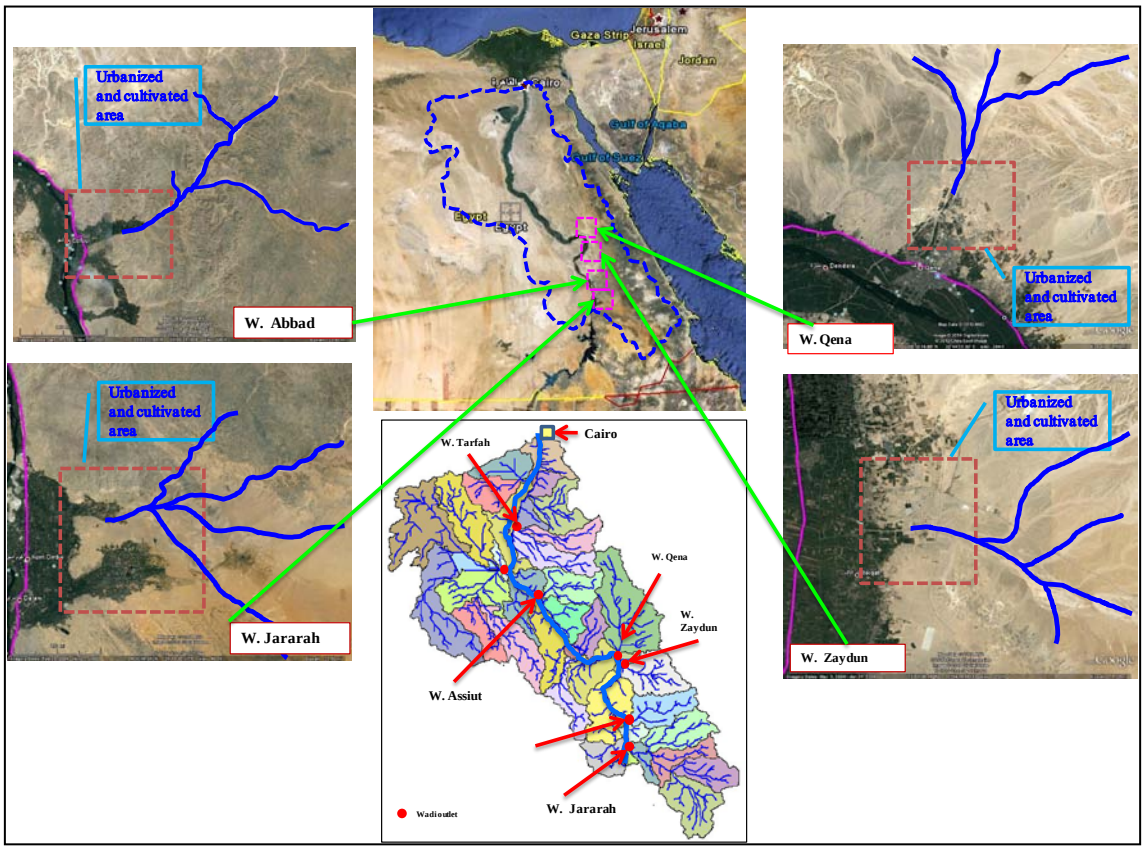

Figure 5.26 Nile River Basin and downstream areas of the affected wadis maps during the flash flood of Jan, 2010 showing the most prone regions for flash floods based on the simulated results of **Figure 5.25**.

The most affected areas in this event are the downstream outlet of wadi Qena, wadi Zaydun, wadi Abbad, and wadi Jaraah as illustrated in **Figure 5.26**. Most of downstream regions are urbanized cultivated regions which have been suffering from this flash flood. The reasons why these regions at the downstream have been affected by the flash flood are the steepness slope of the catchments which make the travel time is short to the downstream area. The wadi bed channel is not so permeable which does not give a chance for infiltration process during the flash flood event due to the high velocity of flow. The last reason is the effect of heavy rainfall throughout short period affecting on this regions.

In the real situation the area around Aswan city which is representing in wadi Abbad and wadi Jaraah have been affected by this flash flood and from the government announcement that more than 14 persons have been killed in Aswan and Sinai Peninsula as well as thousands of people becomes homeless. The current results of our simulation show how much the performance of the proposed model to predict the flash flood in such regions as well as the evaluation of the most affected regions as depicted in the results of distribution maps and **table 5.8**. The simulated results dedicate that wadi Qena and wadi Abbad show flow rate about 502 (m^3/s) and 174 (m^3/s) and total flow volume about 6.85286E+07 m^3 and 2.27200E+06 m^3 which can reach to the downstream area during the flash flood event. On the other hand, wadi Jararah and wadi Zaydun have affected by the flow rate and flow volume less than the other two wadis.

So, these results indicate that the possibility of estimating spatiotemporal flow volume of the flash flood affecting the target regions and consequence, the risk maps and the prone areas of flash flood can be easily detected and determined in wadi basins as illustrated in this work.

Table 5.8 Simulation results of event (2010/Jan.18-20)

Wadi Name	Location	Time to peak (hours)	Peak disch. (m^3/s)	Flow Volume (m3)
Jararah (1)	32.9E, 24.5N	4	19.7	8.01921E+05
Abbad (2)	32.9E, 24.9N	3	174	2.27200E+06
Zaydun (3)	32.8E, 25.9N	3	9.97	4.24185E+05
Qena (4)	32.7E, 27.3N	11	502.7	6.85286E+07
Assiut (5)	31.3E, 27.2N	5	2.9	3.02180E+05
W. Desert(6)	32.0E, 26.1N			
At-Tarfah (7)	30.7E, 28.4N			
Total				7.23289E+07

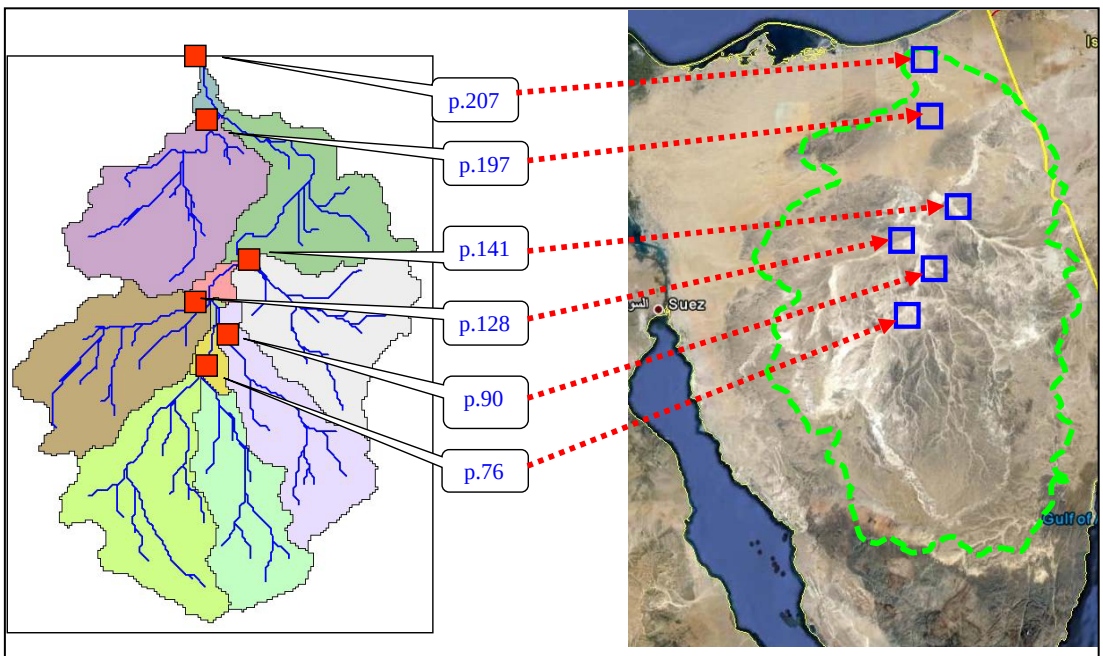

Sub-catchments of Wadi El-Arish Outlets	Location	Time to peak (hours)	Peak discharge (m3/s)	Flow Volume (m3)
W. El-Arish (p.207)	33.8E, 30.7N	17	2864.84	3.54E+08
W. El-Arish (p.197)	33.8E, 30.4N	14	1080.38	1.26E+08
W. Griha (p.141)	33.9E, 29.9N	13	1050.41	1.26E+08
W. Elbarok (p.128)	33.7E, 29.8N	10	885.38	9.9E+07
W. Eqabah (p.90)	33.8E, 29.5N	7	386.66	4.5E+07
W. Abu-Tarifieh (p.76)	33.7E, 29.4N	8	240.52	2.7E+07

Figure 5.27 Nile River Basin and downstream areas of the affected wadis maps during the flash flood of Jan, 2010 showing the most prone regions for flash floods based on the simulated results of **Figure 5.25**.

Moreover, wadi El-Arish, Sinai Peninsula also has been affected by the flood event which hit Egypt on Jan. 18-20, 2010; but it was more devastating in this area than Nile River basin at Aswan City. It is so important to evaluate and discuss the threat of flash flood at this wadi which is important because Al-Arish city is located mainly at the downstream part of its wadi channel course as well as a lot of Bedwins (are nomadic peoples that have traditionally occupied Sinai) are living in

different location along this wadi. Along the main stream of wadi El-Arish, some downstream points of sub-catchments have been studied and the simulated results show that the maximum affected regions is the downstream of wadi El-Arish which has flow rate about 2864 (m^3/s) and flow volume about 3.54E+08 m^3. The effect of flash flood is reducing towards the upstream area for example at wadi Abu-Tarifieh is affected by flow rate about 240 (m^3/s) and flow volume about 2.7E+07 m^3 as illustrated in **Figure 5.27**.

As a future work, a comprehensive integrated management of flash flood warning system is our main target to minimize the human life loss and infrastructure damage causing by flash flood is desperately needed in the whole Egypt as well as for the effective and sustainable management of water resources to improve the water situation.

5.11. CONCLUSION

In the arid regions, the flash flood is characterized as flood leading to damage caused by heavy rainfall for short duration, steep slope and impervious layer as well as climate change which make it more sever and devastating. Due to the scarcity of high quality observations, an attempt is made to use Global Satellite Mapping of Precipitation (GSMaP) for flash flood simulation in the wadi basins at Nile River in Egypt. GSMaP product has been compared with the monitored data of Global Precipitation Climatology Centre (GPCC); gauge-based gridded monthly precipitation data sets. Monthly and 0.1° x 0.1° (10km × 10km) spatial resolutions data is used. Statistics analysis has been done to calculate the bias of these data for different arid areas such as, N. Africa, Arabian Peninsula, S. Africa, South-West USA, Australia, China.

The results of comparative show an acceptable agreement between GSMaP and GPCC however the occurrence of overestimated or underestimated systematic seasonal bias which is variable relying on the selected regions. Relying on these

results, GSMaP product has been corrected in the target basin. HydroBEAM as a physical-based hydrological model is used to simulate various flash flooding events at wadi outlets of Nile River using GSMaP data. The simulation has been done to the flood event which hit Egypt on Jan. 18-20, 2010; it was devastating where some people died with a big demolition of their infrastructure. Furthermore, Simulation of flash flood events of Feb. 2003, Dec. 2004, and Apr. 2005 have also carried out in this paper for more understanding of the flash flood behaviors and characteristics.

The simulated results present remarkable characteristics of flash flood hydrograph as reaching to maximum peak flow more than (174 m3/s) throughout three hours in W. Abbad in Egypt. Additionally, the distribution results of flash flood corresponding to rainfall data show that there are high variability in occurrence of flash flood from in both space and time in terms of wadi characteristics and the time of the flash flood event. It can be concluded that GSMaP precipitation product is very effective in use with the physical-based hydrological model (HydroBEAM) to predict the flash flood not only in wadi basins on Nile River but also in wadi basin in different arid regions.

As well known, the flash flooding is one of the most devastating hazards in terms of loss of human life and infrastructures. So simulation of Flash flood has been carried in the wadi basins in Nile River at the Egyptian part using the remote sensing data such as GSMaP product in. The Nile River Basin in Egypt is selected due to its significant as the main water resources for domestic, agricultural and industrial purposes.

GSMaP product as real time rainfall data can be used as linkages with the flood forecasting technique in order to provide the flash flood forecast well in advance for taking the emergency actions for evacuating the people so that their lives may be saved and the losses of the properties may be minimized.

For simulation of flash flood, a physically-based, distributed hydrological model (HydroBEAM) has been used for this target after calibrating it in wadi Al-Khoud

in Oman model as well as parameters identification of wadi system. The simulation for the strongest events has been only chosen in this study. The simulated results of flash flood event in the studied wadi basins exhibit that the flow characteristics of flash flood where it takes a few hours to reach to the maximum peak and then gradually reducing until cessation of the event.

The distribution maps of flash flood events of (Feb., 2003; Dec., 2004; Apr., 2005, and Jan., 2010) in the whole catchment of Nile River in Egypt part show that highly variation of flash flood in space and time in the selected targets. It reveals the high variability of discharge distribution due to the spatiotemporal variability of rainfall during the selected four events. It is noticed that the effect of catchments areas and geomorphologic conditions of wadi catchments. It is clear that how much of flash flood of wadi can contribute into the Nile River as additional water resources however its difficulty to control and management it to avoid or avert the devastating effect on the downstream areas along the Nile River. The contributed water flow volume in the downstream point of wadis is varying from one wadi to the others.

It can be concluded that GSMaP can be used with or without bias correction based on the selected regions as well as the proposed model of HydroBEAM using such Satellite remote sensing data can be applied effectively for flash flood forecasting at different wadi basins in arid and semi-arid regions.

We can summarize our findings and advantages of our results as flow:

1- Simulation of flash flood has been successfully achieved in wadi basins in very large catchment of Nile River basin as well as wadi El-Arish, Sinai Peninsula, Egypt
2- Using remote sensing Data to overcome the problem of data paucity in arid regions is analyzed and introduced by using GSMaP
3- Evaluation of Water contribution of flash flood into the Nile River from its wadi sub-catchments and wadi El-Arish sub-catchments.

Chapter Six

Summary and Recommendations

6.1 Overall conclusion

In this dissertation, the proposed and developed of hydrological approaches as well as numerical simulation of distributed runoff have been achieved for arid and semi-arid environment model in regard of water resources management and flash flood simulation. Throughout this study, understanding of wadi system characteristics and hence its hydrological processes have been accomplished and depicted. Additionally, runoff behaviors and factors affecting it, initial and transmission losses and its effect on both surface flow and subsurface storage are successfully evaluated.

This study is formulated into the following main five parts; the first one declaration of characteristics of the arid and semi-arid regions and their current problems as described in chapter one and chapter two. The second part is devoted to introduce the developed and proposed physically-based hydrological approaches. The third parts are to discuss the numerical simulation results of wadi runoff. The last part is focusing on the flash flooding simulation in the Nile River basin, in Egypt.

The characteristics of wadi basins can be summarized briefly as follow; i) More than one third of the world can be described as arid regions. Ii) They are suffering from the severe situation of water resources shortage. iii) the ephemeral streams in arid areas are characterized by discontinuous occurrence of flow in both space and time. In terms of geomorphology, most of the arid terrains can also be called deserts which has not enough water and low vegetations; Climatic

conditions in arid environment (rainfall is commonly characterized by extremely high spatial and temporal variability, and the climatic pattern in the arid zones is frequently characterized by a relatively "cool" dry season, followed by a relatively "hot" dry season, and ultimately by a "moderate" rainy season. In general, there are significant diurnal temperature fluctuations within these seasons, and because of the scarcity of vegetation that can reduce air movements, arid regions typically are windy. Winds remove the moist air around the plants and soil and, as a result, increase evapotranspiration.); and surface water–groundwater interactions in arid and semi-arid drainages are controlled by transmission losses.

This thesis also presents homogenization method of upscaling hydrological parameters related to a distributed runoff model from microscopic aspects up to macroscopic ones. It is concluded that the homogenized parameters k^* and n^* are equivalently derived from the mathematically formulated descriptions based on the conservation of surface and subsurface water quantities, these parameters are relied on Darcy's law and Manning's law. The obtained Equations of the equivalent parameters are different considering the cell conditions. Also, a trial is made to adopt Hydrological Basin Environmental Assessment Model (Hydro-BEAM) which has been originally developed for humid regions application; it has been chosen for simulation the wadi runoff model with incorporating of the initial and transmission losses models. The adopted Hydro-BEAM is a physically-based numerical model and it mainly consists of: i) the watershed modeling using GIS technique is processed. ii) Surface runoff and stream routing modeling based on using the kinematic wave approximation is applied. iii) the initial and transmission losses modeling are estimated by using SCS (1997) method (an empirical model for rainfall abstractions suggested by the U.S Soil conservation Service) and Walter's equation (1990) respectively. iv) Groundwater modeling based on the linear storage model is used. Moreover, due to the importance of initial and transmission losses; In this study, basically, the initial losses is figured out through the empirical equation of the SCS (Soil Conservation Service) method,

and transmission losses along wadi river channels are estimated from the empirical equation of regression model in wadi discharges. The consistency and compatibility between empirical (empirically proposed transmission losses) and theoretical (kinematic wave) models are then established.

Furthermore, in this work, simulation and evaluation of wadi basin surface and subsurface runoff in addition to understand the flow characteristics and the factors affecting on its behaviors have been successfully accomplished. In addition to, a comparative study has been done between some wadi basins in the Arabian regions of Egypt, Oman, and Saudi Arabia.

It is concluded that the simulated runoff are completely coincide in their behaviors with the monitored one that prove an appropriate performance of the proposed model to predict the future flood events. From the distribution maps of surface runoff in the wadi system, the discontinuously surface flow is perfectly depicted as one of the most import characteristics of ephemeral streams. Transmission loss is affected by the volume of surface runoff as evidence that the rate of losses is linearly related to the volume of surface discharge.

A comparative study between some Arabian wadis is performed. Results of simulation declared that the runoff features are affected by the catchments area, slope, and rainfall events frequency and duration as declared in chapter four. Runoff features in the ephemeral streams are characterized by different behaviors from the runoff in the humid area based on the results as follow: i) the time to peak is short (i.e. the time of flow to reach to the discharge peak); ii) Flood event time including starting and cessation is short; iii) Initial and transmission losses are considered the main source of subsurface water recharge; and v) Discontinuous surface flow in space and time occurrence.

The proposed approaches could be found applicable methodologies in wadi basins in arid and semi-arid regions and consequently, a vital contribution to estimate the distributed surface runoff and transmission losses regionally not only in some Arabian wadis but also in the other arid regions.

The flash flooding simulation using the Global Satellite Mapping of Precipitation (GSMaP) has been achieved in the Nile River Basin and wadi El-Arish, Sinai Peninsula, Egypt. Due to the scarcity of high quality observations, an attempt is made to use Global Satellite Mapping of Precipitation (GSMaP) for flash flooding simulation in wadi basins at the Nile River in Egypt. GSMaP product has been compared with the monitored data of Global Precipitation Climatology Centre (GPCC) which are gauge-based gridded monthly precipitation data sets. Monthly and 1.0° x 1.0° spatial resolutions data is used. Statistics analysis has been done to calculate the bias of these data for different arid areas such as, N. Africa, Arabian Peninsula, S. Africa, South-West USA, Australia, and China. The results of comparative show an acceptable agreement between GSMaP and GPCC but the occurrence of overestimated or underestimated systematic seasonal bias which is variable relying on the selected regions. Relying on these results, GSMaP product has been corrected in the target basin. HydroBEAM as a physical-based hydrological model is used to simulate various flash flooding events at wadi outlets of the Nile River using GSMaP data. The simulation has been done to the flood event which hit Egypt on Jan. 18-20, 2010; it was devastating where some people died with a big demolition of their infrastructure. Furthermore, Simulation of flash flood events of Feb. 2003, Dec. 2004, and Apr. 2005 have also carried out in this paper for more understanding of the flash flood behaviors and characteristics. The simulated results present remarkable characteristics of flash flood hydrograph as reaching to maximum peak flow more than (174 m3/s) throughout three hours in W. Abbad in Egypt. Additionally, the distribution results of flash flood corresponding to rainfall data show that there are high variability in occurrence of flash flood from in both space and time in terms of wadi characteristics and the time of the flash flood event. It can be concluded that GSMaP precipitation product is very effective in use with the physical-based hydrological model (HydroBEAM) to predict the flash flood not only in wadi basins on the Nile River but also in wadi basin in different arid

regions.

GSMaP product as real time rainfall data can be used as linkages with the flood forecasting technique in order to provide the flash flood forecast well in advance for taking the emergency actions for evacuating the people so that their lives may be saved and the losses of the properties may be minimized.

For simulation of flash flood, a physically-based, distributed hydrological model (HydroBEAM) has been used for this target after calibrating it in wadi Al-Khoud in Oman model as well as parameters identification of wadi system. The simulation for the strongest events has been only chosen in this study. The simulated results of flash flood event in the studied wadi basins exhibit that the flow characteristics of flash flood where it takes a few hours to reach to the maximum peak and then gradually reducing until cessation of the event.

The distribution maps of flash flood events of (Feb., 2003; Dec., 2004; and Apr., 2005, Jan., 2010;) in the whole catchment of the Nile River in Egypt part show that highly variation of flash flood in space and time in the selected targets. It reveals the high variability of discharge distribution due to the spatiotemporal variability of rainfall during the selected four events. Moreover, it is noticed that the effect of catchments areas and geomorphologic conditions of wadi catchments. It is clear that how much of flash flood of wadi can contribute into the Nile River as additional water resources however its difficulty to control and management it to avoid or avert the devastating effect on the downstream areas along the Nile River. The contributed water flow volume in the downstream point of wadis is varying from one wadi to the others.

It can be concluded that GSMaP can be used with or without bias correction based on the selected regions as well as the proposed model of HydroBEAM using such Satellite Remote Sensing data can be applied effectively for flash flood forecasting at different wadi basins in arid and semi-arid regions.

Consequently, our findings and advantages of flash flood simulation results can be summarized as flow:

1- Simulation of flash flood has been successfully achieved in wadi basins in very large catchment of the Nile River basin and wadi El-Arish, Sinai Peninsula, Egypt
2- Using Remote Sensing Data to overcome the problem of data paucity in arid regions is analyzed and introduced by using GSMaP
3- Evaluation of water contribution of wadi basins during the flash flood in to the Nile River and wadi El-Arish, Sinai Peninsula.

6.2 Recommendation for future research

1. Further powerful and appropriate approaches are recommended for the wadi system modeling based on the observed data and the regional application considering the physical based approaches are totally needed. In the arid regions, the observational data are so rare, thus, setting up of observational stations for multiple measurements (discharge, rainfall, evaporation, etc) are important to improve the hydrological models which have been developed in such regions.
2. Field work to investigate the initial and transmission losses in wadi basins are highly recommended for more understanding of the intricate hydrological processes in such areas. The infiltration process in wadi system is so intricate because it is controlled by many factors such as (soil types, wadi bed channel, land use, geomorphology and geology of wadi basin, and slope, etc). In order to understand such phenomena (transmission loss or infiltration in wadi channel), detailed field work are also recommended to enhance the proposed approaches as well as more understanding of the hydrology of wadi system. Moreover, field work considering geomorphologic, topographic, geologic properties as well as land use and soil types to get a comprehensive view of its actual circumstances and behaviors which might be useful for developing the physical based hydrological modeling for flash flood warning system and

water resources management at wadi environment not only in Egypt but also in other arid regions all over the world.

3. In the current research using Hydro-BEAM, the linear storage model is used for the subsurface water modeling and replacement into a physically-based ground water approach is also needed. As well known, the groundwater in arid areas is so essential. Thus, developing the physical based models of groundwater flow and contaminant transport are desperately needed in order to find the appropriate management strategies in such regions to save the minimum base of water resources.
4. In terms of flash flood in arid regions, the flash floods simulation have been done in the Nile River in this study, but, the effective flash flooding warning system is urgently requested based on collecting the observed data as well as considering the climate change and its effect on the flash floods in arid regions. In Egypt and many Arabian countries, it is noticed that during this year 2010, the flash floods have been repeated just during a few months, but before that they were infrequently occurring. This is an indication of the effect of the climate change on the wadi hydrological conditions recently.

REFERENCES

Abdulrazzak, M. J. and Sorman, A. U. (1994): Transmission losses from ephemeral stream in arid region, *J. of Irrigation and Drainage Eng.*, 20, 3, pp. 669-675.

Alsharhan, A. S, Rizk, Z. A., Nairn, A. E. M, BAkhit, D. W. and Alhajari, S. A. (2001): Hydrogeology of an arid region: the Arabian Gulf and adjoining areas, *Elsevier Science B.V., The Netherlands*, 354pp.

Andersen, N. J., Wheater, H. S., Timmis, A. J. H. and Gaongalelwe, D. (1998): Sustainable development of alluvial groundwater in sand rivers of Botswana. In Sustainability of Water Resources under Increasing Uncertainty, *IAHS Pubn*. No. 240, pp. 367-376.

Bell, V. A. and Moore, R. J. (2000): The sensitivity of catchment runoff models to rainfall data at different spatial scales, *Hydrol. Earth Syst. Sci*., 4, pp. 653–667.

Biswas, A. K. (1994): International waters of the Middle East: from euphrates - Tigris to Nile. *Oxford University Press*, p. 221.

Boughton, W. C. and Stone, J. J. (1985): Variation of runoff with watershed area in a semi-arid location, *Journal of Arid Environment*, 9, pp. 13–25.

Bowers, J. E. (1982): The plant ecology of inland dunes in Western North America. *Journa1 ofArid Environments*, 5: 199-220.

Choudhury, B.J. and Monteith, J.L., 1986. Implications of stomatal response to saturation deficit for the heat balance of vegetation. *Agric. For. Meteorol.*, 36: 215-225.

Collier, C. (2007): Flash flood forecasting: What are the limits of predictability? *Quarterly Journal of the Royal Meteorological Society*, 133: 622A, pp. 3–23.

Conway, D. and Hulme, M. (1993): Recent fluctuations in precipitation and runoff over the Nile sub-basins and their impact on main Nile discharge. *Clim Change,* 25: pp. 127–151.

Cordery, I., Pilgrim, D. H. and Doran, D. G. (1983): Some hydrological characteristics of arid western New South Wales. *Hydrol. and Water Resour. Symp*, Inst. Engrs Aust., Natl. Conf. Publ.83/13, pp. 287-292.

Crerar, S., Fry, R. G., Slater, P. M., van Langenhove, G. and Wheeler, D. (1988): An unexpected factor affecting recharge from ephemeral river flows in

SWA/Namibia. In Estimation of Natural Groundwater Recharge, ed. Simmers, I. Dordrecht: D. Reidel Publishing Company, pp. 11–28.

Creutin, J. D. and Borga, M. (2003): Radar hydrology modifies the monitoring of flash flood hazard. *Hydrological Processes* 17(7): pp. 1453–1456, 10.10002/hyp.5122.

Dames and Moor (1985): Sinai development study-phase 1, water resources volumes II-A and II-B, submitted to the advisory committee for reconstruction, ministry of development, Cairo, Egypt.

Digital Elevation Model: http://dds.cr.usgs.gov/srtm/.

Digital Elevation Model: http://seamless.usgs.gov/.

Dittmer, H. J. (1959): A study of the root systems of certain sand dune plants in New Mexico. ECO~OQ40,: 265-273.

ECOCLIMAP:http://www.cnrm.meteo.fr/gmme/PROJETS/ECOCLIMAP/frame_text_ecoclimap.html#licence

FAO (1989): Arid Zone Forestry. A Guide for Field Technicians. *Food and Agriculture Organization*, Rome.

Farquharson, F. A., Meigh, J. R. and Sutcliffe, J. V. (1992): Regional flood frequency analysis in arid and semi-arid areas. *J. Hydrol* 138: pp. 487–501.

Few, R., Ahern, M., Matthies, F. and Kovats, S. (2004): Floods, health and climate change: a strategic review. *Tyndall Centre: Norwich*; 138 (Working Paper 63).

Flerchinger, G. N. and Cooly, K. R. (2000): A ten-year water balance of a mountainous semi-arid watershed. *J Hydrol* 237: pp. 86–99.

Georgakakos, K. P. (1986): On the design of natural, real-time warning systems with capability for site-specific, flashflood forecasts. *Bulletin American Meteorological Society*, 67: pp. 1233–1239.

GLCC:http://edc2.usgs.gov/glcc/glcc.php

Goosen, M. F. A. and Shayya, W. H. (1999): Water Management, Purification and Conservation in Arid Climates. In: Water Management, Purification and Conservation in Arid Climates: Volume I Water Management. M. F. A. Goosen and W. H. Shayya (eds.), *Technomic Publishing Co., Lancaster*, Pennsylvania, pp.1-6.

Goutorbe, J. P., Dolman, A. J., Gash, J. H. C., Kerr, Y. H., Lebel, T., Prince, S. D. and Stricker, J. N. M. (1997): HAPEX-SAHEL, Special Issue. *Journal of Hydrology*, pp. 188-189.

GPCC; http://gpcc.dwd.de

Grantz, D.A., 1990. Plant response to atmospheric humidity. Plant, Cell Environ., 13: 667-679.

GSMAP http://sharaku.eorc.jaxa.jp/GSMaP_crest/

Hansen, J., Lacis, A., Rind, D., Russell, G., Stone, P., Fung, I., Ruedy, R. and Lerner, J., 1984. Climate sensitivity: analysis of feedback mechanisms. In: J.E. Hansen and T. Takahashi (Edi tors), Climate Processes and Climate Sensitivity. *Geophysical Monographs, AGU, Washington*, DC, 29, pp. 130-163.

Hawkins, R. H., Jiang, R., Woodward, D. E., Hjelmfelt, A. T.,Van Mullem, J. A. and Quan, Q. D. (2002): Runoff Curve Number Method: Examination of the Initial Abstraction Ratio, in: *Proceedings of the Second Federal Interagency Hydrologic Modeling Conference, Las Vegas, Nevada, U.S. Geological Survey, Lakewood, Colorado,ASCE*.

http://en.wikipedia.org/wiki/Desert#cite_note-usgs-0

http://geology.com/records/sahara-desert-map.shtml

Hughes, D. A., and Sami, K. (1992): Transmission losses to alluvium and associated moisture dynamics in a semi-arid ephemeral channel system in southern Africa. *Hydr. Proc.*, 6, pp. 45–53.

Hughes, D. A., (1995): Monthly rainfall–runoff models applied to arid and semiarid catchments for water resource estimation purposes. *Hydrol. Sci. J.*, 40 (6), pp. 751–769.

Hulme, M., Doherty, R., Ngara, T. and New, M. (2005): Global warming and African climate change: a reassessment. *Cambridge University Press, Cambridge*, 338 pp

IPCC (1997): An introduction to simple climate models used in the IPCC Second Assessment Report. In Houghton JT, Filho LGM, Griggs DJ, Maskell K, IPCC Working Group I. Available online at http://www.ippc.ch.

Jiang, R. (2001): Investigation of Runoff Curve Number Initial Abstraction Ratio.

MS Thesis, *Watershed Management, University of Arizona*, pp. 120.

Jordan, P. R. (1977): Stream flow transmission losses in Western Kansas. *Jul of Hydraulics Division, ASCE,* 108, HY8, pp. 905-919.

Knighton, A. D. and Nanson, G. C., (1997): Distinctiveness, diversity and uniqueness in arid zone river systems. *In Arid Zone Geomorphology*: Process, form and Change in Dry lands (2nd edn), Thomas DSG (ed.). John Wiley & Sons: Chichester; pp. 185–203.

Kojiri, T., Tokai, A., and Kinai, Y. (1998): Assessment of river basin environment through simulation with water quality and quantity. *Annuals of Disaster Prevention Research Institute, Kyoto University,* No. 41 B-2, pp. 119-134 (in Japanese).

Korner, C. and Bannister, Up., 1985. Stomatal responses to humidity in Nothofagus menziesii. N.Z.J. Bot., 23: 425-429.

Lane, L. J. (1994): Estimating transmission losses. Proc. Spec. Conf., Development and Management Aspects of Irrigation and Drainage Systems, Irrig. And Drain. Engr. Div., A. S. C. E., San Antonio, Texas, pp. 106-113.

Lebel, T., and Le Barbe, L. (1997): Rainfall monitoring during HAPEX-Sahel.2. Point and areal estimation at the event and seasonal scales. *J.Hydrol*. 188-189, pp. 97-122.

Leopold, L. B. and Maddock, T. (1953): The hydraulic geometry of stream channels and some physiographic implications. *U.S. Geological Survey Professional Paper* 252, 56 p.

Malhotra, S. P. (1984): Traditional agroforestry practices on arid zone of Rajasthan. *In*: Agroforestry in arid and semi-arid zones. Eds. Shamkarnarayan et.al.CAZRI, Jodhpur, pp. 263-266.

McGuire and Thomas (2004): "Weather Hazards and the Changing Atmosphere". Earth Science: The Physical Setting. Amsco School Pubns Inc. pp. 571. ISBN 0-87720-196-X. http://www.amscopub.com/images/file/File_67.pdf. Retrieved 2008-07-17.

McMahon, T. A. (1979): Hydrological characteristics of arid zones. Proc. Symposium on the Hydrology of Areas of Low Precipitation, Canberra, *IAHS*,

No. 128, pp.105–23.

Mishra, S. K. and Singh, V. P. (2004): Long-term hydrological simulation based on the Soil Conservation Service curve number, *J. Hydrol. Process*. 18, pp. 1291–1313.

Mohamed, Y. A., van den Hurk BJJM, Savenijeand HHG, Bastiaanssen WGM (2005): Hydroclimatology of the Nile: results from a regional climate model. J *Hydrol Earth Syst Sci* 9: pp. 263–278.

National Weather Service, (2008): Definitions of flood and flash flood".. http://www.srh.noaa.gov/mrx/hydro/flooddef.php. Retrieved 2008-08-19.

Nile Basin Initiative (NBI) Shared vision program (2001): report on Nile River Basin: transboundary environmental analysis. United Nations Development Programme World Bank and Global Environment Facility

Nouh, M. (2006): Wadi flow in the Arabian Gulf states. *Hydrol. Process.*, Vol. 20, pp. 2393-2413.

Obled, C., Wendling, J. and Beven, K. (1994): Sensitivity of hydrological models to spatial rainfall patterns: An evaluation using observed data, *J. Hydrol.*, 159, pp. 305–333.

Osterkamp, W. R., Lane, L. J. and Savard, C. S. (1994): Recharge estimates using a geomorphic/distributed-parameter simulation approach, Amargosa river basin. *Water Resources Bulletin, American Water Resources Association*, 30, 3, pp. 493-507.

Palmer, T. N. and R¨ais¨anen, J. (2002): Quantifying the risk of extreme seasonal precipitation events in a changing climate, *Nature,* 415, pp. 512–514.

Parry, M., Canziani, O., Palutikof, J., van der Linden, P., and Hanson, C. (2007): Climate Change 2007: *Impacts, Adaptation and Vulnerability, Cambridge University Press*, 840 p.

Pilgrim, D. H., Chapman, T. G., and Doran, D. G. (1988): Problems of rainfall-runoff modeling in arid and semi-arid regions. *Hydrol. Sci. J.*, Vol. 33, No. 4: pp. 379‑400.

Rosso, R. and Rulli, M. C. (2002): An integrated simulation method for flash flood risk assessment: 2. Effects of changes in land-use under a historical perspective;

Hydrology and Earth System Sciences, 6(3), pp. 285–294.

Şen Z (2004) Hydrograph Methods, Arid Regions, Saudi Geological Survey (SGS), Technical Report

Şen Z (2008) Wadi Hydrology, CRC Press, New York

Smith, M. B., Seo, D. J., Koren, V. I., Reed, S. M., Zhang, Z., Duan, Q., Moreda, F. and Cong, S. (2004): The distributed model intercomparison project (DMIP): motivation and experiment design, *J. Hydrol.*, 298, pp. 4–26.

Smith, S. I., EL-Shamy, and H. El-Monsef (1997): "Locating Regions of High Probability for Groundwater in Wadi El Arish Basin, Sinai, Egypt". *Journal of African Earth Sciences,* Vol. 25, No. 2.

Soil Conservation Service (SCS) (1997): Hydrology. National Engineering Handbook, Chapter 5, Stream Flow Data, USDA: Washington, DC, USA.

Soil Conservation Service (SCS) (1985): National Engineering Handbook, section 4: hydrology, US Department of Agriculture, Soil Conservation Service, Engineering Division, Washington, DC.

Sorman, A. U. and Abdulrazzak, M. J. (1993): Infiltration - recharge through Wadi beds in arid regions. *Hydr. Sci. Jnl.*, 38, 3, pp. 173-186.

Tamura, N. and Kojiri, T. (2002): Water quantity and turbidity simulation with distributed runoff model in the Yellow River basin. Flood Defence ‘2002, Wu et al. (eds.), *Science Press, New York Ltd.*, Vol. 2, pp. 1699-1705.

Telvari, A., Cordery, I. and Pilgrim, D. H. (1998): Relations between transmission losses and bed alluvium in an Australian arid zone stream. In: Wheater H, Kirby C (eds) Hydrology in a Changing Environment, vol. II. Wiley, pp. 361–36

Tokai, A., Kojiri, T. and Yoshikawa, H. (2002): Case study of basin wide environmental quality assessment based on the distributed runoff model. *6th Water Resources Symposium, Japan*, pp. 229-234 (in Japanese).

U. Hornung, ed., Homogenization and Porous Media, Interdisciplinary Applied Mathematics Series, Vol. 6, Springer, New York, 1997.

UNEP. 1992. World Atlas of Desertification. Edward Arnold, London, UK.

UNEP. 1997. United Nations Environment Programme. World Atlas of

Desertification, 2nd edition. Edited by N. Middleton and D. Thomas. London: UNEP. 182pp.

UNESCO (1977): World Distribution of Arid Regions. Map Scale: 1/25,000,000, UNESCO, Paris.

United Nations Environment Program/Global Resource Information Database. Prepared by U. Diechmann and L. Eklundh. (1991): Global Digital Datasets for Land Degradation Studies: a GIS Approach. Nairobi, Kenya:UNEP/GEMS and GRID.

UNSO/UNDP. (1997): Office to Combat Desertification and Drought/ United Nations Development Programme. An Assessment of Population Levels in the World's Drylands: Aridity Zones and Dryland Populations. Office to Combat Desertification and Drought. New York, NY. 23pp.

Vivarelli, R. and B. J. C. Perera (2002): "Transmission Losses in Natural Rivers and Streams – a review." Riversymposium Papers and Presentations. Riverfestival Brisbane Pty Ltd, South Brisbane, Australia.

Walters, M. O. (1990): Transmission losses in arid region. *J. of Hydraulic Engineering,* 116, 1, pp. 127-138.

Walton, W. C. (1969): Ground Water Resources Evaluation, *McGraw-Hill Book Co., New York.*

Wheater, H. S., Jakeman, A. J. and Beven, K. J. (1993): Progress and directions in rainfall-runoff modelling. In Modelling Change in Environ. Systems, ed. Jakeman, A. J. Beck, M. B. and McAleer, M. J. Chichester: Wiley, pp. 101–32.

Wheater, H., S. Sorooshian and G. Sharma (2008): Hydrological Modelling in Arid and Semi-Arid. *Areas, Cambridge University Press, New York*, 195pp.

Wheater, H. S., Woods Ballard, B. and Jolley, T. J. (1997): An integrated model of arid zone water resources: evaluation of rainfall-runoff simulation performance. In: Sustainability of Water Resources under Increasing Uncertainty, *IAHS* Pubn. No.24.

Willis, A. J., Folkes, B. F. & Yemm, E. W. (1959): Branton Burrows: the dune

system and its vegetation. Part II.Jouma1 of Ecology, 47: 249-88.

Woods, R. A. and Sivapalan, M. (1999): A synthesis of space-time variability in storm response: Rainfall, runoff generation and routing, Water Resour. Res., 35, pp. 2469–2485.

World Meteorological Organization (WMO), UNEP, Climate Change (2001): Impacts, Adaptation and Vulnerability, Contribution of Working Group II to the Third Assessment Report (TAR) of the Intergovernmental Panel on Climate Change (IPCC).

WRI (2002): World Resources Institute. Drylands, People, and Ecosystem Goods and Services: A Web-based Geospatial Analysis. Available online at: http://www.wri.org.

Younis, J., Anquetin, S. and Thielen, J. (2008): The benefit of high-resolution operational weather forecasts for flash-flood warning. Hydrology and Earth System Sciences and Discussion 5: pp. 345–377.